

UNIVERSITÀ DEGLI STUDI DI PADOVA
LEOPOLD-FRANZENS UNIVERSITÄT INNSBRUCK
ALBERT-LUDWIGS UNIVERSITÄT FREIBURG

HOME INSTITUTION: UNIVERSITÀ DEGLI STUDI DI PADOVA,
DIPARTIMENTO DI FARMACOLOGIA ED ANESTESIOLOGIA

HOST INSTITUTION: LEOPOLD-FRANZENS UNIVERSITÄT INNSBRUCK,
INSTITUT FÜR BIOCHEMISCHE PHARMAKOLOGIE

HOST INSTITUTION: ALBERT-LUDWIGS UNIVERSITÄT FREIBURG,
INSTITUT FÜR EXPERIMENTELLE UND KLINISCHE
PHARMAKOLOGIE UND TOXIKOLOGIE

DOCTORAL DISSERTATION
in

"MOLECULAR AND CELLULAR PHARMACOLOGY"
"FARMACOLOGIA MOLECOLARE E CELLULARE"
SSD: BIO/14

DOCTORAL PROGRAMME
XX CICLE

THE EFFECTS OF OXYSTEROLS ON CELL VIABILITY IN VASCULAR ENDOTHELIAL AND SMOOTH MUSCLE CELLS: ROLE OF REACTIVE OXYGEN SPECIES

COORDINATOR: *Prof. Sisto Luciani*
Department of Pharmacology and Anestesiology, University of Padova

SUPERVISOR: *Prof. Sisto Luciani*
Department of Pharmacology and Anestesiology, University of Padova

DOCTORAL CANDIDATE: Chiara Poggiani

January 31st, 2008

INDEX

ABBREVATIONS

25-OHC	25-hydroxycholesterol
7-KC	7-ketocholesterol
7*β*-OHC	7β-idrossicolesterolo
ACAT	cholesterol acetyltransferase
AGEs	advanced glycation end products
AIF	apoptosis inducing factor
Akt	protein kinase B
Ang II	angiotensin II
ASK-1	apoptosis signal regulating kinase-1
ATP	adenosine triphosphate
bFGF	basic fibroblast growth factor
BSA	bovine serum albumin
CCCP	
CCCP	cyanide m-chlorophenylhydrazone
cGMP	cyclic guanosine phosphate
DMSO	dimethylsulfoxide
DNA	deoxyribonucleic acid
EGF	endothelial growth factor
eNOS	endothelial nitric oxide synthase
eNOS	endothelial nitric oxide synthase
EPOX	epoxycholesterol
ER	endoplasmic reticulum
ERK	extracellular regulated kinases
ET-1	endothelin-1
FBS	fetal bovine serum
GPx	gltathione peroxidase
GSH	glutathione
GTPase	guanosinetriphsphataes
H_4B	tetraidrobiopterina
HDL	high density lipoprotein
HMG-CoA	hydroxymethylglutaryl coenzyme A

HUVEC	human umbilical vein endothelial cell
IAPs	inhibitor of apoptosis proteins
ICAM-1	intercellular adhesion molecule-1
ICAM-1	intracellular adhesion molecule-1
IL-1	interleukin-1
JNK	c-jun-N terminal kinase
LDL	low density lipoprotein
LDL	low density lipoprotein
LXR	liver X receptor
M199	medium 199
MAPK	mitogen activated protein kinases
MAPK	mitogen-activated protein kinase
MCP-1	monocyte chemoattractant protein-1
MEK	
MEK	extracellular signal-regulated kinase
MEM	minimum essential medium eagle
MPO	myeloperoxidase
MPTP	mitochondrial permeability transition pore
MTT	3-(4,5-dimethylthiazol-2-yl)-2,5-diphenyltetrazolium bromide
NADPH	nicotinamide adenin dinucleotide phosphate
NFκB	nuclear factor κB
NO	nitric oxide
NOS	nitric oxide synthase
oxLDL	oxidized low density lipoprotein
oxLDL	oxidized low density lipoprotein
PARP	Poly(ADP-Ribose) polymerase
PBS	phosphate-buffered saline solution
PDGF	platelet derived growth factor
PGI_2	prostacicline
PI3K	phosphatidylinhositol 3 kinase
PKC	protein kinase C
PSS	physiological salin solution
PTPs	protein tyrosine phpsphatases
ROS	reactive oxygen species

SDS	sodiumdodecylsulfate
SOD	superoxide dismutase
SOD	superoxide dismutase
TNFα	tumor necrosis factor α
TRAF4	TNF-receptor-associated factor 4
Trx	thioredoxin
TTFA	tenoyltrifluoroacetate
TXA_2	tromboxane A_2
VCAM-1	vascular adhesion molecule-1
VEGF	vascular endothelial growth factor

Abstract

Oxidized low density lipoproteins (oxLDLs) are involved in the pathogenesis of atherosclerosis and the cytotoxicity of oxLDLs has been linked to the formation of oxysterols (Schroepfer et al, 2000). 7-ketocholesterol (7-KC) and 7β-hydroxycholesterol (7*β*-OHC) are the major oxysterols found in oxLDLs. High concentrations (> 20 *μ*g/ml) of 7-KC and 7*β*-OHC have been shown to induce apoptosis in human endothelial cells (Lizard et al, 1999). Preliminary results obtained in our laboratory have shown that 7*β*-OHC and 7-KC, at concentrations below 20 *μ*g/mL, induce an increase in cell viability. Furthermore, it has been recently reported that oxLDLs induce proliferation and apoptosis in vascular cells, depending on the concentration and that both effects are mediated by superoxide formation (Galle, *et al*, 2001). In fact, besides the known cytotoxicity of reactive oxygen species (ROS), evidences have been accumulated indicating that these molecules are involved in several signal transduction pathways leading to antiapoptotic and proliferative effects (Haendeler *et al*, 2004). The aim of this study was to investigate the role of ROS on cellular effects of 7-KC and 7*β*-OHC in endothelial and vascular smooth muscle cells.

Treatment of human umbilical vein endothelialcells (HUVEC) and A7r5 (rat vascular smooth muscle cells) for 24 and 48 hours with 7-KC or 7*β*-OHC (1-10 *μ*g/mL) increased cell viability, while a cytotoxic effect was induced at 20 *μ*g/mL. Both oxysterols induced an increase in intracellular ROS production in a time dependent manner. ROS production by 7*β*-OHC was partially dependent on NADPH oxidase. Analysis of phosphatidylserine translocation and caspase-3 activation in HUVEC treated with 7*β*-OHC showed an antiapoptotic effect of the oxysterol against bFGF deprivation and staurosporine treatment. Incubation of HUVEC with the NADPH oxidase inhibitor hydralazine or with the antioxidant N-acetilcysteine was not able to prevent the antiapoptotic effect of 7*β*-OHC. Although 7*β*-OHC did not induce an increase in ERK activation, treatments of HUVEC with two different MEK inhibitors (PD98059, U0126) antagonized the protective effect of the oxysterol. The results show that 7*β*-OHC, at concentration below 20 *μ*g/mL is antiapoptotic by a mechanism independent on ROS production and dependent on activation of MEK/ERK pathway.

Riassunto

Le lipoproteine a bassa densità (oxLDL) sono coinvolte nella patogenesi dell'aterosclerosi e la citotossicità delle stesse oxLDL è dovuta alla presenza degli ossisteroli tra i suoi componenti. Il 7-chetocolesterolo (7-KC) e il 7β-idrossicolesterolo (7β-OHC) sono i principali ossisteroli che costituiscono le oxLDL ed è stato riportato che alte concentrazioni di 7-KC e di 7β-OHC inducono apoptosi nelle cellule endoteliali umane (Lizard et al, 1999). Risultati preliminari del nostro laboratorio hanno dimostrato che il 7β-OHC e il 7-KC inducono un aumento della vitalità cellulare a concentrazioni inferiori a 20 μg/mL. Inoltre, è stato recentemente dimostrato che le oxLDL possono indurre sia proliferazione che morte nelle cellule vascolari, a seconda della concentrazione; entrambi gli effetti sono mediati da un aumento del livello delle specie reattive dell'ossigeno (ROS) (Galle, et al, 2001). In accordo con tale evidenza, sono stati riportati i dati sperimentali circa il duplice effetto dei ROS, che possono indurre sia proliferazione che apoptosi, dipendentemente dalla loro concentrazione nelle cellule endoteliali (Haendeler et al, 2004). Lo scopo di questo lavoro è stato quello di studiare il ruolo dei ROS negli effetti cellulari di 7-KC e 7β-OHC nelle cellule endoteliali umane della vena ombelicale (HUVEC) e nelle cellule muscolari lisce vascolari di ratto (A7r5).

Il trattamento delle HUVEC e delle A7r5 con 7-KC o 7β-OHC per 24 ore induceva un aumento della vitalità cellulare a concentrazioni inferiori a 20 μg/mL, mentre a 20 μg/mL si evidenziavano effetti citotossici. Entrambi gli ossisteroli provocavano un aumento dei ROS concentrazione-dipendente. La produzione di ROS indotta dal 7β-OHC era in parte dovuta all'attività della NADPH ossidasi. Analisi della traslocazione della fosfatidilserina e dell'attivazione della caspasi-3 in HUVEC trattate con 7β-OHC hanno evidenziato un effetto antiapoptotico dell'ossisterolo contro l'apoptotosi indotta da deprivazione di bFGF o da staurosporina. Né l'idralazina, inibitore della NADPH ossidasi, né l'antiossidante N-aceticisteina erano in grado di prevenire l'effetto antiapoptotico del 7β-OHC. Infine, anche se l'ossisterolo induceva la fosforilazione delle ERK, il trattamento delle HUVEC con due inibitori della MEK (PD98059, U0126) era in grado di antagonizzare l'effetto aniapoptotico del 7β-OHC. In conclusione, il 7β-OHC a concentrazioni inferiori a 20 μg/mL ha un'azione antiapoptotica non mediata dai ROS, ma dipendente dall'attivazione della via di sopravvivenza cellulare MEK/ERK.

1. INTRODUCTION

1.1 VASCULAR WALL AND ENDOTHELIAL FUNCTION

The arterial vessel wall is divided into three components: *tunica intima*, *tunica media* and *tunica adventitia* (Fig. 1) *Tunica intima* consists of a single layer of endothelial cells between the vessel lumen and the internal elastic lamina membrane. *Tunica media* comprises the muscular portion of the blood vessel, whereas *tunica adventitia* includes the external elastic lamina, terminal nerve fibres and surrounding connective tissue, which contains fibroblasts and tissue macrophages. Each of these three layers has specific properties and exerts different effects which are crucial to regulation of vasomotor tone, protection against thrombosis and response to injury (Hürlimann *et al*, 2002).

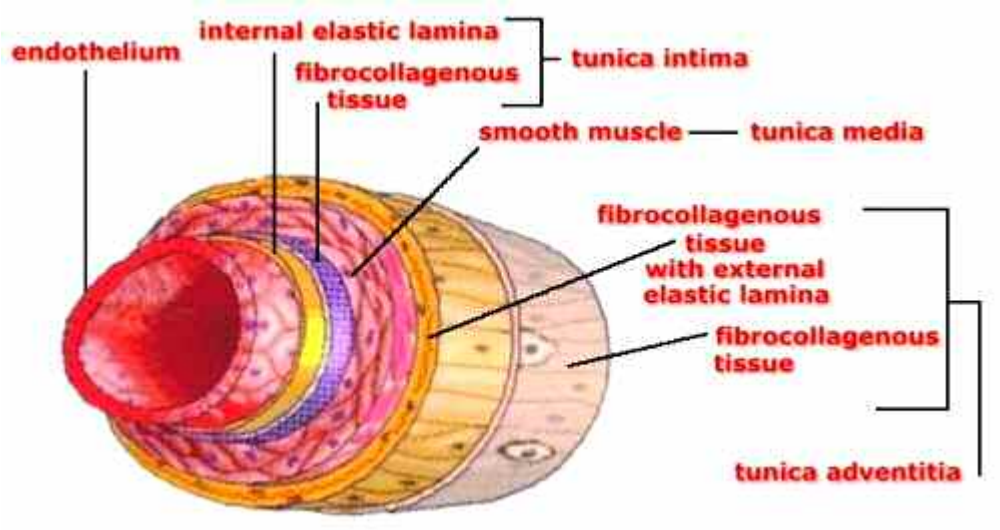

Fig. 1 Scheme of artery wall.

The endothelium is a monolayer of endothelial cells located between the circulating blood and vascular smooth muscle cells of the media. It is a paracrine autocrine, and endocrine organ, playing a key role in regulation of vascular tone, thrombogenesis, inflammation and vessel growth. Therefore, the integrity of

endothelium layer is necessary to maintain vascular homeostasis. Endothelial cells can have indirect and direct effects on vascular structure and their presence is necessary to prevent both migration and proliferation of vascular smooth muscle cells.

To exert its vascular regulatory functions, endothelium release several mediators with capacity to modulate the contractile state and proliferative responses of vascular smooth muscle cells. Endothelium has also capacity to control platelet function, coagulation and monocyte adhesion. Endothelial cells exert protective role during tissue injury, by producing cytokines regulating vascular permeability and chemotaxis.

Migration is another property of endothelial cells, important to enhance blood vessel repair after cardiovascular lesions (Hürlimann *et al* 2002).

To control contractile state of blood vessels, endothelial cells produce nitric oxide (NO), the most important vasodilator mediator (Radomski *et al*, 1987) originally named 'endothelium-derived relaxing factor'. NO is released from endothelial cells in response to both shear stress (produced by blood flow) and mediators such as acetylcholine, bradykinin, substance P and serotonin. NO is a free radical gas with an in vivo halflife of only a few seconds, and is able to cross biological membranes. NO is synthesized by NO synthase (NOS) from L-arginine and is released by endothelial cells via a diffusion mechanism. NO acts at level of vascular smooth muscle cells of the media where it increases intracellular cyclic-GMP (cGMP) concentrations by activation of the guanylate cyclase. This leads to relaxation of smooth muscle cells. Systemic inhibition of NO synthesis increases arterial blood pressure. NO has also anti-aggregation, anti-thrombotic and anti-inflammatory properties. In addition to that, NO acts as signalling molecule involved in endothelial antiapoptotic and protective pathways in cells (Hürlimann *et al,* 2002). Continuous production of NO helps to maintain integrity of endothelium and prevents the expression of endothelia adhesion molecules (VCAM-1 and ICAM-1) responsible for the attachment and sequestration of monocytes through the endothelial cells monolayer during atherogenesis.

Another vasoprotective factor produced by endothelial cells is prostacycline (PGI_2), a vasodilator factor with antiaggregation properties, which enhances vessels permeability.

Both NO and PGI_2 inhibit endothelin production via a cGMP-dependent mechanism.

On the other hand, endothelin-1 (ET-1) is a vasoconstrictor factor, produced by both endothelial cells and vascular smooth muscle cells, under the stimulation of

hypoxia, shear stress, angiotensin II, vasopressin, insulin, thrombin, and interleukin-1 (Miyauch and Masaki, 1999).

1.2. REACTIVE OXYGEN SPECIES IN ENDOTHELIAL FUNCTION

Reactive oxygen species (ROS) are partially reduced and highly reactive metabolites of oxygen (O_2), produced as a consequence of aerobic metabolism. ROS include free radicals such as superoxide anion ($O_2^{\bullet -}$), hydroxyl radicals ($^{\bullet}OH$) and the non-radical hydrogen peroxide (H_2O_2) (Thannikal and Fanburg, 2000).

They are particularly transient species due to their high chemical reactivity, so they can react with many biomolecules such as DNA, proteins, carbohydrates and lipids in a destructive manner.

The equilibrium between intracellular ROS production and the activity of antioxidant defence systems determines intracellular redox status and defines redox homeostasis. If ROS production overcomes the capacity of antioxidant enzymes, redox homeostasis is altered and oxidative damages occurs in cells undergoing a condition called oxidative stress (Thannikal and Fanburg, 2000).

This condition of oxidative stress is implicated in the pathogenesis of several diseases including Huntington's, Parkinson's, Alzheimer's diseases.

1.2.1. Chemistry of ROS

ROS are highly reactive metabolites coming from molecular oxygen. They are often considered as free radicals, but this definition is not always correct. A free radical is any

molecular or atomic species capable of independent existence that contains one or more unpaired electrons in one of its molecular orbitals. Molecular O_2 itself can be defined a free radical, because it has two unpaired electrons with parallel spin in two different π-antibounding orbitals. This spin restriction accounts for its relative stability and paramagnetic properties. O_2 is capable of accepting electrons in its antibounding orbitals becoming partially reduced. The partially reduced forms of oxygen are strong oxidizing agents because of their tendency of becoming completely reduced and form water (H_2O), as shown below (Halliwell and Gutteridge, 1989):

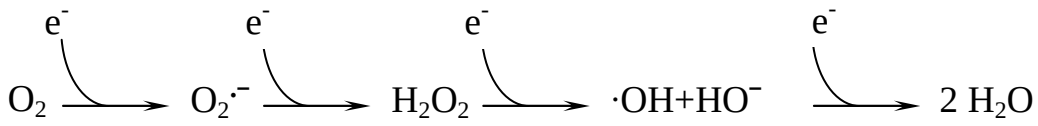

One-electron reduction of O_2 results in the formation of $O_2^{\bullet -}$ and it can be due to either enzymatic catalysis or electron leaks from various oxidoreductase reactions. In aqueous solution $O_2^{\bullet -}$ is short-lived because of its instability and its tendency of dismutate to H_2O_2. This dismutation is facilitated in acidic conditions when superoxide is protonated ($HO_2^{\bullet}$). In intracellular compartments this spontaneous dismutation is in competition with the same dismutation catalyzed by superoxide dismutase (SOD), the principal antioxidant defence enzyme (Huie and Padmaja, 1993). Thus, in most biological systems the production of $O_2^{\bullet -}$ results in the formation of H_2O_2, a non-radical molecule more stable than the other ROS. It can cross biological membranes and because of its higher half-life it's weaker oxidant agent than $O_2^{\bullet -}$. H_2O_2 can act as signaling molecule in both physiological and pathological conditions. H_2O_2 plays also an important role in antimicrobial response: it can be converted to hypochlorous acid (HOCl) by myeloperoxidase (MPO), an enzyme present in phagosomes and neutrophils. HOCl has strong bactericide oxidant properties (Rossi *et al*, 1985).

In presence of reduced forms of transient metals such as iron (Fe^{2+}) and copper (Cu^{+}), H_2O_2 can lead to the formation of the higher reactive and toxic $^{\bullet}OH$ (*Fenton Reaction*) which rapidly induce the oxidation of biological substrates to be reduced to H_2O. For example $^{\bullet}OH$ induces lipid peroxidation damaging biological membranes. The oxidized transient metals coming from the *Fenton Reaction* can be reduced again in the *Haber Weiss Reaction* with $O_2^{\bullet -}$, which is converted to O_2.

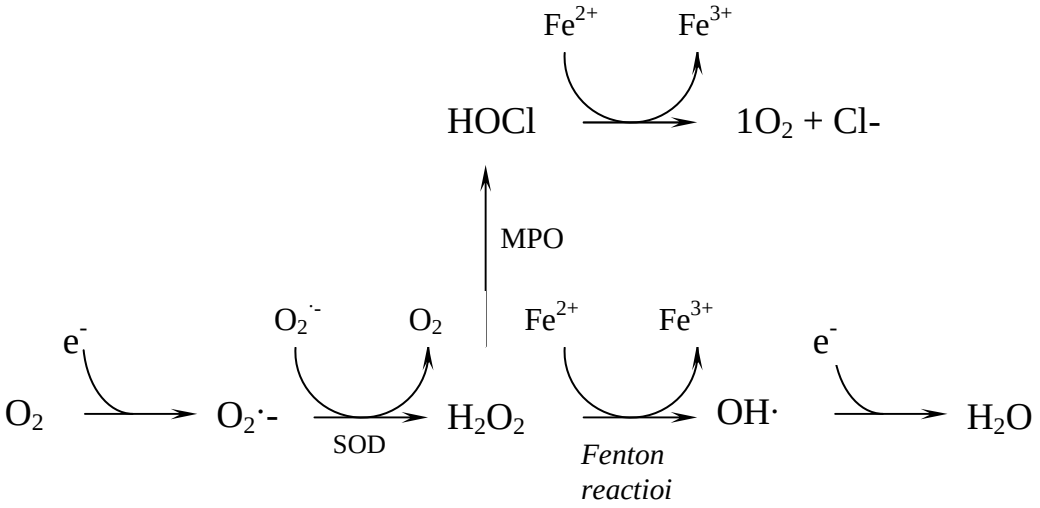

Fig. 2 Main reactions of reactive oxygen species (SOD: superoxide dismutase. MPO: myeloperoxidase).

1.2.2. Intracellular antioxidant defence systems

To maintain intracellular redox homeostasis at physiological levels (Droge, 2002), cells have antioxidant defence systems as summarized below:

- Superoxide dismutase (SOD), catalyzing the dismutation of $O_2^{\bullet -}$ to H_2O_2 as the following reaction shows:

$$2O_2\cdot\text{-} + 2H+ \xrightarrow{\text{SOD}} H_2O_2 + O_2$$

- Catalase, heme-proteine, containing four oxidized heme groups (Fe^{3+}). This enzyme can neutralize H_2O_2 with two alternative mechanisms:
  - dismutation of H_2O_2 to O_2 and H_2O

$$2H_2O_2 \xrightarrow{\text{catalase}} 2H_2O + O_2$$

  - Reduction of H_2O_2 with a reduced substrates.

- Peroxidases, heme-proteins containing only one oxidized heme group (Fe3+), that catalyzes the reduction of H_2O_2 with a reduced substrates.

- Glutathione peroxidase system (GPx), composed of glutathione peroxidase and

glutathione reductase. This system catalyzes the reduction of both H_2O_2 and peroxides using reduced glutathione (GSH) which is oxidized (glutathione disulfide, GSSG). GSSG is then reconverted to GSH by glutathione reductase under consumption of NADPH

- Thioredoxin (Trx) system, composed of thioredoxin reductase (TrxR) and thioredoxin. Reduced Trx is highly efficient in reducing disulfides in proteins and peptides, including glutathione disulfide. TrxR reduces the active site disulfide in Trx and several other substrates directly under consumption of NADPH (Nordberg J and. Arn´er ESJ, 2001).

- Low weight molecular ROS scavangers, such as hydrosoluble ascorbic acid and lipid-soluble tocopherol.

1.2.3. Intracellular sources and regulation of ROS

ROS can be produced by both enzymatic and non-enzymatic sources, as by-product of electron-transfer reactions, carried out by electron-transferring proteins or enzymatic systems.

Mitochondria are the major sources of ROS under physiological conditions (Fig. 3). ROS normally produced by mitochondria corresponds to 1-2% of total O_2 consumption (Freeman and Crapo, 1982). Electrons carried out by the electron transport chain (ETC) can leak out of the pathway and pass directly to oxygen, generating $O_2^{\bullet -}$. Electrons can enter the ETC at the level of either Complex I via the oxidation of NADPH by NADPH-ubiquinone oxidoreductase or Complex II via the oxidation of succinate by the succinate dehydrogenase. After that, electrons are carried from one of these complexes to Complex III (ubiquinol-cytochrome c oxidoreductase) by Ubiquinone, a lipid-soluble electron carrier. The highly reactive semiquinone generated at level of Complex I and III is mainly responsible for the formation of superoxide. The intramitochondrial concentrations of $O_2^{\bullet -}$ are maintained at very low steady-state levels by the Mn-SOD, which converts $O_2^{\bullet -}$ to H_2O_2. While $O_2^{\bullet -}$ is not able to cross biological membranes, H_2O_2 is able to diffuse across mitochondrial membrane to cytoplasm. Some correlations between intramitochondrial ROS production and the regulation of apoptosis mechanisms induced by different stimuli have been recently found.

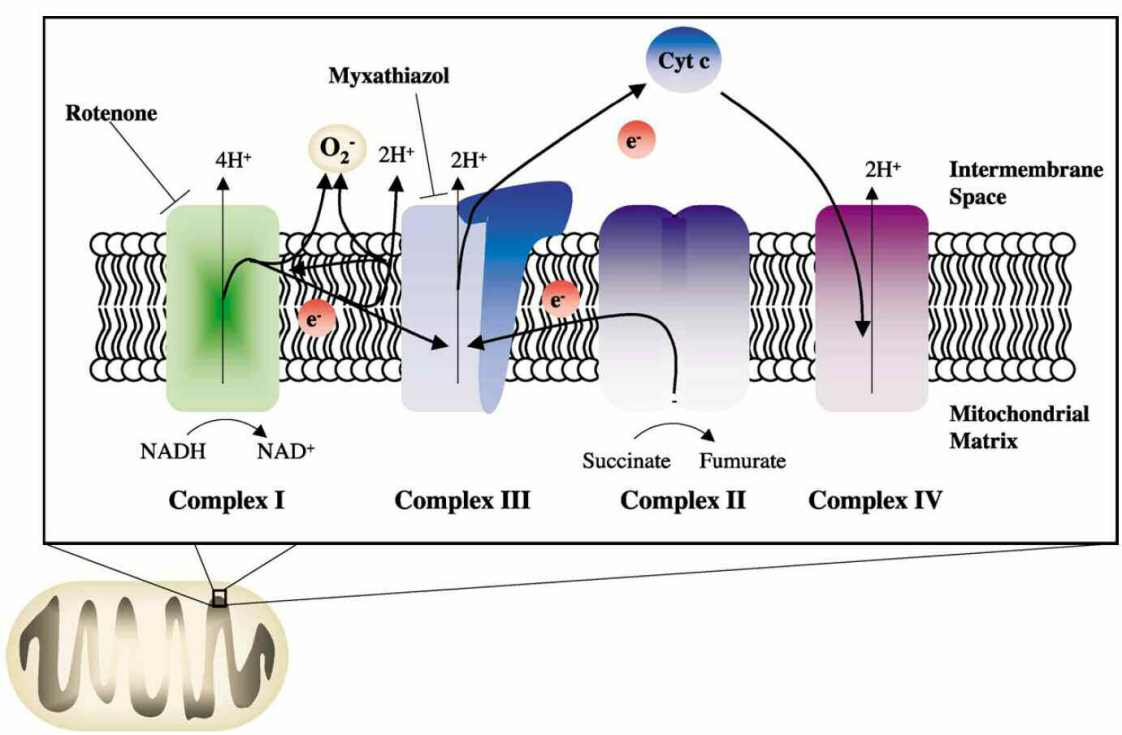

Fig. 3 Superoxide production by mitochondria, at level of different complexes of respiratory chain (Curtin *et al*., 2002).

Endoplasmic reticulum (ER) is another possible source of ROS (Freeman and Crapo, 1982). ER is a membrane-bound organelle involved in lipid and protein synthesis. Smooth ER (lacking bound ribosomes) contains enzymes responsible for the oxidative modifications of lipid soluble drugs and other harmful metabolic products. Cytocrome P450 and b_5 families, are the main important enzymatic systems oxidizing unsaturated fatty acids and xenobiotics and they can reduce molecular oxygen to $O_2^{\bullet -}$. There is evidence for redox-regulation of ER-related functions such as protein folding and secretion (Bader *et al*. 1999).

Peroxisomes are important sources of total intracellular H_2O_2 production (Boveris *et al***.** 1972). They contain a number of H_2O_2-generating enzymes including glycolate oxidase, D-aminoacid oxidase, urato oxidase, L-α-hydroxyacid oxidase and fatty acyl-CoA oxidase. Then peroxisomal catalase utilizes H_2O_2 to oxidize a variety of other substrates in peroxidative reactions. These reactions are particularly important as detoxifying mechanisms to inactivate xenobiotics. A small fraction of peroxisomal

H_2O_2 can escape catalase and diffuse from these organelles to cytoplasm, contributing to either intracellular signalling or oxidative stress, depending on its concentrations.

In addition to intracellular membrane associated oxidases, soluble enzymes such as **xanthine oxidase, aldehyde oxidase, flavoprotein dehydrogenase** can produce ROS during their catalytic cycling. The most relevant enzyme is xanthine oxidase expressed on the luminal surface of the endothelium in many organs It can be formed from xanthine dehydrogenase under condition of hypoxia (McKelvey *et al*. 1988). Usually xantine oxidase catalyzes the oxidation of xanthine to urate with the concomitant reduction of molecular oxygen to superoxide and hydrogen peroxide. The enzyme is normally present as xanthine dehydrogenase, which does not generate $O_2^{\bullet-}$, but is converted to xanthine oxidase either through oxidation or by proteolytic cleavage of a segment of xanthine dehydrogenase. Increased xanthine oxidase-derived $O_2^{\bullet-}$ production may be involved in ischaemia/reperfusion and in endothelial dysfunction in several diseases (McKelvey *et al*. 1988). With respect to signalling, xantine oxidase-derived ROS have been implicated in the control of the endothelial cytoskeleton and mechanoenergetic coupling. Xanthine oxidase is widely used to generate $O_2^{\bullet-}$ in vitro to study the effect of ROS on different cellular processes (Thannikal and Fanburg, 2000).

NADPH oxidase is a membrane associated flavoprotein involved in production of $O_2^{\bullet-}$ directly from molecular O_2 in a one-electron transfer reaction. NADPH oxidase a multicomponent flavoenzyme, which constantly produces intracellular ROS at low levels under physiological conditions. Different stimuli such as growth factors, cytokines, oxLDL, oxysterols, mechanical stress can induce NADPH oxidase activation and this ligand-induced ROS production is involved in the regulation of endothelial function (Ushio-Fukai and Alexander, 2004).

1.2.4. Vascular NADPH Oxidase

NADPH oxidase is a respiratory burst oxidase tipically contained in phagocytes, that catalyzes the one-electron reduction of molecular oxygen to superoxide, leading to hydrogen peroxide production which is important in host defence (see above). This enzyme is normally quiescent, and becomes activated during the neutrophil oxidative burst to generate large amounts of $O_2^{\bullet-}$ (Babior, B, *et al* 2002). The neutrophil oxidase consists of a plasma membrane spanning cytochrome b558 which is an heterodimer, comprising gp91phox and p22phox, and cytosolic components p47phox, p67phox and

the small GTPase Rac1. Even if the catalytic subunit of this complex is gp91phox, defects in any one of the phox components result in the clinical syndrome of chronic granulomatous disease, a disorder characterized by impared host defence and chronic infection. Activation of NADPH oxidase triggers translocation of the cytosolic components to the membrane bound subunits under the guide of Rac 1 protein. This is a highly regulated process that involves post-translational modification of several of the cytosolic subunits and specific protein–protein binding through tandem SH3 (Src homology 3) domains. The resulting protein complex enables electron transfer from NADPH, in the flavin-containing catalytic subunit, to O_2, thereby generating $O_2^{\bullet -}$ (Fig. 4).

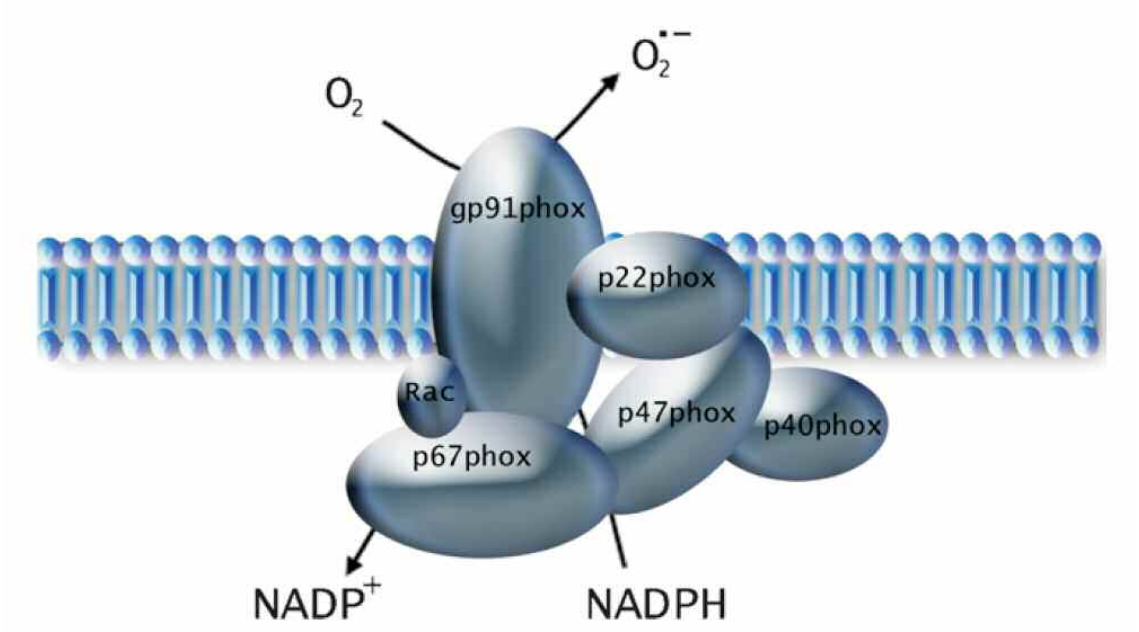

Fig. 4 Neutrophyl NADPH oxidase and superoxide formation (Ray and Shah, 2005).

In the vasculature the $p22^{phox}$, $p67^{phox}$, and $p47^{phox}$ components of the NADPH oxidase are distributed ubiquitously among the major cell types (Bayraktutan *et al*, 1998). In contrast, the catalytic subunit of the vascular NADPH oxidases appears to be distinct from its phagocyte counterpart gp91phox (Cheng, *et al*. 2001). Numerous gp91phox (newly named as Nox2) homologues, including Nox1, Nox3, Nox4, and

Nox5, have been identified in vascular cells, each encoded for by separate genes. Endothelial cells express very low levels of Nox1, intermediate levels of Nox2, and abundant Nox4 mRNA, while vascular smooth muscle cells express predominantly Nox4 and, to a lesser extent, Nox1 with negligible amounts of Nox2 (Jones *et al*, 1996; Griendling KK *et al*, 2000). Analysis of the predicted sequences of Nox family members reveals that despite a relatively high degree of conservation in the overall topology of the Noxs, they differ greatly in their tissue distribution and are also likely to be differentially activated and regulated. Each isoform contains an N-terminal cluster of hydrophobic membrane-spanning regions and C-terminal regions containing a flavoprotein domain and consensus pyridine nucleotide-binding sites.

NADPH oxidase in non-phagocytic cells such as endothelial cells differs from the neutrophil enzyme in several important aspects. Whereas the neutrophil oxidase releases large amounts of $O_2^{\bullet -}$ in bursts, the vascular NADPH oxidase(s) continuously produce low levels of $O_2^{\bullet -}$ in unstimulated cells, yet it can be further stimulated acutely by various stimuli. Then, while in neutrophil $O_2^{\bullet -}$ production occurs mainly in extracellular environment, in endothelial cells $O_2^{\bullet -}$ is produced mainly in intracellular compartments (Fig. 5), depending on the location of the enzyme complex (Thannikal and Fanburg 2000).

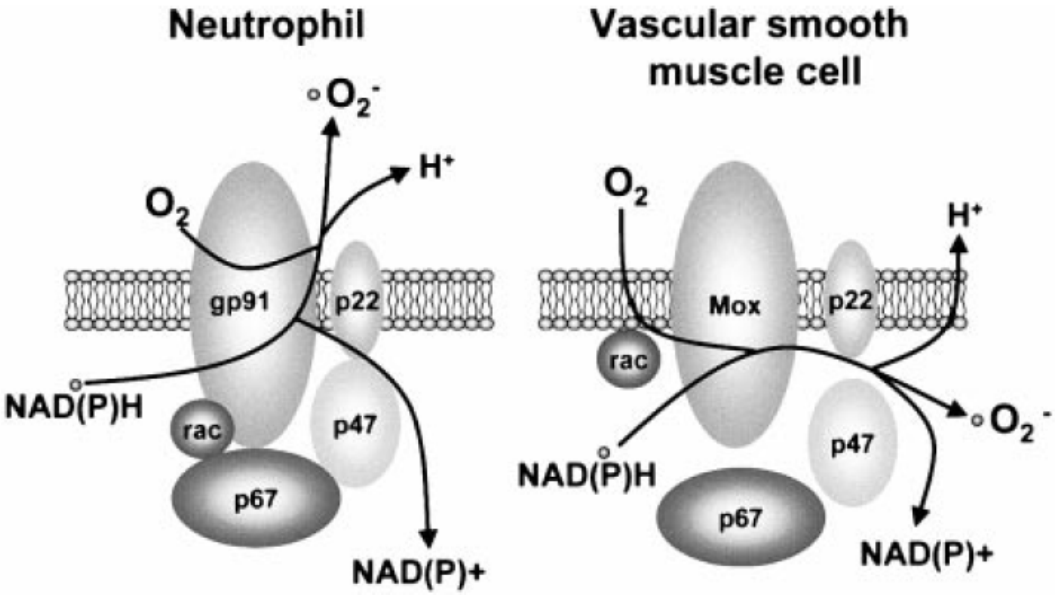

Fig. 5 Neutrophyl and vascular NADPH oxidase in comparison. In vascular cells, superoxide is continously produced in the cytoplasmatic compartment (Griendling KK *et al*., 2000).

Regulation of oxidase activity in cardiovascular cells occurs at least at two levels. First the activation of the enzyme can be enhanced by second messengers, including calcium. In addition to that stimuli, such as angiotensin II, high glucose levels, cytokines, can trigger its overexpression involved in the development of oxidative stress.

The vascular NADPH oxidase is activated and regulated by a variety of hormones and factors (Fig. 6) known to be important in vascular remodeling and disease. These include agonists of G-protein-coupled receptors such as angiotensin II and ET-1, thrombin, platelet-derived growth factor (PDGF), cytokines such as tumor necrosis factor (TNFα), interleukin-1. NADPH oxidase can also be activated by metabolic factors such as increased glucose, insulin, NEFAs (non-esterified fatty acids) or advanced glycation end-products (AGEs), and oxidized LDL (Griendling *et al*. 2000). NADPHox expression can also be modified. For example oxLDL enhance expression of Nox4 in human endothelium (Thum and Borlak 2004). Changes in shear stress are very relevant stimuli in endothelial cells: oscillatory shear stress (zero net forward flow) increases ROS production and upregulates Nox4 as well as Nox2, while pulsatile shear (net forward flow) may actually downregulate these components as compared to static cells (Hwang *et al*. 2003).

One mechanism involved in NADPH oxidase activation is protein kinase C (PKC)-dependent phosphorylation of the p47phox and its translocation to the Nox2/ p22phox heterodimer to form the more fully assembled complex, just as in neutrophils.

The most studied stimulus of the vascular NADPH oxidase is angiotensin II that increases the activity of the NADPH oxidase at three or more levels. At the beginning, there is rapid activation of c-Src and other kinases such as PKC, leading to phosphorylation of p47phox which translocates to the membrane cytochrome complex (Touyz *et al*. 2003). In vascular smooth muscle, the EGF receptor transactivation is also involved, leading to sequential activation of both phosphatidylinositol 3-kinase (PI3K) and small G-protein Rac immediately after angiotensin receptor AT1 activation (Seshiah *et al*. 2002). Activated Rac in its GTP-bound state is thought to bind to the cytosolic p67phox subunit and activate the NADPH oxidase. All these events, following angiotensin II stimulation, serve to activate, promote and sustain electron flow through the cytochrome complex. A further level of action of angiotensin II, and of some other stimuli, is to increase the expression of NADPH oxidase subunits over hours to days (Cai *et al*. 2003).

NADPH oxidase activation is also involved in VEGF induced endothelial proliferation and migration (Ushio-Fukai *et al.*,2002) via PKC-dependent phosphorylation of the p47phox regulatory subunit; this mechanism is implicated in vascular angiogenesis and repair.

In many cases, NADPH oxidase activation is not only triggered by the phosphorylation of p47phox subunit, but also by the p47phox binding to other signaling molecules, such as TNF-receptor-associated factor 4 (TRAF4) during TNF*α* stimulation. This particular mechanism leads to a spatially restricted ROS synthesis targeting some specific MAPK proteins involved in TNF*α* signalling pathway.

An increase in ROS production by NADPH oxidase is involved in NFκB induced expression of adhesion molecules on endothelial cells surface by stimulation of cytokines or under condition of hypercholesterolemia (True *et al*., 2000).

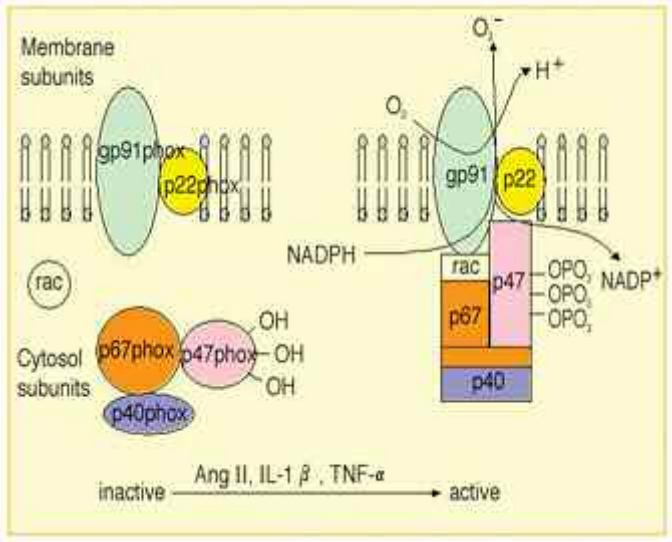

Fig. 6 Molecular composition and regulation of NAPH oxydase

1.2.5. ROS as signaling molecules in the vascular system

ROS have always been considered as toxic agents because of their oxidant properties leading to destructive modifications on different biomolecules, such as DNA, proteins, lipids and carbohydrates. On the other hand, evidence are about a role of ROS as signaling molecules involved in regulation of many intracellular pathways concerning to cell survival, growth, apoptosis and death. The mechanism through which

ROS act as signaling molecule is due to modification of redox sensitive proteins (Thannikal and Fanburg, 2000):

a. Formation of intramolecular disulfide linkages.
b. Protein dimerization by intermolecular disulfide linkages.
c. Dithyrosine formation by H_2O_2/peroxidases-dependent reactions.
d. Metal-catalyzed reaction oxidation of proteins by *Fenton*-like chemistry.

An alternative protein modification by which ROS exert their signalling function is protein S-glutathiolation**.** (Biswas *et al*, 2006) That is a GSH-dependent trapping mechanism wherein protein–SH are at the first oxidized to a thiyl radical or sulfenic acid as followed:

$$\text{Protein-}S^- + ROO^{\bullet} \longrightarrow \text{protein-}S^{\bullet}\ (\text{thiyl radical}) + ROO^-$$

$$\text{Protein-}SH^- + R^{\bullet}/HO^{\bullet} \longrightarrow \text{protein-}S^{\bullet}\ (\text{thiyl radical}) + RH/H_2O$$

$$\text{Protein-}SH^- + H_2O_2 \longrightarrow \text{protein-}SOH\ (\text{sulfenic acid}) + H_2O$$

and then they are converted to mixed disulfide adduct in conjunction with cellular GSH. This S-glutathiolation of proteins is a reversible mechanism that convert cystein proteins to an inactive state. In the absence of sufficient glutathione, partially oxidized protein cysteins may react with oxygen or other oxidants to produce irreversibly oxidized sulfinic and sulfonic acid species: this condition is associated with oxidative injury:

$$\text{Protein-}S + O_2 \longrightarrow \text{protein-}SO_2H/\text{protein-}SO_3H$$

- **Redox regulation of phosphorylation/dephosphorylation mechanism.** Protein-tyrosine phosphatases (PTPs) play an important role in the dynamics of cell regulation due to phosphorylation-dephosphorylation mechanisms during extracellular signalling (Choa *et al*, 2004). Phosphorylation of tyrosine residues of various target proteins have been recorded in response to cytokines and growth factors and have been found to be at least partly mediated by the generation of ROS, due to a redox regulation of PTPs. PTPs action is usually in equilibrium with the

action of protein tyrosine kinases, and both kind of proteins are involved in important cellular processes such as cell growth, proliferation and differentiation. PTPs contain an essential cystein residue in the active site. The cystein thiol group at neutral pH exist as thiolate anion, which forms a thiolate-phosphate intermediate in the catalytic mechanism of PTPs. In presence of physiological levels of ROS, the cystein thiol group can be reversibly oxidized to cystein-sulfenic acid (Cys-SOH) undergoin glutathiolation. This mechanism leads to a reversibly inhibition of PTPs activity with stabilization of phosphotyrosine moieties of the isozymes at conserved sites in the catalytic domain and phosphorylation-dependent signalling pathways are potentiated. This mechanism of redox regulation can activate Mitogen-Activated Protein Kinases (MAPK) cascades, leading to an activation of extracellular signal–regulated kinases (ERK), responsible for endothelial cell protection. Also PI3K-dependent pathways can be activated, with consequent activation of Akt, a protective kinase able to activate endothelial NOS by phosphorylation (see below), thus enhancing NO production (Choa *et al*, 2004).

- **GSH and thioredoxin: redox-sensitive systems.** This two proteins make part of two important antioxidant defence systems. In addition, they play an important role in cellular signaling depending on intracellular redox status. A reducing environment is necessary to maintain both GSH and Trx in a reduced active form. In endothelial cells it has been shown that decrease in GSH induces apoptosis and inhibit cell proliferation (Droge *et al*, 1994). It has been demonstrated that Trx has antiapoptotic properties, due to its capacity to inhibit proapoptotic proteins by binding them. Trx is a small multifunctional protein (Nordberg and Arnér, 2001) with two redox-active cysteines within a conserved active site (Cys-Gly-Pro-Cys). In reduced form this protein can bind some proteins through its –SH moiety, leading to their reversible block. A target of Trx is apoptosis signal-regulating kinase 1 (ASK-1), involved in the activation of the c-Jun N-terminal kinase (JNK) and p38 kinase, which are two stress-activated components of the MAPK system. Thioredoxin complex formation inactivates ASK-1 and this process is reversed by ROS production in response to TNF. In presence of ROS Cys-SH moiety of Trx undergoes oxidation, so that it can’t bind any other proteins. That is an example of ROS mediated modification of thiol groups. The evidence about Trx as a negative regulator of ASK-1 suggests possible mechanisms for redox regulation of apoptotic pathways (Saitoh *et al* 1998).

1.2.6. Molecular targets of ROS in vascular cells

ROS are normally produced in both endothelial and smooth muscle cells where they can be either mediators of physiological vascular functions, or inducers of vascular dysfunction (Irani, 2000). They can induce cell growth, arrest or promote cell survival or death, depending on both stimulus and cell type. What is determinant for ROS action under different cell stimulations are the subcellular localization of ROS productions, the kinetics of ROS productions and the amount of ROS produced within the cells.

A target of ROS are ERKs, which are members of MAPK family. In both smooth muscle cells and endothelial cells low levels of ROS activate ERKs, under the stimulation of growth factors: it has been shown that VEGF signalling in endothelial cells involves ROS-induced ERK activation leading to cell survival (Gupta et al, 1999).

Kinases belonging to the stress-activated protein kinase (SAPK) family, which include c-Jun N-terminal kinases (JNKs) and p38 MAPK regulated by small GTPases proteins such as Rac1, are also sensitive to redox modulation. In contrast to ERKs, JNKs and their downstream target c-Jun, have been implicated in H_2O_2 and other stress-induced apoptosis of endothelial cells (Wang et al, 1999). Moreover, p38 MAPK has been implicated in upregulation of ICAM-1 and, therefore, endothelial dysfunction, leading to a pro-atherosclerotic fenotype (Tamura *et al*, 1998). In smooth muscle cells, redox-sensitive activation of p38 MAPK mediates angiotensin II–induced hypertrophy (Ushio-Fukai, et al, 1998) and has also been implicated in cell migration (Hedges et al, 1999).

The transcription factor NF-kB is another target or ROS particularly ROS generated by a Rac1-regulated NADPH oxidase (Sulciner et al, 1996). In smooth muscle cells, costitutive activation of NF-kB has been reported to be essential for proliferation. In addition, Ang II–induced effects on vascular smooth mucle cells may also be mediated via NF-kB. In endothelial cells, NF-kB is a prime target for ROS, and its activation has been linked to endothelial cell dysfunction and survival.

Akt, a kinase involved in antiapoptotic pathways, is also activated by ROS. In smooth muscle cells Akt is regulated by ROS under Ang II stimulation. In endothelial cells, activation of Akt has been linked to the protective effects of shear stress and VEGF-induced growth and survival. In both vascular smooth muscle and endothelial cells, Akt activation pathway includes a Rac1-regulated, NADPH-dependent oxidase (Irani, 2000).

1.3. NO AS SIGNALING MOLECULE IN ENDOTHELIAL FUNCTION

Under physiological conditions, NO regulates vascular tone, provides anti-inflammatory activity and inhibits endothelial cell apoptosis by increasing intracellular concentration of cyclic GMP (as seen above). Increasing evidence suggests that cGMP-independent processes contribute to cellular signaling by NO. Specifically, S-nitrosylation of Cyst-SH groups has been recognized as an important mechanism involved in dynamic regulation of protein function (Porasuphatanaa *et al*, 2003).

These alternative mechanism can be mediated by different reactive nitrogen species (RNS) produced by reaction of NO with superoxide anion. RNS include nitrosonium cation (NO^+), nitroxyl anion (NO^-) or peroxynitrite ($ONOO^-$). If produced at high doses, in condition of oxidative stress, $ONOO^-$ can be highly toxic, due to its unspecific oxidant properties. Moreover high levels of RNS indicate that NO biodisponibility has decreased due to its completely reaction with ROS, affecting endothelial function. On the contrary, at low levels these species act as signaling molecules.

Apart from low molecular weight SNO molecules, such as *S*-nitrosoglutathione (GSNO), *S*-nitrosothiols are associated with high molecular weight proteins.

One mechanism of protein–NO adduct formation may involve transnitrosylation of proteins by low molecular weight S-nitrosothiols, such as GSNO, as shown by the following reaction:

$$\text{Protein-SH} + \text{RSNO} \rightarrow \text{protein-SNO} + \text{R-SH}$$

Other possible mechanisms of protein S-nitrosylation requires formation of either a reactive protein intermediate or some reactive low molecular weight species other than S-nitrosothiol (Biswas S *et al*, 2006):

(1) $\text{Protein-SH} + ONOO^- \rightarrow \text{protein-S}^\bullet + HNO_3$

$\text{Protein-S}^\bullet + NO^\bullet \rightarrow \text{protein-SNO}$

(2) $4NO^\bullet + O_2 \rightarrow 2N_2O_3$

$N_2O_3 + \text{protein-SH} \rightarrow HNO_2 + \text{protein-SNO}$

It has been recently demonstrated that redox regulatory activity of Trx is controlled by S-nitrosylation of its Cys-69 residue. At basal level Trx is S-nitrosylated at this site, and if this process is inhibited the antioxidant defence function of Trx (seen above) is destroyed, leading to an increase in intracellular ROS at high toxic level (Haendeler *et al*, 2002).

It has been shown that NO in cardiomyocytes exerts its antiapoptotic action by inhibiting caspase activity (Maejima *et al* 2005). Caspases are key regulator of apoptotic signaling pathway and generally they are divided into two category: initiator (caspase-8, -9) and executioner caspases (caspase-3, -6, -7). Under normal conditions, caspases exist as latent zymogens as procaspases, that can be cleaved into active forms via other activated caspases in the apoptotic process. In their active site, caspases have a cysteine residue, and the activity of the enzymes can be regulated by S-nitrosylation of that cystein residue. It has been demonstrated both *in vivo* and *in vitro* that caspase-3 can be inhibited by S-nitrosylation at cystein 163.

1.3.1. NO synthesis and eNOS regulation

Three isoforms of NOS have been identified. The neuronal NOS (nNOS o NOS1, 150 kDa protein encoded by NOS1 gene) principally expressed in neurons; the inducible NOS (iNOS or NOS2, 130 kDa protein encoded by NOS2 gene) expressed in endothelial cells in response to stimulation of cytokines under injury conditions; the endothelial NOS (eNOS or NOS3 135 kDa, protein encoded by NOS3 gene) expressed constitutively in endothelial cells, cardiac myocytes, and blood platelets. The three isoforms are highly homologous in their primary structure.

While iNOS is regulated only at transcriptional level, eNOS is highly regulated at both transcriptional and post-transcriptional level.

Each of the NOS isoforms is composed of both a reductase domain that is flavin-containing C-terminal with binding sites for FAD, FMN and NADPH, and a catalytic N-terminal oxygenase heme-containing domain with binding sites for L-arginine and 6-*R*-tetrahydrobiopterin (H_4B). These two domains are connected by a calmodulin (CaM)-binding domain.

During NO synthesis L-arginine is oxidized to L-citrulline, in a two step reaction. The first step involves the *N*-hydroxylation of L-arginine to N^{ω}-hydroxyl-L-arginine, while in the second step N^{ω}-hydroxyl-L-arginine is converted to L-citrulline and NO.

All three isoforms of NOS are functionally active as homodimer, so that electrons can pass from the reductase domain of one monomer, to the heme-oxigenase domine of the other monomer, leading to the concomitant reduction of molecular oxygen (O_2). Different stimuli can activate eNOS inducing its dimerization through mechanisms of post-traslational regulation involved in endothelial function (Fleming *et al*, 2003).

The enzyme is highly regulated by different proteins such as caveolin, heat shock protein 90 and eNOS interacting protein. Furthermore motor proteins regulate both the formation of the protein complex and its intracellular localization important in determining eNOS activity. All together, these regulatory proteins and activated eNOS form the so called eNOS signalling complex.

Intracellular calcium level is the main regulator of eNOS activation. The association of Ca^{2+}/CaM complex to the CaM-binding domain of eNOS triggers its activation facilitating the dimerization process, thus all stimuli increasing intracellular calcium (Ca^{2+}) levels activate the enzyme (Fleming *et al*, 2003).

Activation of eNOS is also dependent on the phosphorylation status of two critical aminoacids: a serine residue in the reductase domain (Ser^{1177}), and a threonine residue in the CaM-binding domain (Thr^{495}). At basal level Thr^{495} is usually phosphorylated, leading to an inactive state of eNOS. It is thought that the phosphorylated Thr^{495} interferes with the association of Ca^{2+}/CaM complex to the CaM-binding domain. Thr^{495} has to be dephosphorylated during activation of eNOS (Fleming *et al*, 2003). On the other hand the phosphorylation of Ser^{1177} occurs during eNOS activation and it's triggered by kinases such as Akt (Dimmeler *et al* 1999) after their association with eNOS signaling complex. Generally, stimuli elevating intracellular Ca^{2+} levels, such as bradykinin, histamine, and Ca^{2+} ionophores, lead to changes in the phosphorylation status of both Ser^{1177} and Thr^{495} facilitating the association of Ca^{2+}/CaM complex to the CaM-binding domain. These stimuli increase eNOS activity by 10- to 20-fold over basal levels. Growth factors and hormones usually activate eNOS exclusively increasing the phosphorylation of Ser^{1177}, triggering an increase in eNOS activity by two- to fourfold over basal levels (Fleming and Busse, 2003). On the other hand, it has been shown a correlation between eNOS activation by Akt phosphorylation and intracellular ROS production: at lower levels ROS can enhance the activation of Akt-eNOS complex, while at higher levels, associated with a decrease in GSH levels, ROS inhibit eNOS activation (Tanaka *et al*. 2005**)**

Another important aspect in the activation of eNOS is its subcellular localization. Normally when eNOS is not activated the two monomers are not associated and they are myristoylated and palmitoylated and thus can associate with intracellular membranes. Moreover, in the plasma membrane eNOS is mainly targeted to the caveolae where it is inhibited by binding to caveolin-1. Activating stimuli, after the binding of Ca^{2+}/CaM motif to the CaM binding site, can dissociate eNOS from cav-1, leading to activation of the enzyme after its translocation to distinct subscellular compartments. The selective movement of eNOS to different cellular compartments may be an essential step in determining the physiological outcomes of NO production (Fleming and Busse 2003).

The principal mechanisms of regulation of eNOS are represented in Fig. 7.

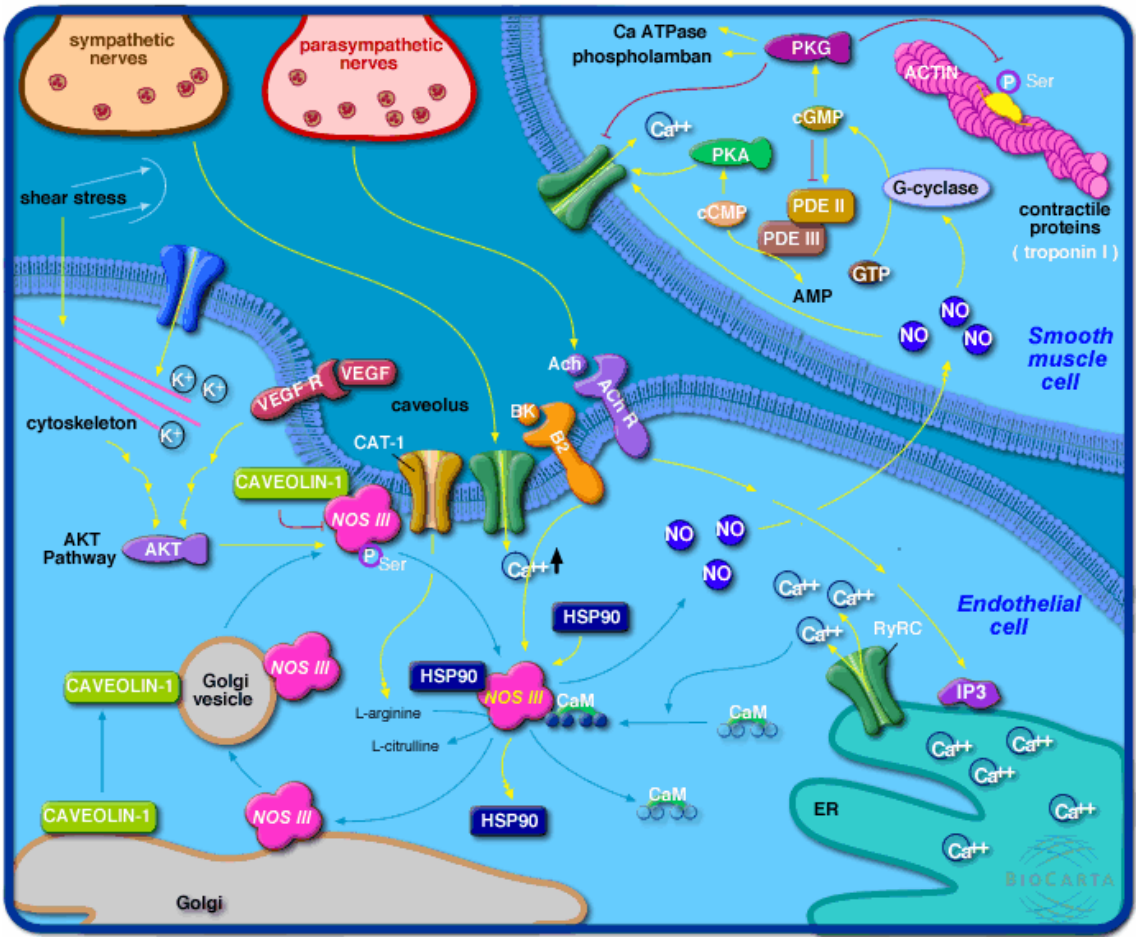

Fig. 7 Endothelial nitric oxide synthase (eNOS) regulation in response to endogenous stimuli, such as shear stress, acetylcoline (Ach) and sympathetic innervation.

1.4 ENDOTHELIAL DYSFUNCTION AND ATHEROSCLEROSIS

Atherosclerosis is a multifactor inflammatory disease characterized by the accumulation of cholesterol in large- and medium-sized arteries. This deposition leads to chronic inflammation state, infiltration of monocytes under the endothelium, proliferation of smooth muscle cells within the arterial wall inducing the formation of atherosclerotic plaque with progressive hardening of the arteries.

Hypercholesterolemia is a central pathogenic factor for atherogenesis and endothelial dysfunction and is one of the earliest events of atherosclerosis. One of the characteristics of endothelial dysfunction is impaired endothelium-dependent vasodilation.

Damages to endothelium are associated to many typical risk factors of atherosclerosis, such as smoke, lipid diet, hypertension, diabetes (Puddu *et al*, 2005).

It has been shown that ROS are involved in both initial and progressive development of atherosclerosis, enhancing a condition of oxidative stress. This lead to decrease in NO biodisponibility triggering to loss of endothelial function and alteration of vascular homeostasis.

Endothelial lesion leads to infiltration of Low-Density-Lipoproteins (LDL) under the endothelium leading to an oxidative stress condition in the *tunica intima*. This ROS overproduction triggers expression of both intercellular adhesion molecules (ICAM-1) and macrophages chemoattractant protein-1 (MCP-1) on the endothelial surface. Therefore, monocytes can adhere on endothelial cells and than migrate under the endothelium where they differentiate to macrophages.

Under condition of oxidative stress, different components of LDL can undergo oxidation, leading the formation of oxidized LDL (ox-LDL). Oxidation can occur at level of both lipid and protein components of the lipoproteins. Macrophages and smooth muscle cells possess the so-called scavenger receptors for ox-LDL.

Ox-LDL have been identified as the main factors involved in developing atherosclerosis due to their multiple actions against cardiovascular homeostasis, as reviewed by Puddu *et al*, in 2005:

- Ox-LDL induce leukocyte adhesion to endothelial cells, through the stimulation of many cytokines, such as TNF-α and interleukin-1 which in turn induce the surface expression of adhesion molecules.

- Ox-LDL can stimulate smooth muscle cells to proliferate, inducing the expression of basic fibroblast growth factor (bFGF) in both endothelial cells and smooth muscle cells, and to migrate, enhancing the expression of platelet-derived growth factor (PDGF) in endothelial cells. Ox-LDL act also as mitogen on smooth muscle cells, inducing the release of endothelin-1.
- Ox-LDL have also a pro-coagulant activity on the endothelium, by triggering platelet adhesion and aggregation and by decreasing prostacyclin (PGI_2) production.
- Ox-LDL stimulate apoptosis in endothelial cells, smooth muscle cells and macrophages leading to the formation of foam cells, and thereby contribute to plaque rupture. Evidence suggests that the pro-apoptotic action of ox-LDL is due to their capacity to decrease levels of protein S-nitrosylation in endothelial cells, triggerin activation of caspases (Hoffmann *et al*, 2001).

In vitro studies in endothelial cells by have demonstrated that high concentrations of oxLDLs (40 μg/ml) are cytotoxic but lower concentrations induce cell proliferation (Galle *et al*. 2001). This dual effect is mediated by different levels of ROS. In particular, ROS inducing cell proliferation are produced by NADPH oxidase (Heinloth *et al*. 2000) These results are in accord with the evidence about a dual role of ROS on endothelial cells. In fact it has been shown that treatment of endothelial cells with low doses of H_2O_2 leads to anti-apoptotic action, through the stimulation of thioredoxin expression (Haendeler J *et al*, 2004). Finally it has also been demonstrated that in human umbilical vein endothelial cells (HUVECs), both gp91phox expression and $O_2^{\bullet -}$ formation are increased by ox-LDL (Rueckschloss *et al*. 2001)

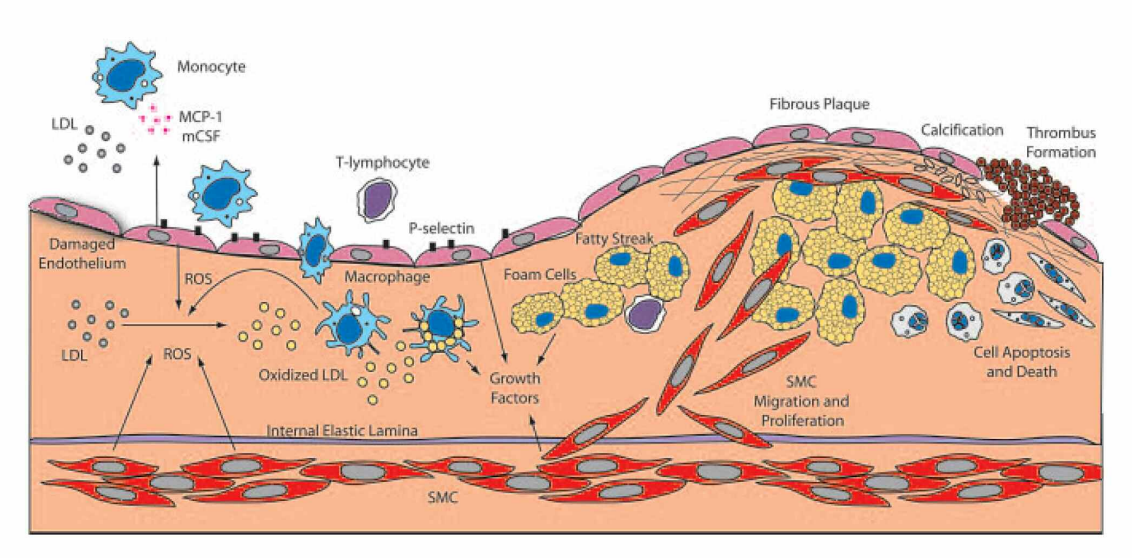

Fig. 8 Formation of atherosclerotic plaque.

1.5 OXYSTEROLS

Oxysterols are 27-carbon products of cholesterol oxidation (Fig. 9) which have been shown to possess many potent and diverse biological activities in vitro, several of which may implicate them in the initiation and development of atherosclerosis.

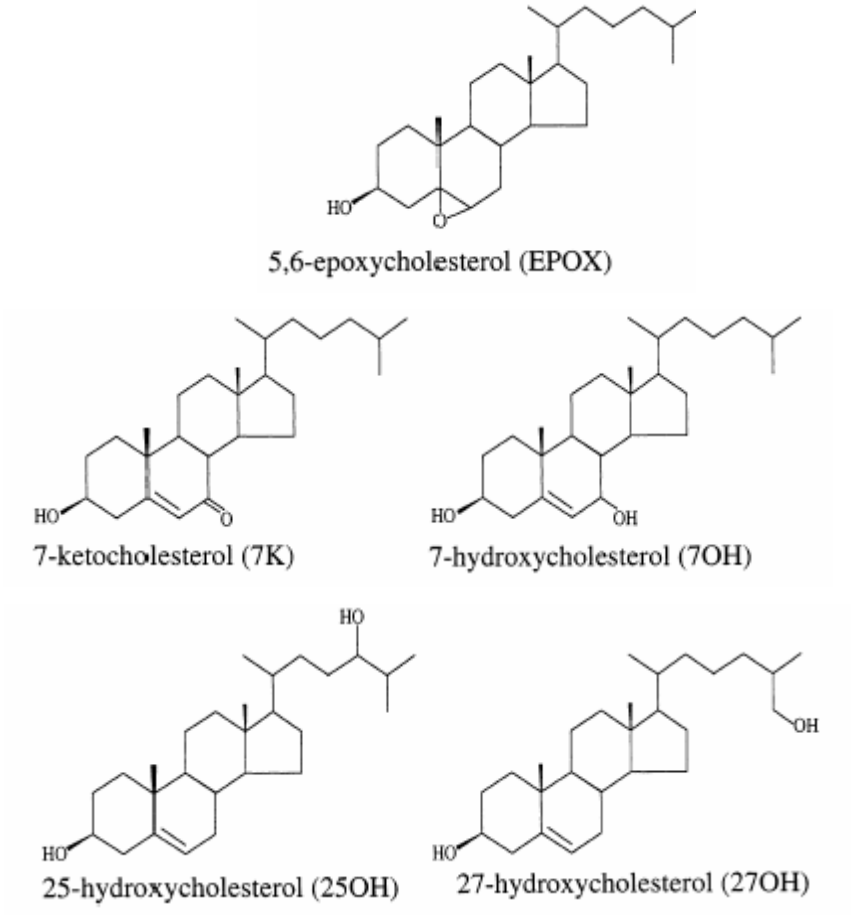

Fig. 9 Chemical structure of some oxysterols.

Oxysterols are mainly found in ox-LDL and the amount of total oxysterols in atherosclerotic plaque is much higher than in normal tissues or plasma, due to oxidative stress induced by inflammatory processes .

Oxysterols can be introduced also with diet, and then transported in chylomicrons. The most commonly detected oxysterols in foods are the major products of cholesterol autoxidation, such as 7-ketocholesterol (7-KC), 7 α-hydroxycholesterol (7α-OHC), 7 β-hydroxycholesterol (7β-OHC), 5, 6 α-epoxycholesterol (α-EPOX) and 5, 6 β -epoxycholesterol (β-EPOX) (Tai C-Y *et al*., 1999).

Some oxysterols can be formed directly *in vivo* as a consequence of both enzymatic processes and cholesterol autoxidation. Some of the most abundant oxysterols found *in vivo* are enzymatic products of cholesterol metabolism. For example, 7α -hydroxylation of cholesterol in the liver by the microsomal cholesterol 7α -hydroxylase (to produce 7α-OHC) was traditionally considered as the first and rate-limiting step in bile acid synthesis (Leonarduzzi *et al*., 2002).

In cells oxysterol esters are present in the same low-density cytosolic cell fraction as cholesteryl esters: this is due to oxysterol esterification triggered by acyl coenzyme A: cholesterol acyltransferase (ACAT) activity leading to cellular oxysterols uptake (Guardiola *et al*., 1996).

Cytotoxicity of oxysterols to many cell types has been widely reported including vascular cells such as endothelial cells, macrophages, smooth muscle cells and lymphocytes. Death of any of these cell types might promote atherogenesis. Smooth muscle cell death is also associated with aneurysm development. Moreover, oxysterols have been demonstrated to have a proapoptotic action on endothelial cells, associated with an increase in intracellular ROS production (Hodis *et al*., 1991).

The most extensively studied oxysterols in vitro are 25-OHC, the 7-oxygenated series and 27-OHC. Generally, in atherosclerotic tissues 27-OHC is more concentrated than 7-oxygenated sterols which in turn are more concentrated than 25-OHC (Brown and Jessup, 1999).

Cholesterol is ubiquitously present in mammalian tissues and is essential for the formation and function of cellular membranes. Since oxysterols are thought to be involved in the regulation of cholesterol homeostasis, they could influence membrane function, synthesis of steroid hormones and bile acids and cell growth and proliferation. Several oxysterols, especially those hydroxylated on the side-chain, such as 25-OHC, have been shown to exert inhibitory effects on the activity of HMG-CoA reductase, an enzyme which converts HMG-CoA to mevalonate, the rate limiting step in the cholesterol biosynthetic pathway (Schroepfer *et al*., 2000). Thus, cells may form oxysterols in order to facilitate the elimination of excess cholesterol. Inhibition of HMG-CoA reductase in actively dividing cells could result in deficient cholesterol synthesis and impaired membrane function. Studies have suggested that this inhibitory effect is due to a reduction in de novo synthesis of HMG-CoA reductase as well as stimulation of its degradation. Oxysterols can modify the activity of different enzymes related to sterol metabolism like acetoacetyl CoA thiolase (ACAT), cholesterol 7a-

hydroxylase, cholesterol-5,6-epoxide hydrolase, HMG-CoA synthase, methylsterol oxidases and mevalonate kinase (Guardiola *et al.*, 1996).

1.5.1 Oxysterols as ligands of LXRs.

As intermediates of cholesterol metabolism, oxysterols have a biological role in maintaining cholesterol homeostasis. At physiological concentrations, oxysterols are natural ligands of Liver X receptors (LXR), which are members of the nuclear receptor superfamily playing a critical role in cholesterol homeostasis and lipid metabolism. There is considerable evidence indicating that LXR function as whole body cholesterol sensors. Concerning with this physiological role, the endogenous ligands for LXRs are likely to be intermediates or end products of sterol metabolic pathways. Both LXRα and LXRβ are activated by physiological concentrations of sterol metabolites such as 22(R)-hydroxycholesterol, 24(S)-hydroxycholesterol, 27-hydroxycholesterol, and 24(S), 25-epoxycholesterol. The two LXR forms share considerable sequence homology and appear to respond to the same endogenous ligands. These proteins contain a zinc finger DNA-binding domain and a ligand-binding domain which accommodates specific small lipophilic molecules. Ligand binding triggers a conformational change that promotes interaction with coactivator proteins and facilitates the activation of specific target genes. LXRs bind to their target DNA sequences in heterodimeric complexes with the retinoid X receptor (RXR). LXR/RXR is a so-called permissive heterodimer which can be activated by ligands for either LXR or RXR. It has been shown that LXRα null mice exhibit dramatically increased plasma LDL cholesterol and decreased HDL cholesterol levels (Tontonoz *et al*, 2003).

LXR activation induce the expression of different genes involved in cholesterol metabolism as shown in table I (Edwards *et al* 2002).

Target gene	Humans (H)/Mice (M)	Function
SREBP-1 FAS	H, M H, T	Synthesis of fat acids
CYP7A1 ApoE	H H, M	Clearance of cholesterol
LXRα	H	Control lipid homeostasis
CETP LPL	H, M H, M	Triglycerids metabolism
ABCA1 ABCG1	H, M H, M	Efflux of phospholipids and/or cholesterol
ABCG5 ABCG8	H H	Efflux of cholesterol/phytosterols
ABCG4	H	Not known

Table I. Genes regulated by the activation of Liver X receptors (LXR). SREBP-1 = sterol regulatory element binding protein; FAS = fatty acid synthase; CYP7A1= cytocrome P450 isoform; ApoE = apolipoprotein E; LXR α= liver X receptor α; CETP= cholesteryl ester transfer protein; LPL= lipoprotein lipase; ABCA1= ATP-binding cassette transporter A1; ABCG = ATP-binding cassette, subfamily G (Edwards *et al* 2002).

1.5.2 Oxysterols and atherosclerosis

At physiological levels the main oxysterols found in the blood are 27-OHC, 24-OHC and 7*α*-OHC and they are present at nanomolar concentrations (Schroepfer, 2000). Higher plasma concentrations of oxysterols have been found in patients with cardiovascular diseases and particularly high plasmatic levels of both 7*β*-OHC and 7-KC have been associated to the development of the atherosclerotic plaque (Zhou *et al*., 2000).

Oxysterols are present in the vascular wall, mainly during atherogenesis. 7*β*-OHC and 7-KC are more abundant than other oxysterols during the early formation of atherosclerotic plaque when the accumulation of both LDL and macrophages occurs under the endothelium (Brown and Jessup, 1999). It has been shown that during atherogenesis high levels of oxysterols are in macrophages, leading to the activation of

macrophage NADPH oxidase. Thus, ROS overproduction triggers LDL oxidation (Rosenblat and Aviram, 2002). These events lead to inflammatory processes and then macrophages are induced to die becoming foam cells. All these events lead to development of atherosclerosis (Peng *et al*., 1985).

Both *in vivo* and *in vitro* studies have demonstrated the cytotoxicity of oxysterols in endothelial cells, smooth muscle cells and macrophages. Exposure of the vasculature to these compounds leads to endothelial dysfunction, inducing platelet aggregation, leucocyte adhesion and smooth muscle cells proliferation (Peng *et al*., 1985).

1.5.3 Oxysterols and apoptosis

There is evidence about the capacity of oxysterols to induce cell death. Normally there are two major apoptotic pathways, known as the extrinsic, or death receptor pathway and the intrinsic, or mitochondrial pathway. In vascular cells oxysterols have been shown to induce apoptosis. In vascular smooth muscle cells 7β-OHC and 25-OH upregulated the expression of death mediators, p53, Fas and Fas ligand, tipically involved in the extrinsic apoptotic pathway (Lee and Chau, 2001).

The second major apoptotic pathway, the intrinsic pathway, is mediated by mitochondrial release of proapoptotic molecules. Perturbation of the mitochondria results in the opening of the mitochondrial permeability transition pore (MPTP), a non-specific pore in the inner mitochondrial membrane thought to open under conditions of elevated calcium concentration. Opening of the MPTP causes a massive swelling and depolarisation of the mitochondria, a condition referred to as the mitochondrial permeability transition (MPT). The MPTP, once opened, is thought to play a role in apoptosis through the release of proapoptotic molecules such as cytochrome c, Smac/DIABLO (second mitochondrial activator of caspases/direct IAP-binding protein of low isoelectric point -pI) and apoptosis inducing factor (AIF). Once released, cytochrome c interacts with apoptotic protease-activating factor-1 (Apaf-1), ATP/dATP and recruits pro-caspase-9 to form the apoptosome. Active caspase-9 in turn cleaves and activates caspase-3, leading to the morphological and biochemical changes characteristic of apoptosis. Smac/DIABLO may promote caspase activation by binding to inhibitor of apoptosis proteins (IAPs) and directly eliminating IAP inhibition of caspases. The ability of oxysterols to induce apoptosis through the intrinsic pathway has been well studied. It was found that 7β-OHC and 7-KC induce apoptosis in U937 cells via loss of mitochondrial potential, caspase-3 activation, PARP degradation and DNA

fragmentation. Both oxysterols were also found to enhance superoxide anion ($O_2^{\bullet -}$) production before and after the loss of mitochondrial potential. It has been reported that in U937 cells 7*β*-OHC-induced apoptosis involved a decrease in glutathione levels followed by activation of caspase-9, caspase-3 (Miguet-Alfonsi *et al*., 2002). On the other hand, 7-KC has been shown to induce apoptosis via release of cytochrome c from mitochondria with subsequent caspase-9 and caspase-3 activation in a variety of cell lines.

There is experimental evidence about effects of oxysterols on different regulators of apoptosis:

- **Bcl-2 Family.** Bcl-2 proteins are crucial regulators of apoptosis. On the basis of function and sequence similarity they can be divided into three groups. Proteins belonging group I (Bcl-2/Bcl-XL/Bcl-w/Mcl-1/A1/Bfl 1) inhibit apoptosis by binding to and sequestering proapoptotic Bcl-2 family members. Group II includes Bax and Bak, promoters of cell death, whose activity is necessary to induce cytochrome c release from the mitochondria. Group III is comprised of proapoptotic proteins (Bid/Bad/Bik/Bim) which translocate from the cytosol to the mitochondria, in response to apoptotic stimuli, and then activate Bax or Bak to induce the release of apoptogenic mitochondrial proteins. It has been shown that both 7-KC and 7*β*-OHC induce apoptosis, in U937 cells, by downregulation of Bcl-2 protein (Lizard G *et al* 1997). Similar results were found in smooth muscle cells, after treatment with either 7-KC or 25-OHC (Harada K *et al,* 1997).
- **Caspases**. Caspases are a family of cystein proteases that are the primary drivers of apoptosis. All caspases are present as inactive precursors in cells that must be proteolytically cleaved in order to be activated. Each caspase consists of a pro-domain, a large (~20 kDa) subunit and a small (~10 kDa) subunit. Cleavage and subsequent heterodimerization of the larger and smaller subunits result in caspase activation (Robertson JD *et al*., 2000). An active caspase can cleave and activate other caspases leading to a caspase cascade and ultimately cell death. To date, a number of mammalian caspases have been identified. Based on the length of their pro-domain caspases can be divided into two distinct groups: group I that contain a relatively long pro-domain (caspases -1, -2, -4, -5, -8, -9, -10, -11, -12, -13) and group II containing a short pro-domain (caspases -3, -6, -7, -14). Caspases -1, -4, -5, -11, -12 and -14 are primarily involved in cytokine processing (Slee EA *et al* 1999). Many group I caspases are initiator proteases (caspases -2, -8, -9, -10),

activated with the help of adaptor molecules such as Apaf-1 and FADD/MORT1. Group II caspases (not including caspase-14) are also known as effector caspases. They lack the ability to self-activate and appear to require cleavage by activated initiator caspases (Kumar S., 1999). Once activated, caspases cleave various proteins leading to the biochemical and morphological features characteristic of apoptosis. Both 7*β*-OHC and 7-KC can induce apoptosis in U937 cells by activating caspase cascade, in association with loss of mitochondrial potential (Miguet-Alfonsi C *et al*, 2002).

- **Oxidative stress**. In some experiments it has been shown that 7*β*-OHC-induced apoptosis in U937 is associated with a decrease in intracellular glutathione (GSH) levels, with an increase in the activity of superoxide dismutase (SOD) and with a decrease in intracellular nitric oxide production. It has been demonstrated that 7-KC-induced apoptosis in U937 cells, similarly to 7*β*-OHC, involved a decrease in GSH levels and production of ROS (Lizard G *et al*, 1998).

2. AIM

Oxidized low density lipoproteins (oxLDLs) are mainly involved in the pathogenesis of atherosclerosis. *In vitro* studies (Galle *et al*. in 2001) in endothelial cells have demonstrated that high concentrations of oxLDLs (40 μg/mL) are cytotoxic whereas lower concentrations induce cell proliferation. This dual effect is mediated by different levels of ROS coming from NADPHox activation. A large body of evidence shows that low concentrations of ROS act as signalling molecules and regulate vascular cell functions, while sustained ROS levels are cytotoxic and are implicated in the pathogenesis of various cardiovascular diseases (Thannickal and Fanburg, 2000).

Cytotoxicity of oxLDLs has been linked to the formation of oxysterols (Schroepfer *et al*, 2000) such as 7-KC and 7β-OHC. Evidence on the proapoptotic effect of oxysterols on vascular cells has been reported (Lizard *et al*, 1999). It was also demonstrated that 7-KC-induced apoptosis involves both ROS production and decrease in GSH levels, an important antioxidant defence system, (Lizard *et al.* 1998). Moreover, it has been shown that proapoptoic action of 7-KC is due to loss of mitochondrial membrane potential, with cytocrome c release and all these events are prevented by antioxidants (Lizard *et al*, 2000). All these findings indicate an important role of ROS in the effects of oxysterols.

Preliminary studies from our laboratory indicate that 7KC and 7β–OHC, like oxLDLs, posses a dual effect on HUVEC viability. They induce cell death at high concentrations ($\geq$ 20 μg/mL), while they induce an increase in cell viability at lower concentrations (< 20 μg/mL).

The aim of this work was to determine the mechanism involved in the protective effects of the oxysterols on HUVEC, in particular for 7β–OHC, whose effects are more relevant than 7KC. Considering the involvement of ROS in the action of both oxLDL and oxysterols in vascular cells, the role of ROS in the mechanism of action of 7β–OHC was investigated.

.

3. MATERIALS AND METHODS

3.1 CHEMICALS

M199 and DMEM media, fetal bovine serum (FBS), basic fibroblastic growth factor (bFGF), trypsin, penicillin/streptomycin solution, 7*β*-hydroxycholesterol (7*β*-OHC), 7-ketocholesterol (7-KC), 3-(4,5-dimethylthiazol-2-yl)-2,5-diphenyltetrazolium bromide (MTT), sulfanilamide, N-1-napthylethylendiamine dihydrochloride, rotenone, tenoytrifluoroacetate (TTFA), cyanide m-chlorophenylhydrazone (CCCP), hydralazine, N-acetylcysteine (NAC), N-Nitro-L-Arginine Methyl Ester (L-NAME) and solution of propidium iodide (IP, 1.5 mM), were from Sigma. Solution of annexin-V conjugated with the fluorophore Alexa Fluor 488, fluorescent dye 5-(-6)-cloromethyl-2',7'-dichlorodihydrofluoresceinadiacetate acetylester (CM-H_2DCFDA) and EnzChek Caspase-3 Assay Kit #2 were from Molecular Probes. Type 2 Collagenase was from Worthington. Mouse monoclonal IgG_{2a} antibody to phosphorylated ERKs (phospho-ERK-1 and phospho-ERK-2) and rabbit polyclonal IgG to overall ERKs (ERK-1 and ERK-2) were purchased from Santa Cruz.

MTT was dissolved in phosphate-buffered saline solution (PBS, 137 mM NaCl, 2.7 mM KCl, 8.1 mM Na_2HPO_4, 1.8 mM KH_2PO_4) at concentration of 5 mg/mL and stored at + 4°C. Both 7*β*-OHC and 7-KC were dissolved in ethanol at concentration of 5 mg/mL. Hydralazine was always freshly dissolved in water (25 μM). Solutions of rotenone, TTFA and CCCP were freshly prepared in dimethylsulfoxide (1 mM). NAC was freshly dissolved in water (1 mM). Staurosporine was dissolved in methanol (500 μM) and stored at -20°C. L-NAME was dissolved in water at 100 mM concentration. CM-H_2DCFDA was dissolved in dymethylsulfoxide (10 mM) and stored at -20°C. Annexin-V and IP were stored at + 4-8°C. Collagenase was dissolved freshly just before use in PBS without Ca^{2+} and Mg^{2+} at concentration of 1 mg/mL.

3.2. METHODS

3.2.1. Extraction of endothelial cells from human umbilical vein

HUVEC were isolated in our laboratory as described by Jaffe *et al*. (1973). Human umbilical cords were obtained at normal delivery or caesarean section.

Experimental protocol

1. Immediately after delivery, the cords were placed into sterile MEM solution containing penicillin (400 U/ml) and streptomycin (400 μg/mL), and kept at 4°C;
2. the umbilical vein was cannulated with a cannula (Scalp Vein Set 19G), which was then clamped into place. The vein was washed with 20 ml of MEM (prewarmed to 37 °C) to remove any blood clots,
3. one end of the cord was clamped and the opposite end was infused with 0.1% (w/v) collagenase type 2;
4. the cord was then incubated at 37 °C in an atmosphere of 5% CO_2/95% air;
5. after 18 min the cord was removed and the contents of the cord were flushed out with 20 ml of MEM with 20% (v/v) FBS;
6. cell suspension was collected and centrifuged at 500 x g for 5 min. Cells were resuspended in 5 ml of M199 containing 20% (v/v) FBS with 2% (v/v) antibiotics solution (penicillin 400 U/ml and streptomycin 400 μg/ml) and plated into one 75 cm flask. This flask was then incubated at 37 °C in an atmosphere of 5% CO_2/95% air.

After one day HUVEC were washed with 2 ml of MEM to remove any blood, contaminant cells and cell debris. The medium was replaced with a further 5 ml of M199 containing 10% (v/v) FBS, 5 ng/mL bFGF, 25 U/mL heparin, 4mM l-glutamine, 100 U/mL penicillin-G and 100 μg /mL streptomycin.

3.2.2. Cell culture

HUVEC were grown on 1% (v/v) gelatin-coated culture flasks in M199 containing 10% (v/v) fetal bovine serum (FBS), 5 ng/mL bFGF, 25 U/mL heparin, 4mM l-glutamine, 100 U/mL penicillin-G and 100 μg/mL streptomycin. HUVEC were used from passages two to six. All the experiments were conducted with different preparations of endothelial cell.

A7r5 (cell line of vascular smooth muscle cells from rat embryo aorta) were from "Istituto Zooprofilattico Sperimentale" (IZS) of Brescia (Italy). They were grown in DMEM containing 10% (v/v) FBS, 2 mM l-glutamine, 100 U/mL penicillin-G and 100 μg/mL streptomycin.

3.2.3. Cell treatments

HUVEC: After trypsinization, cells were plated into 96, 12 or 6 well plates coated with gelatin 0.5% with M199 containig bFGF (5 ng/mL). Treatments with oxysterols at indicated concentrations and time were performed in bFGF deprived M199 medium (10% FBS).

A7r5: cells were trypsinized and plated into 96 well plates with DMEM containing 10% FBS. Treatments with oxysterols at indicated concentrations and time were performed in DMEM without FBS containing BSA 0.5%.

For both HUVEC and A7r5, control cells were treated with the medium containing ethanol 0.4%.

3.2.4. Measurement of cell viability with MTT test

MTT (3-(4,5-dimethylthiazol-2-yl)-2,5-diphenyltetrazolium bromide) test is based on the capacity of viable cells to reduce MTT to blue formazan (Fig. 10). MTT is soluble in aqueous solution, and can enter cells by endocytosis. Then it is reduced by different intracellular flavin enzymes. Blue formazan in soluble in organic solvent such as dimethyl sulfoxide (DMSO).

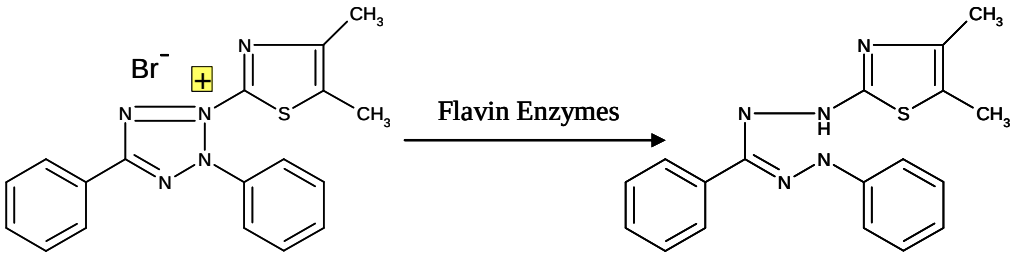

3-(4,5-dimethylthiazol-2-yl)-2,5-diphenyltetrazolium bromide (MTT)

blu-formazan

Fig 10. Reduction of (3-(4,5-dimethylthiazol-2-yl)-2,5-diphenyltetrazolium bromide (MTT) to blue Formazan

Experimental protocol

1. sub-confluent cells were plated in 96-well plate (10000 HUVEC/well, 5000 A7r5 cells/well);
2. cells were treated with 100 μL of cell culture medium containing either 7β-OHC or 7-KC at different concentrations (1, 5, 10, 20 μg/mL) for 24 hours. HUVEC were treated in M199 medium without bFGF, and A7r5 were treated in DMEM medium containing 0,5% (w/v) BSA. Cells treated with ethanol 0.4% were used as control. The only medium was used as blank;
3. 10 μL of MTT (5 mg/mL) was added to treated cells, control and blank samples 4 hours before the end of the treatment,
4. at the endo of treatment, medium was removed and 100 μL DMSO were added to each well to dissolve formazan crystals.
5. absorbance was measured at 570 nm 630 nm with a microplate reader (VICTOR^2, Wallak).

Data elaboration

1. Absorbance values of blank were subtracted to values of related samples to avoid background signal interference;
2. difference between values at 570 and 630 were calculated;
3. results were expressed as percentage of MTT reduction with respect to control.

3.2.5. Flow cytometric analysis of annexin-V and propidium iodide binding

Cells have an asymmetric composition of membrane bilayer, due to different location of phospholipids: neutral phospholipids are exposed on the extracellular side of the membrane, while negative charged phospholipids, such as phosphatidylserine, are exposed on the cytoplasmatic side of the membrane.

An early event in cells undergoing apoptosis is translocation of phosphatidylserine from the inner to the outer side of the membrane. Annexin-V is a peptide able to bind selectively phosphatidylserine in presence of Ca^{2+}, thus binding to apoptotic cells. This event delivers apoptotic cells to be removed from the healthy tissues by physiological scavenger mechanisms.

Annexin-V binding on cell surface is a widely used parameter to detect apoptotic events. For this purpose, annexin-V is conjugated to fluorochromes such as fluorescein derivatives. The signal of annexin-V conjugate is proportional to the amount of apoptotic cells (Fig. 11).

Propidium iodide (PI) is used as marker of necrotic cells. This is a fluorescent dye which enters cells with broken membrane and binds quantitatively DNA. The signal of PI is proportional to the amount of necrotic cells.

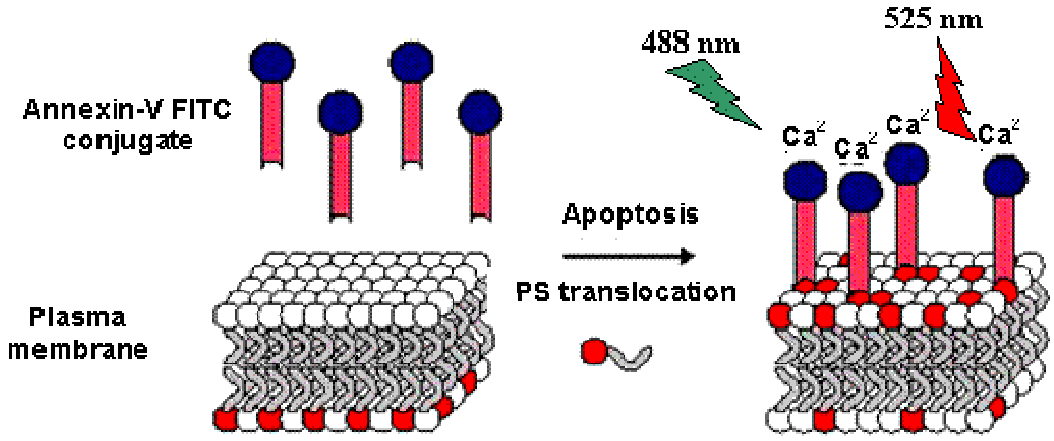

Fig. 11 Schematic representation of the annexin-V assay

Experimental protocol:

1. After cell treatment, the medium of each sample was collected;
2. after trypsinization, cells were collected by centrifugation (500 x g, 10min) and resuspended in 100 μL of calcium containing binding buffer (140 mM NaCl, 2.5 mM $CaCl_2$, 10 mM HEPES/NaOH, pH 7.4);
3. cells were labelled in suspension with both 2 μL annexin-V Alexa Fluor 488 conjugated solution and 1.25 μL PI solution. After that, cells were incubated in the dark for 15 min, at room temperature. Blank sample was used to determine background signal due to autofluorescence of cells;
4. cell suspension was diluted with 400 μL binding buffer (140 mM NaCl, 2.5 mM $CaCl_2$, 10 mM HEPES/NaOH, pH 7.4) to obtain a cell density not higher than 10^6 cells/mL;
5. cells were analyzed flow cytometry using excitation wavelength of 488 nm and emission wavelength of 525 and 620 nm for annexin-V and PI respectively (EPICS XL, Beckman Coulter equipped with EXPO^{TM} 32 ADC software). For each sample, 10,000 events were collected.

Data elaboration

Results are plotted in a two dimensional scatter plot, reporting PI fluorescence on y axe and annexin-V conjugate fluorescence on x axe (Fig. 12).

Cell population was defined on the basis of forward and side scatter properties. Viable cells are collocated in the left quadrant on the bottom (P3) of the graphic. Annexin-V positive cells are collocated in the right quadrant on the bottom (P4). PI positive cells are represented in the left quadrant on the top (P1) of the scatter plot. Double stained cells are in the right quadrant on the top (P2).

To quantify apoptosis for each treatment, results were expressed as percentage of annexin-V positive cells.

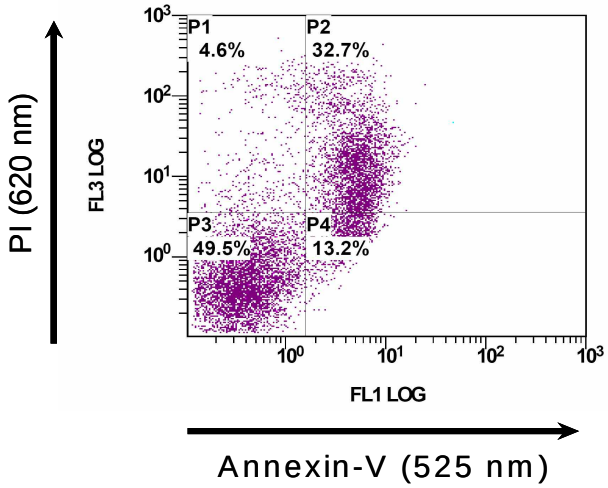

Fig. 12 Two dimensional scatter plot of results from the cytofluorimetric analysis of the binding of annexin-V and propidium iodide (PI) to determine cell apoptosis.

3.2.6. Determination of of caspase-3 activation

The EnzChek Caspase-3 Assay Kit #2 provides a simple and reliable method for assaying caspase-3 activity. The basis for the assay is the rhodamine 110-derived substrate Z-DEVD-R110. This substrate is a nonfluorescent bisamide that is first converted by caspase-3 to the monoamide and then to the bright, green-fluorescent rhodamine 110 (excitation/emission maxima ~496/520 nm, Fig. 13).

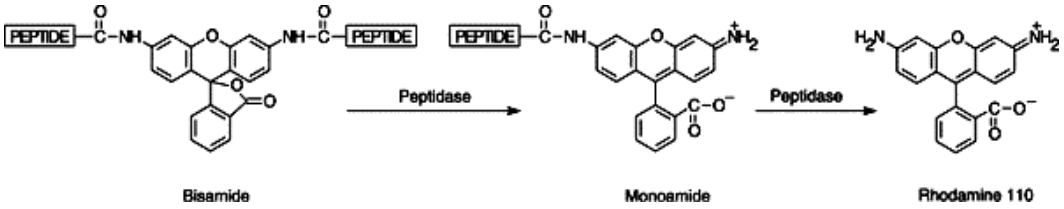

Fig. 13. Sequential cleavage of a peptidase rhodamine 110–based substrate. The nonfluorescent bisamide substrate is first converted to the fluorescent monoamide and then to the highly fluorescent rhodamine 110.

Experimental protocol

1. After the treatment of the cells (300,000 HUVEC in 6-well plate, the media was removed and the cells were wash twice with PBS;
2. HUVEC were scraped into 200 µl lysis buffer (100 mM NaCl, 1 mM Tris, 1 mM EDTA, 0,01% Triton X-100, pH 7.5) on ice and were centrifuged at 12000 x g for 20 minute at + 4 °C;
3. the clear supernatant was transfered to a new tube and kept on ice;
4. the protein content of the supernatant was measured with Lowry procedure;
5. in a microplate (1508-0010 Black 96-well microplate, PerkinElmer) 50 μl reaction buffer (20 mM PIPES, 4 mM EDTA, 0.2% CHAPS, 10 mM DTT, pH 7.4) with caspase substrate (50 μM) was added to 50 μl cell lysate. The blank controls (50 μl reaction buffer with caspase substrate and 50 μl lysis buffer) showed the background absorbance and were subtracted from the experimental readings;

6. the microplate was incubated at room temperature for 30 minutes. Fluorescence was measured at 485 nm for excitation and 535 nm for emission with a multilabel plate counter (VICTOR^2-Wallac).

Data elaboration

Fluorescence signal was normalized to the protein content of the related sample. Caspase activity was expressed as percentage with respect to control.

3.2.7. Determination of intracellular ROS production

To determine intracellular ROS production, the fluorescent probe Chloromethyl-dichlorodihydrofluoresceindiacetate (CM-H_2DCFDA) was used. Diesterified probe can enter cells by simple diffusion across membrane. Once diffused in both cytoplasm and different organelles, the ester moieties are idrolized and the fluorescent dye is entrapped inside cells. Then, the probe can be oxidized, preferentially by hydrogen peroxide (H_2O_2), into the dehydrogenated form with excitation wavelength of 480 nm and emission wavelength of 530 nm (Fig. 14). Fluorescence signal is an index of intracellular ROS levels.

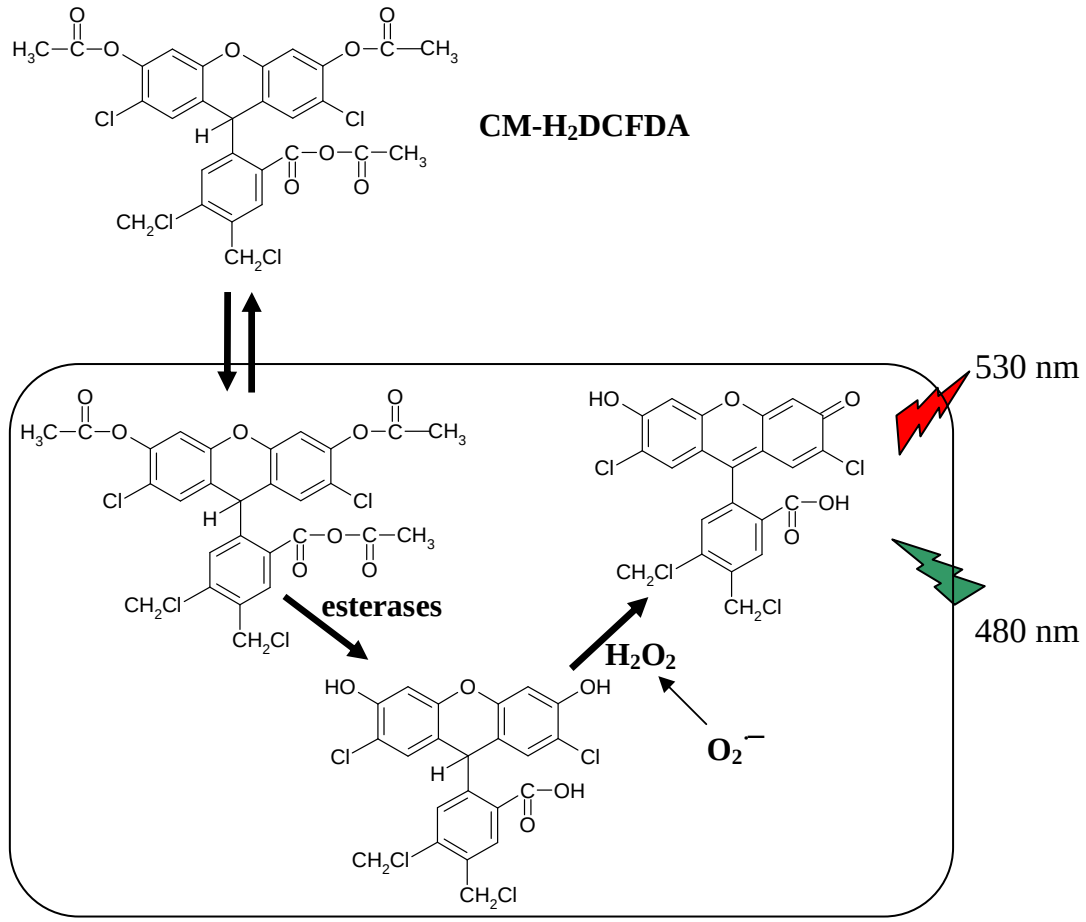

Fig. 14 Schematic representation of ROS detection with the fluorescent dye Chloromethyl-dichlorodihydrofluoresceindiacetate (CM-H_2DCFDA).

Experimental protocol

1. Cells were plated in 96 well plates at confluence (20000 HUVEC/well, or 10000 A7r5 cells/well);
2. cells were put to quiescence for 4 hours before the experiments: HUVEC were bFGF deprived and A7r5 cells were incubated in medium containing 0.5% (w/v) BSA;
3. cells were than washed three times with physiological salt solution (PSS, 140 mM NaCl, 11.5 mM glucose, 5.9 mM KCl, 1.8 mM $CaCl_2$, 1.4 mM $MgCl_2 \cdot 6H_2O$, 1.2 mM NaH_2PO_4, 5 mM HEPES, pH 7.4) and loaded with CM-H_2DCFDA (20 μM in PSS) for 30 min at 37°C;

4. than cells were incubated in PSS containing either 10% (v/v) FBS (HUVEC) or 0.5% (w/v) BSA (A7r5) for 15 min at 37°C.
5. cells were washed again with PSS to remove extracellular traces of the probe and then treated with different concentrations (1, 5, 10, 20 μg/mL) of either 7-KC or 7β-OHC. Treatments were performed in 100 μL PSS containing either 10% (v/v) FBS or 0,5% (w/v) BSA for HUVEC or A7r5 respectively;
6. fluorescence was measured with a microplate reader (VICTOR^2, Wallak). Fluorescence was detected in time course at 10 min intervals for either 3 or 4 hours for HUVEC or A7r5 respectively.

Data elaboration

Average of fluorescence values of blank samples was subtracted to each measurement, to remove background signal.

Fluorescence was expressed as percentage of the basal signal measured at time zero.

3.2.8. Determination of NO production by the Griess reaction

NO are partially converted by oxidation to nitrite (NO_2^-) and nitrate (NO_3^-), two products detectable in the culture medium as index of intracellular NO production.
The Griess Reaction method is based on the chemical reaction shown in Fig. 4, which uses sulfanilamide (SULF) and N-1-napthylethylenediamine dihydrochloride (NEDD) under acidic (chloride acid) conditions converting NO_2^- to an azo-compound. The azo-compound has a maximum of absorption between 520-550 nm (Fig. 15).

To detect also NO_3^- concentrations, is necessary to convert it into NO_2^- by previous reduction.

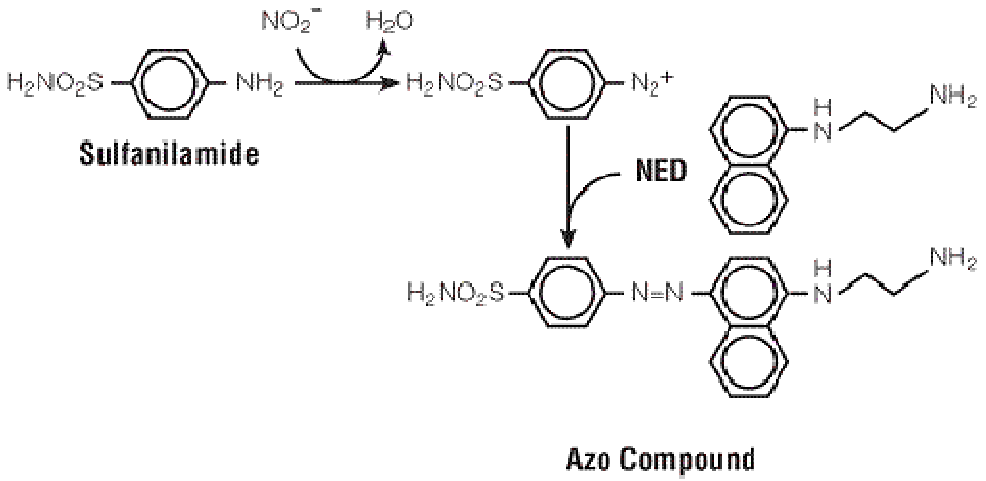

Fig. 15 Reaction of formation of the azo-compound to detect nitrite with the Griess method.

Experimental protocol

1. Medium from 24 hours treatment of HUVEC with different concentration (5, 10 μg/mL) of 7β-OHC was collected (at least 500 μL);
2. the medium was centrifuged (13000 x g, 10 min) to eliminate cell debris and any membrane component;
3. a standard curve was prepared for each experiment with standard solutions of NO_2^- at known concentrations (0-100 μM). These solutions were prepared in the same medium of treatment;

4. 50 μL of each sample or standard was pipeted in 96 well plates in duplicate;
5. the reaction mix was freshly prepared as follow (mix for each well):

   - 40 µL VCl_3 (saturated solution in HCl 1 M)
   - 10 µL SULF (1% w/v in HCL 1 M)
   - 10 µL NEDD (0,1% w/v in HCL 1 M)

   VCl_3 is a reducing agent which converts NO_3^- to NO_2^- to detect total nitrites;
6. 60 μL of reaction mix was added to each sample or standard;
7. the plate was incubated at 37°C, 5% CO_2, for 30 min;
8. after incubation, absorbance was determined at 550 nm in a microplate reader (VICTOR^2, Wallak).

Data elaboration

NO production was expressed as micromolar concentration of total nitrite.

3.2.9 Western blotting analysis

Cell lysates of HUVEC: after treatment, the cells were washed twice in the dish with ice-cold PBS and than PBS was drained off with a syringe. HUVEC were lysed in 150 μl of lysis buffer (10 mM Tris-Hcl pH 7.4, 0.5% SDS, 10% glycerol, Triton-X 100 1%, DOC 0,75%, 75 mM NaCl, 10 mM EDTA, 0,5 mM PMSF, 2 mM $NaPO_4$, 10 µg/mL leupeptin, 25 µg/mL aprotinin, 1.25mM NaF, 1 mM $Na_4P_2O_7$) with a rubber policeman and centrifuged at 10,000*g* for 15 min at 4°C.

30 μg of proteins of each sample were treated with 20% v/v Laemmli buffer (0.07 M Tris HCl pH 6.8, glycerol 22%, SDS 2%, mercaptoethanol 4%) and boiled for 5 min. Then any proteins sample was subjected to 10% SDS-PAGE (10% resolving gel and 4% stacking gel). Protein content of cell lysates was determined by the Bensadoun and Weinstein procedure using bovine serum albumin as standard.

1. Samples were loaded into gel and run in running buffer (25 mM Tris, 192 mM glycin, 1% SDS) for 1h at 40mA (2002 power supply LKB Bromma). A

molecular weights marker was used (BenchMark Prestained Protein Ladder, Invitrogen).

2. Separated proteins were transferred to PDVF membrane (Hybond-P, Amersham), previously soaked in methanol. The gel was sandwiched together with the membrane between Whatman paper, two porous pads, equilibrated in transfer buffer (25 mM Tris and 192 mM glycin) for few minutes, and two plastic supports. The blot sandwich was placed into the Mini-Transblot electrophoresis system (Bio-Rad) filled with the same transfer buffer, the membrane facing the anode. A constant current of 200 mA was applied for 4 h at 4°C.
3. At the end, non specific binding sites were blocked by immersing the membrane in blocking solution, and shaking for 30 min at room temperature.
4. The membrane was exposed to the primary antibody (1:10000) in TBS/Tween-20 containing 5% BSA, overnight at 4°C.
5. After 3x15 min washes with TBS-T 20 at room temperature with gentle agitation, the membrane was incubated with horseradish peroxidase (HRP)-linked secondary antibody (1:100000) in TBS-Tween 20 for 1 hour at room temperature.
6. The membrane was then washed 3x15 min with TBS-Tween 20.
7. The signal was detected by chemiluminescence using the ECL-Advance Western blotting detection kit (Amersham). The detection reagent was pipetted onto the membrane, which was placed with protein side up on a clean surface. After 5 min of incubation at room temperature the membrane was put into clear wrap and exposed to Hyperfilm (Amersham Biosciences) in an X-ray film cassette.
8. For the visualization, the film was developed in developing solution (Kodak). When the bands were at the desired density, the films was transferred into the fixing solution (Kodak), then washed in water and air-dried. Molecular weight standards were used to identify appropriate antibody binding.

3.2.10. Protein assay

Protein content of cell lysates was determined by Lowry procedure (1951) or Bensadoun and Weinstein procedure (1976).

Lowry procedure*:*

1. A tube of 1.0 mg/ml BSA was thawed to prepare BSA standards solution 0, 5, 10, 15, 20, 30, 40, 50. The numbers represent the volume in µl to be used. BSA solution was vortexed to insure homogeneity and pipetted into each standard tube starting from lower concentrations and move up.
2. Two tubes for each buffer blank and for each unknown were prepared. The volumes for unknowns were estimated such that the tubes contain 10-50 µg of protein. Each unknown were measured in duplicate. Volumes of buffer blanks were identical to those of unknowns.
3. 200 µl of DOC 10% were pipeted into each tube. To each tube was added water to make up to 1 ml volume.
4. 100:1:1 mixture of solutions A, B1, B2 was prepared. Solution B1 was added to A first, then solution B2. Usually 20 ml + 0.2 ml + 0.2 ml was sufficient.
5. At t=0 was added exactly 5 ml of the mixture to the first tube and vortexed immediately. The tubes were let sit for exactly 10 min at 25°C.
6. The Folin & Ciocalteu's phenol reagent (2N, Sigma) was diluted 1:1 with distilled H_2O. Usually 1 ml + 1 ml was enough. The solution was vortexed thoroughly.
7. 0.5 ml of the diluted reagent was added to the tubes and vortexed immediately.
8. The tubes were let stand for at least 30 min but no more than 60 min. Absorbance was read at 750 nm. Use the tube with no protein (BSA 0 µl) to set the baseline of the spectrophotometer.
9. The absorbance was plotted as function of µg BSA (i.e. µl BSA). The blank OD was subtracted from each unknown and read the amount, in µg, on the standard curve.

Bensadoun and Weinstein procedure

1. A tube of 1.0 mg/ml BSA was thawed to prepare BSA standards solution 0, 5, 10, 15, 20, 30, 40, 50. The numbers represent the volume in µl to be used. BSA solution was vortexed to insure homogeneity and pipetted into each standard tube starting from lower concentrations and move up.
2. Two tubes for each buffer blank and for each unknown were prepared. The volumes for unknowns were estimated such that the tubes contain 10-50 µg of protein. Each unknown were measured in duplicate. Volumes of buffer blanks were identical to those of unknowns.
3. 25 µl of sodium deoxycholate (DOC) 10% were pipeted into each tube. To each tube was added water to make up to 3 ml volume.
4. The tubes were let stand for at least 10 min at 25°C.
5. 1 ml trichloroacetic acid (TCA) 24% was added to the tubes to precipitate proteins.
6. The precipitate was pelleted in centrifuge by spinning for 20 min at 12500 rpm.
7. The supernatant was aspirated.
8. To each tube was added 300 µl of SDS 10% with 200 µl of water. The solution was vortexed thoroughly. SDS separated membrane proteins from contaminating membrane constituents and denatured the proteins allowing more reproducible results.
9. 100:1:1 mixture of solutions A, B1, B2 was prepared. Solution B1 was added to A first, then solution B2. Usually 20 ml + 0.2 ml + 0.2 ml was sufficient.
10. At t=0 was added exactly 3 ml of the mixture to the first tube and vortexed immediately. The tubes were let sit for exactly 10 min at 25°C.
11. The Folin & Ciocalteu's phenol reagent (2N, Sigma) was diluted 1:1 with distilled H_2O. Usually 1 ml + 1 ml was enough. The solution was vortexed thoroughly.
12. 0.5 ml of the diluted reagent was added to the tubes and vortexed immediately.

13. The tubes were let stand for at least 30 min but no more than 60 min. Absorbance was read at 750 nm. Use the tube with no protein (BSA 0 μl) to set the baseline of the spectrophotometer.
14. The absorbance was plotted as function of µg BSA (i.e. μl BSA). The blank OD was subtracted from each unknown and read the amount, in μg, on the standard curve.

3.2.11. Statistical analysis

To calculate the statistical significance of results, one-way ANOVA test was used together with Dunnet or Bonferroni's multiple comparison test as post test.

Curves of intracellular ROS levels were analyzed by non linear regression analysis with the application of the F-test to calculate statistical significance between two different curves.

Graphs and statistical analysis were performed with Graph Prism version 3.03 for Windows, GraphPad Software.

4. RESULTS

4.1. Effect of 7β-OHC and 7-KC on cell viability of vascular smooth muscle and endothelial cells

Treatment with 7-KC induced an increase of HUVEC viability at 5 and 10 μg/mL after 24 and 48 hours (Fig. 16, a-b). A cytotoxic effect was always present at 20 μg/mL. Also 7β-OHC showed a dual effect on HUVEC viability (Fig. 16, c-d). While at lower concentrations (< 20 μg/mL) an increase in cell viability was induced in a concentration dependent manner, at the highest concentration (20 μg/mL) a cytotoxic effect was observed.

In order to investigate whether the effect of the two oxysterols were specific for HUVEC, some experiments were performed in the vascular smooth muscle cell line A7r5. As shown in Fig. 17, both 7-KC and 7β-OHC caused a transient increase of cell viability. Furthermore, these increases were lower than those found in HUVEC.

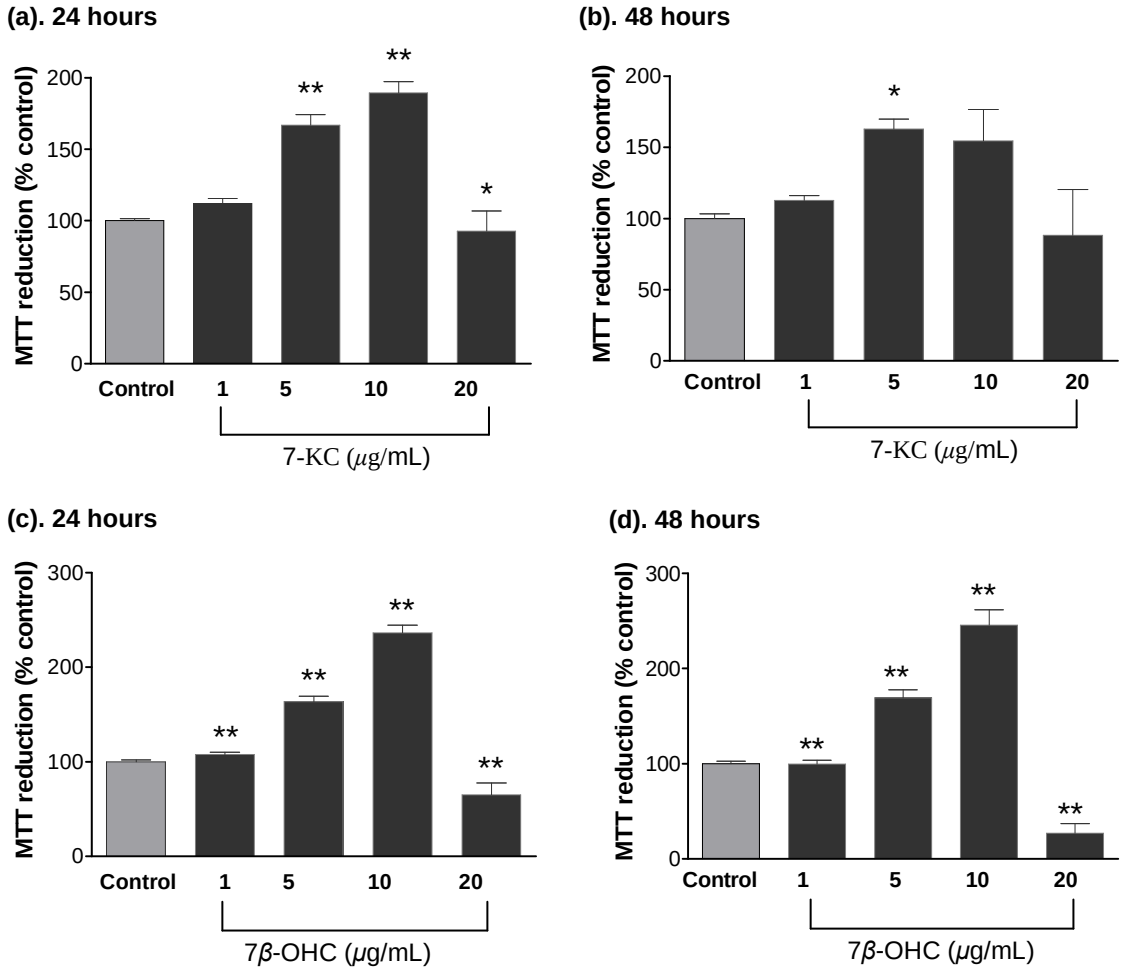

Fig. 16 Effect of 7-KC and 7*β*-OHC on HUVEC viability. Both oxysterols were tested at 1-20 μg/mL concentrations, MTT test was performed after incubation with 7-KC for 24 hours (a) and 48 hours (b) or with 7*β*-OHC for 24 hours (c) and 48 hours (d). Results are expressed as mean $\pm$ SE of % of MTT reduction with respect to control of 4 independent experiments in sextuplicate (*$P < 0.05$, **$P < 0.01$ vs control). Statistical analysis was performed by one-way ANOVA test and Dunnet's comparison post test.

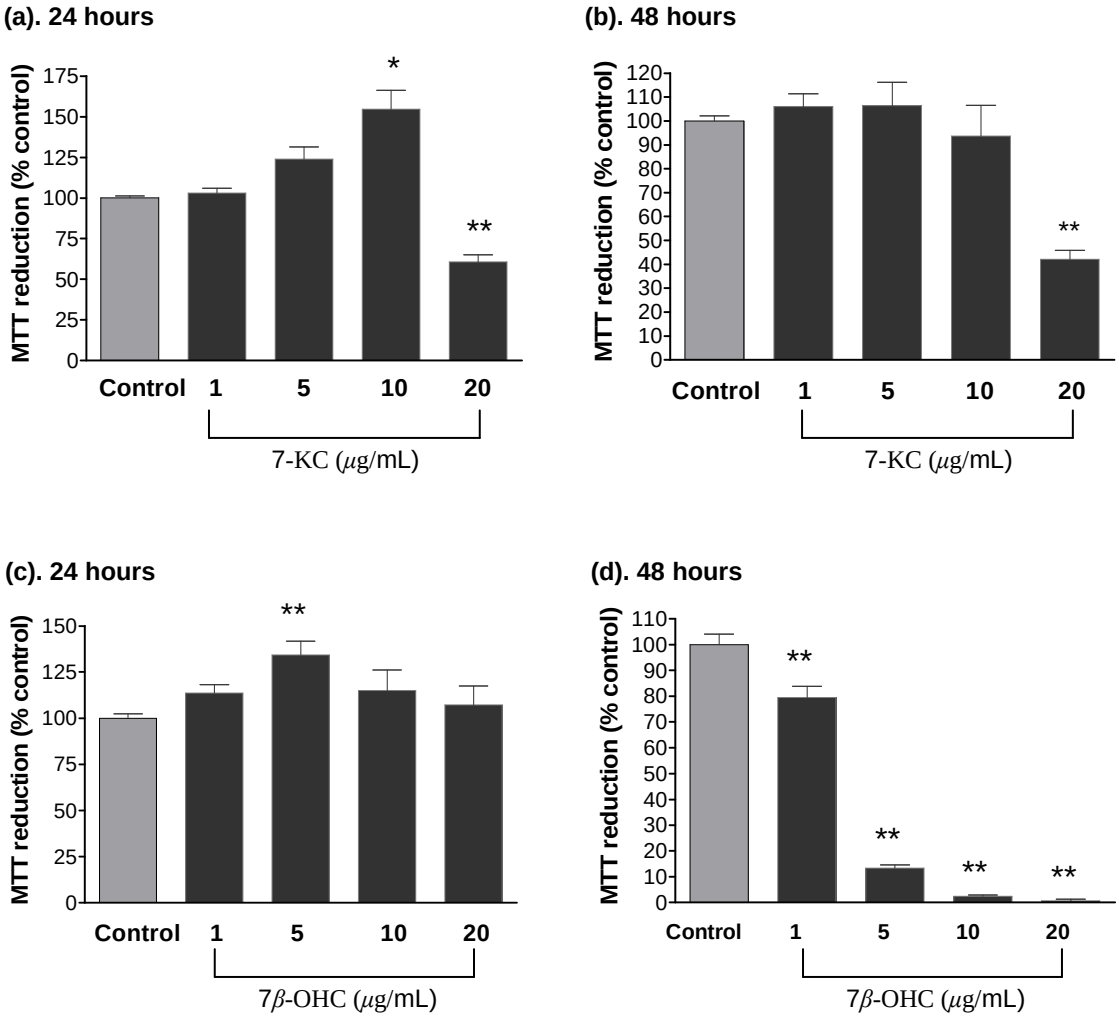

Fig. 17 Effect of 7-KC and 7*β*-OHC on A7r5 viability. Both oxysterols were tested at 1-20 μg/mL concentrations, MTT test was performed after incubation with 7-KC for 24 hours (a) and 48 hours (b) or with 7*β*-OHC for 24 hours (c) and 48 hours (d). Results are expressed as mean $\pm$ SE of % of MTT reduction with respect to control of 4 independent experiments in sextuplicate (*$P < 0.05$, **$P < 0.01$ vs control). Statistical analysis was performed by one-way ANOVA test and Dunnet's comparison post test.

4.2. Effect of 7*β*-OHC on bFGF deprivation induced apoptosis in HUVEC

The effects of the two oxysterols on HUVEC viability reported above were found in cells treated without bFGF, which represents a proapototic condition for HUVEC (Vinci *et al*, 2004; Trevisi *et al*, 2004). Thus, the increase in HUVEC viability induced by both oxysterols could be due to an antiapoptotic action. Since the effect of 7*β*-OHC was more relevant, the analysis of the antiapoptotic effect was performed in 7*β*-OHC-treated HUVEC.

Analysis annexin-V and PI binding and caspase-3 activation in HUVEC were performed after 24 hours treatment with 7*β*-OHC in the absence of bFGF. Figures 18 and 19 show that 7*β*-OHC (< 20 μg/mL) was able to significantly decrease the number of annexin-V positive cells with respect to control in a concentration-dependent manner, indicating an antiapoptotic action of the oxysterol.

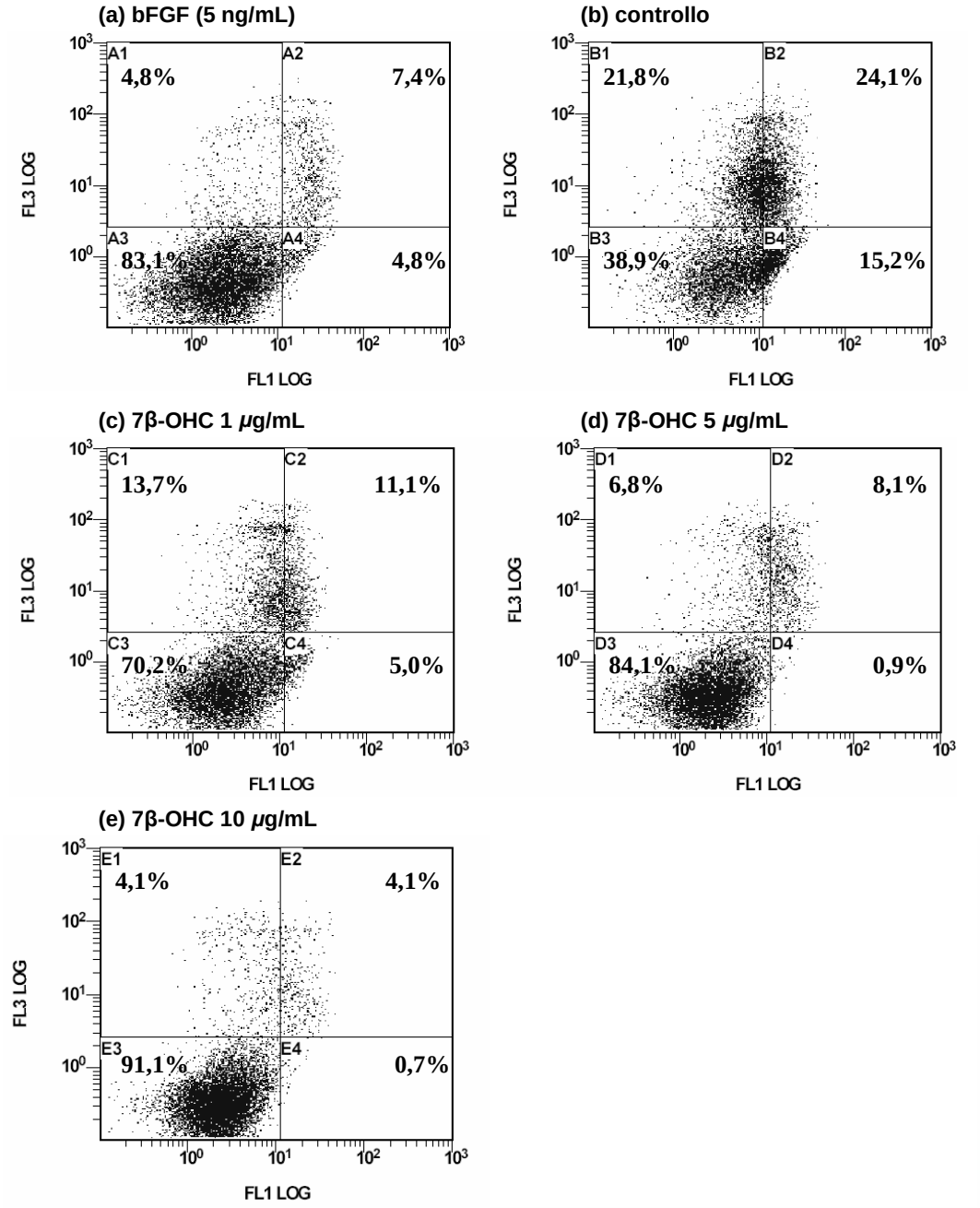

Fig. 18 Representative cytograms of annexin-V and PI binding showing the effect of 7*β*-OHC on bFGF deprived HUVEC. HUVEC were treated with or without 7*β*-OHC (10 *μ*g/mL) for 24 hours. Unlabelled cells (viable cells) are collocated in the left quadrant on the bottom (3). Annexin-V positive cells (apoptotic cells) are collocated in the right quadrant on the bottom (4). PI positive cells (necrotic cells) are represented in the left quadrant on the top (1) of the scatter plot. Double stained cells (late apoptotic cells) are in the right quadrant on the top (2).

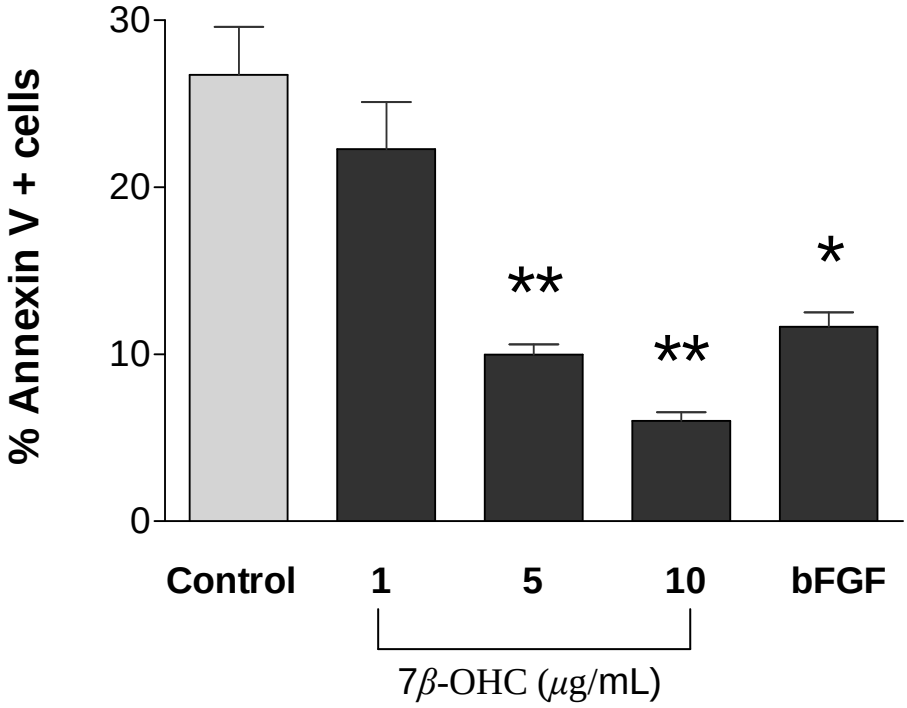

Fig. 19 Antiapoptotic effect of 7*β*-OHC in bFGF deprived HUVEC. The cells were treated with or without 7*β*-OHC (1-10 *μ*g/mL) for 24 hours, then flow cytometric analysis of annexin-V/PI binding was performed. Results are expressed as mean ± SE of percentage of annexin-V labelled cells of 4 independent experiments performed in duplicate (*P < 0.05, ** *P* < 0.01 vs control). Statistical analysis was performed by one-way ANOVA test and Dunnet's post test.

The antiapoptotic action of 7β-OHC against apoptosis induced by bFGF deprivation was confirmed by the caspase-3 assay. 7β-OHC was able to significantly inhibit caspase-3 activation after 6 hours treatment (Fig. 20)

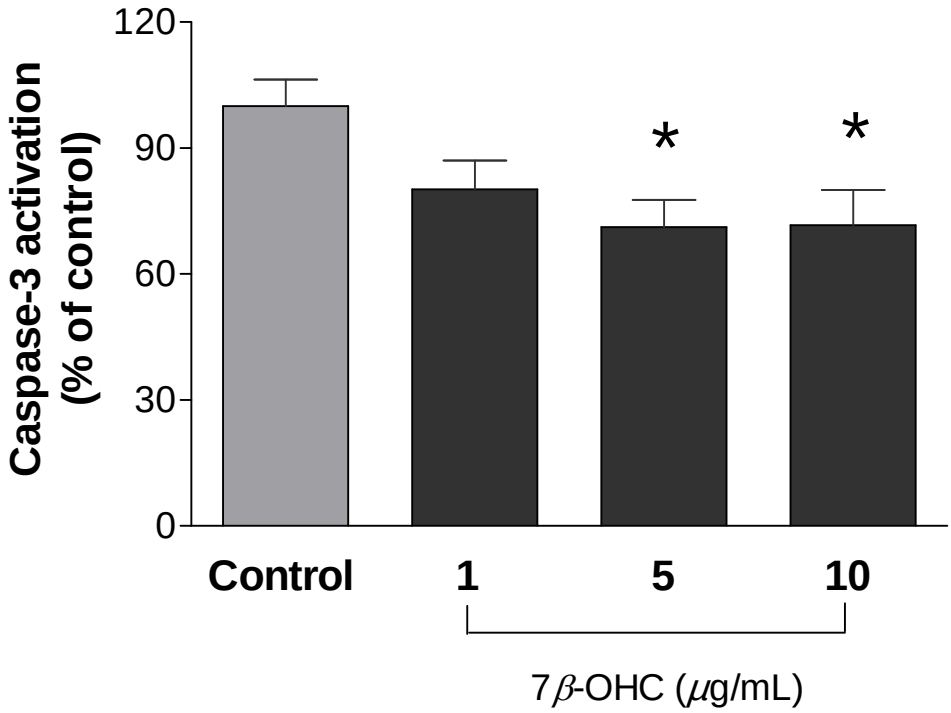

Fig 20. Antiapoptotic effect of 7β-OHC in bFGF deprived HUVEC. Cells were treated with or without 7β-OHC (1-10 μg/mL) for 6 hours, then caspase 3 activity was determined in cell lysates. Results are expressed as mean $\pm$ SE of percentage of caspase-3 activation of 4 independent experiments performed in duplicate (*P < 0.05 vs control). Statistical analysis was performed by one-way ANOVA test and Dunnet's post test.

All together, the results of both annexin-V binding and caspase-3 activation revealed the capacity of 7β-OHC to prevent bFGF induced apoptosis in HUVEC.

4.3. Effect of 7*β*-OHC on staurosporine induced apoptosis in HUVEC

The antiapoptotic effect of 7*β*-OHC in HUVEC was tested also against apoptosis induced by staurosporine (from *Streptomyces staurospores*), a relatively non-selective protein kinase inhibitor. Staurosporine is often used as a general stimulus for inducing apoptosis (Kabir et al, 2002). Thus, the effect of staurosporine (50 nM, 3 hours) on annexin-V and PI binding and caspase-3 activation was investigated in HUVEC pretreated with 7*β*-OHC (10 μg/mL) for 15 hours.

The oxysterol was able to significantly reduce the percentage of annexin-V labelled cells induced by staurosporine treatment (Fig.21, 22), thus confirming the antiapoptotic action of 7*β*-OHC.

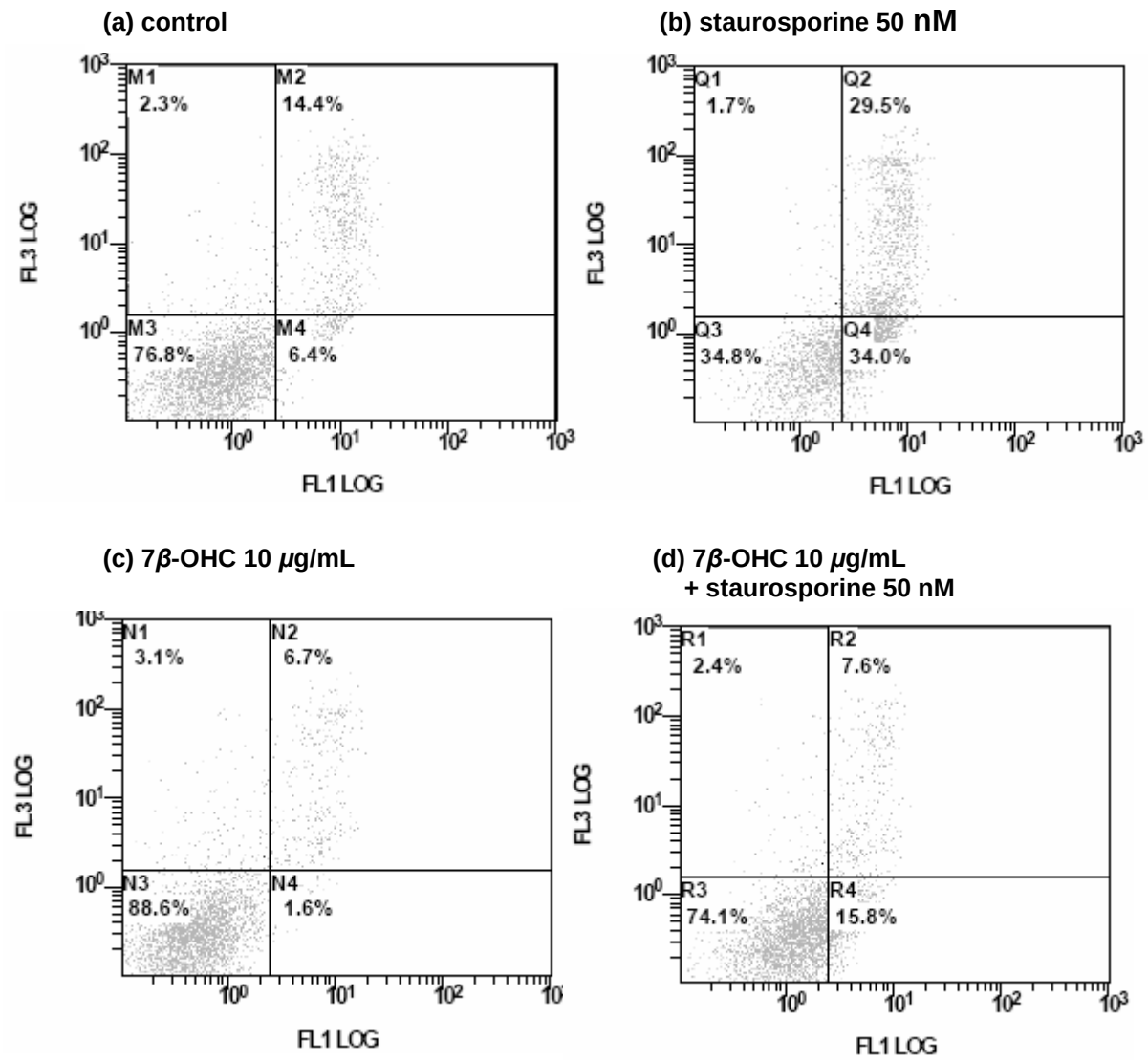

Fig. 21 Representative cytograms of annexin-V and PI binding showing the effect of 7*β*-OHC on HUVEC treated with staurosporine. HUVEC were treated with or without 7*β*-OHC (10 *μ*g/mL) for 15 hours, then staurosporine (50 nM) was added for 3 hours. Unlabelled cells (viable cells) are collocated in the left quadrant on the bottom (3). Annexin-V positive cells (apoptotic cells) are collocated in the right quadrant on the bottom (4). PI positive cells (necrotic cells) are represented in the left quadrant on the top (1) of the scatter plot. Double stained cells (late apoptotic cells) are in the right quadrant on the top (2).

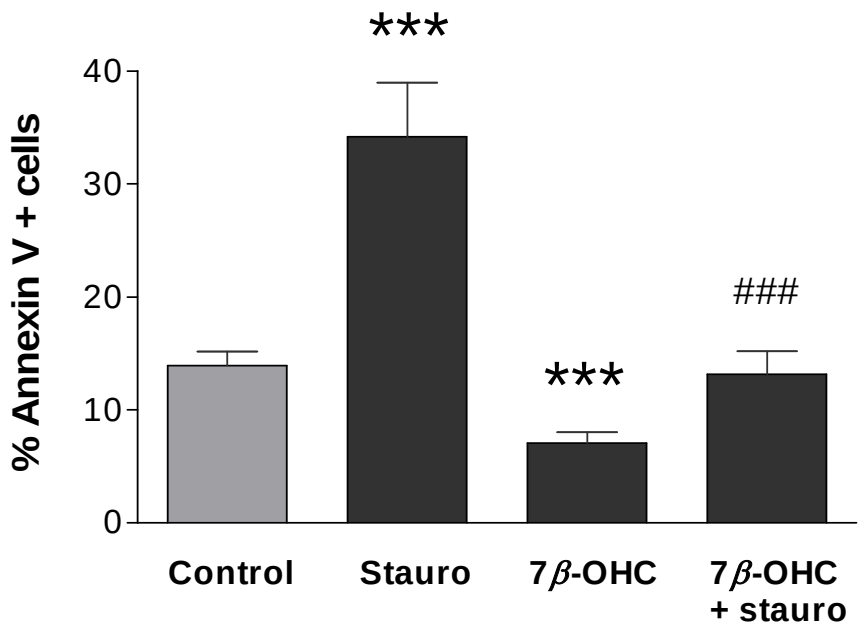

Fig. 22 Antiapoptotic effect of 7β-OHC in HUVEC against staurosporine treatment. HUVEC were treated with or without 7β-OHC (10 μg/mL) for 15 hours, then staurosporine (50 nM) was added for 3 hours. Results are expressed as mean $\pm$ SE of percentage of annexin-V labelled cells of 4 independent experiments performed in duplicate (** $P < 0.01$, *** $P < 0.001$, vs control; ###P < 0.001 vs staurosporine treated cells). Statistical analysis was performed by one-way ANOVA test and Bonferroni's multiple comparison post test.

The antiapoptotic action of 7*β*-OHC against apoptosis induced by staurosporine was confirmed by the analysis of caspase-3 activation in HUVEC lysates (Fig. 23). In fact, 7*β*-OHC was able to significantly inhibit the increase in caspase-3 activity due to staurosporine treatment.

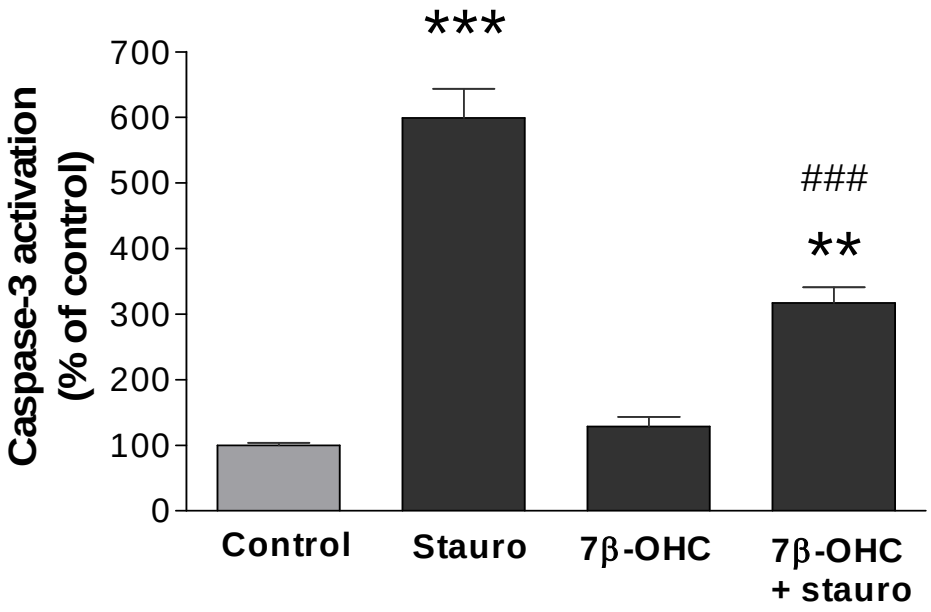

Fig 23. Antiapoptotic effect of 7*β*-OHC in HUVEC against staurosporine treatment. HUVEC were treated with or without 7*β*-OHC (10 μg/mL) for 15 hours, then staurosporine (50 nM) was added for 3 hours. Results are expressed as mean $\pm$ SE of percentage of caspase-3 activation of 4 independent experiments performed in duplicate (** $P < 0.01$, *** $P < 0.001$, vs control; ###P < 0.001 vs staurosporine treated cells). Statistical analysis was performed by one-way ANOVA test and Bonferroni's multiple comparison post test.

The results demonstrate that 7*β*-OHC has an antiapoptotic action in HUVEC, protecting them from apoptotis induced by either bFGF deprivation or staurosporine.

4.4. ROS production in vascular cells treated with oxysterols

It has been shown that oxLDL can induce proliferation in HUVEC at concentrations lower than 40 μg/mL with a mechanism dependent on ROS production by NADPH oxidase (Heinloth *et al*, 2000) Furthermore, recently it has been demonstarted the protective effect of low concentrations of hydrogen peroxide on apoptosis induced by serum deprivation in HUVEC (Haendeler J *et al*., 2004). Thus, the involvement of ROS in the action of 7β-OHC and 7-KC was investigated.

Intracellular ROS production was determined with the fluorescent dye CM-H_2DCFDA. In HUVEC, both 7-KC and 7β-OHC (1-20 μg/mL) induced a concentration-dependent increase in ROS production (Fig. 24). 7β-OHC was more effective than 7-KC in increasing intracellular ROS levels.

Intracellular ROS levels were also measured in A7r5 treated with 7-KC or 7β-OHC. As shown in Fig. 25 a slight increase in ROS production was induced by only 7β-OHC.

Taken into account the differences between the two oxysterols in increasing ROS levels in the HUVEC and A7r5, subsequent experiments were performed in HUVEC treated with 7β-OHC.

(a). 7-KC

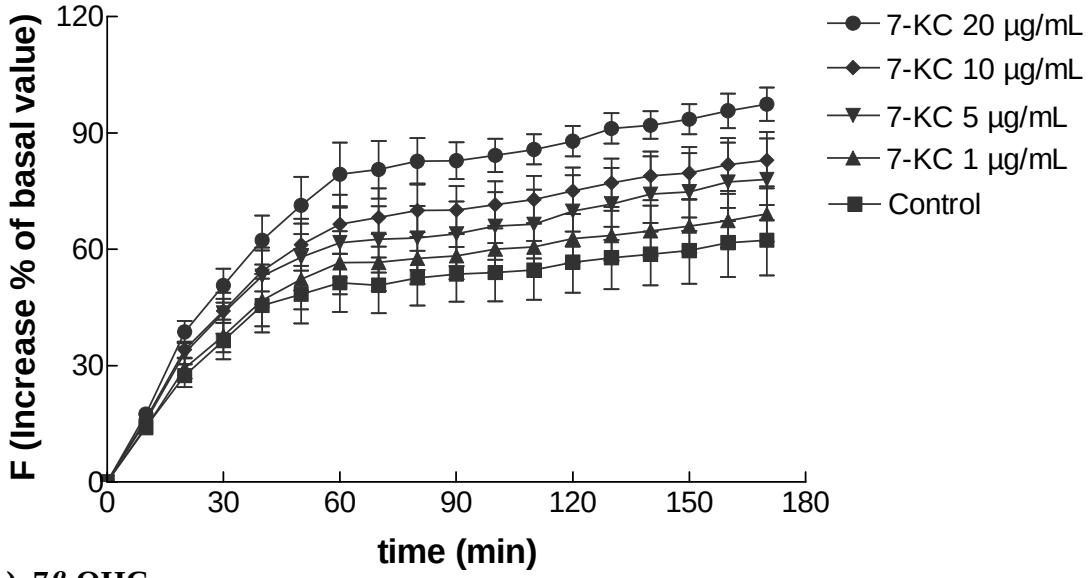

(b). 7*β*-OHC

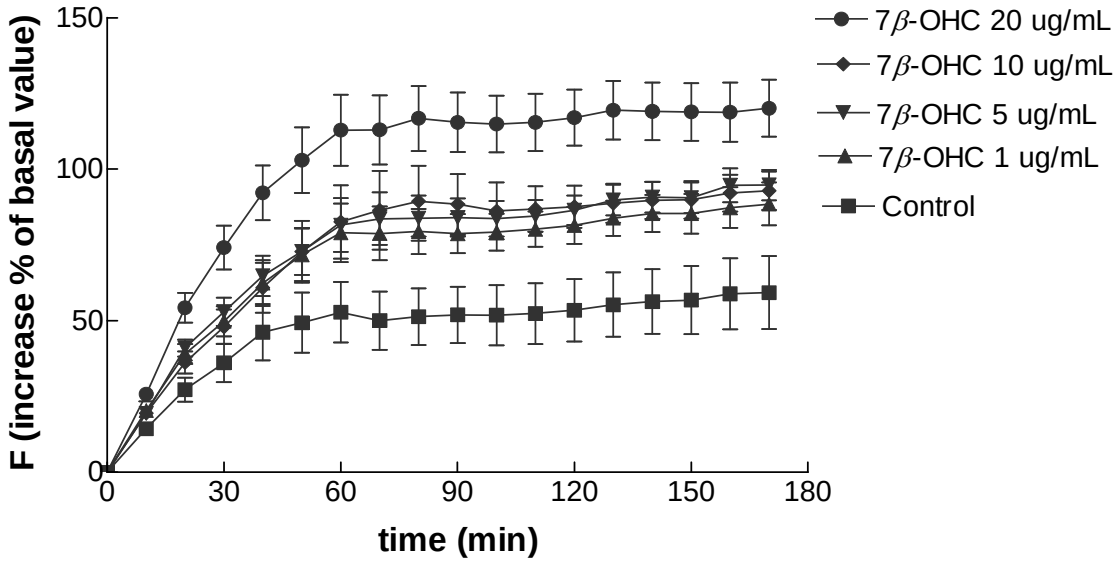

Fig. 24 Effect of 7-KC (a) or 7*β*-OHC (b) on intracellular ROS production in HUVEC. After loading with CM-H_2DCFDA, HUVEC were incubated with the oxysterol (1, 5, 10, 20 μg/mL, or the vehicle). ROS levels were measured as described in methods. Data are expressed as mean $\pm$ SE of 6 independent experiments performed in quadruplicate and are represented as percentage increase of basal value of fluorescence. Increase in ROS production was statistically significant at any concentration ($P < 0.001$). Statistical analysis were performed with non linear regression analysis and F-test.

(a). 7-KC

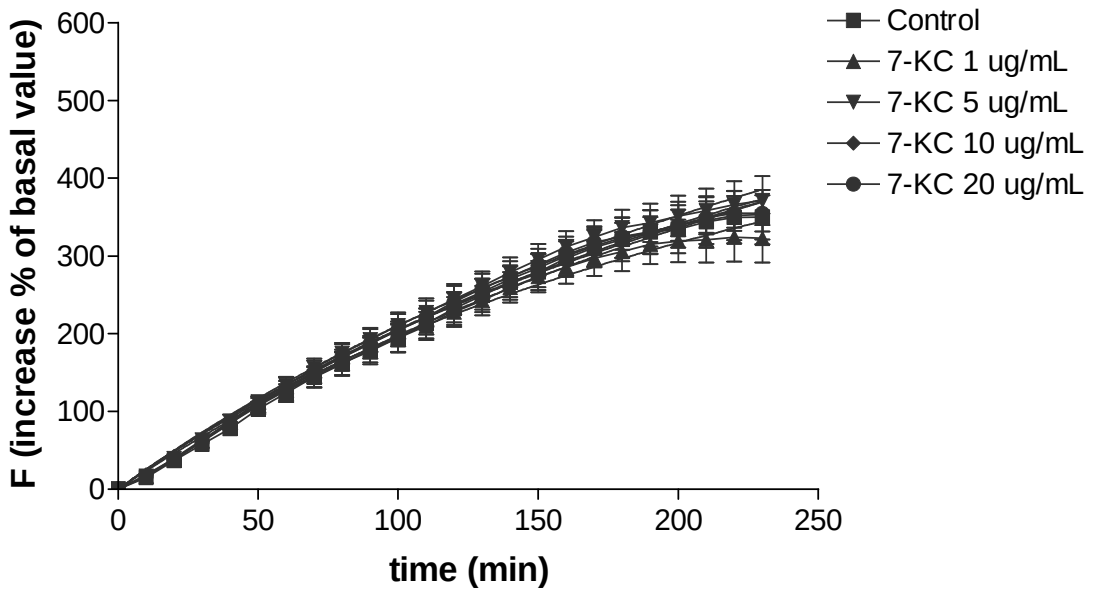

(b). 7*β*-OHC

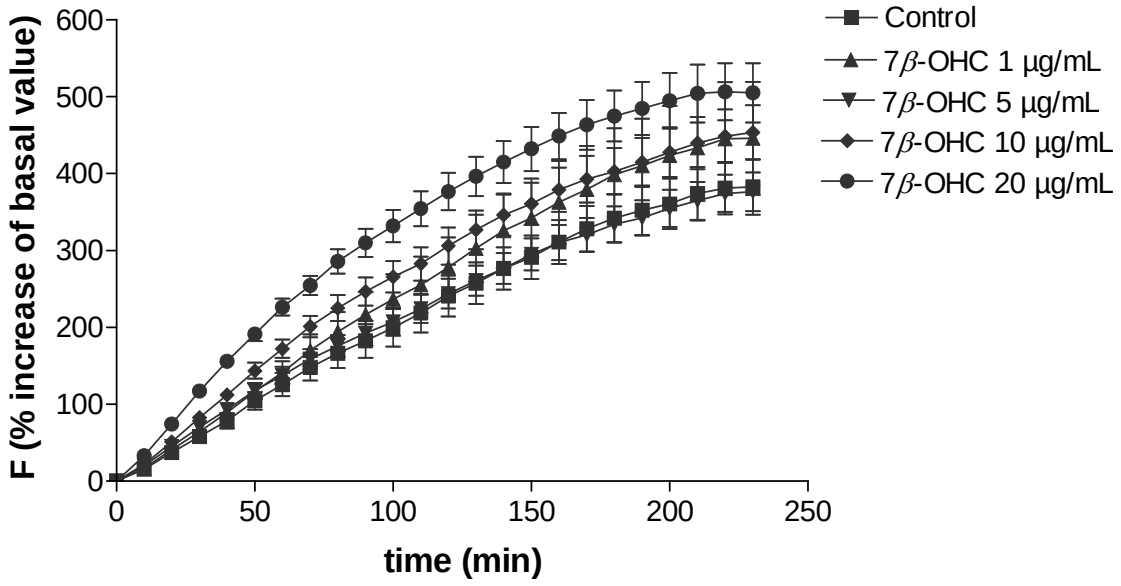

Fig. 25 Effect of 7-KC (a) or 7*β*-OHC (b) on intracellular ROS production in A7r5 cells. After loading with CM-H_2DCFDA, HUVEC were incubated with the oxysterols (1, 5, 10, 20 μg/mL, or the vehicle). ROS levels were measured as described in methods. Data are expressed as mean $\pm$ SE of 4 independent experiments performed in quadruplicate and are represented as percentage increase of basal value of fluorescence. Increase in ROS production was statistically significant only in 7β-OHC treated cells ($P < 0.001$). Statistical analysis were performed with non linear regression analysis and F-test.

4.4.1. Involvement of mitochondria in ROS production

To investigate whether mitochondria is the source of ROS induced by 7β-OHC in HUVEC, ROS production was measured in the presence of two different inhibitors of the respiratory chain.

Rotenone (an inhibitor of complex I) and tenoyltrifluoroacetate (TTFA, an inhibitor of complex II) were unable to block ROS production by 7β-OHC (Fig. 26). In addition, treatment with each inhibitor induced an increase in ROS levels, suggesting that in HUVEC the inhibition of respiratory chain itself causes an overproduction of ROS.

(a). Rotenone

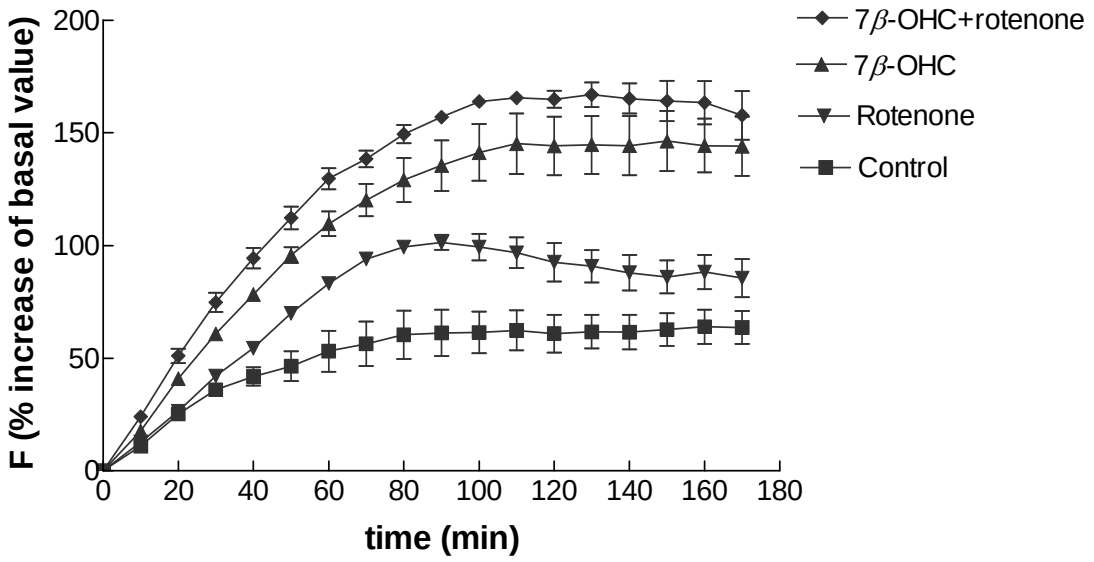

(b). TTFA

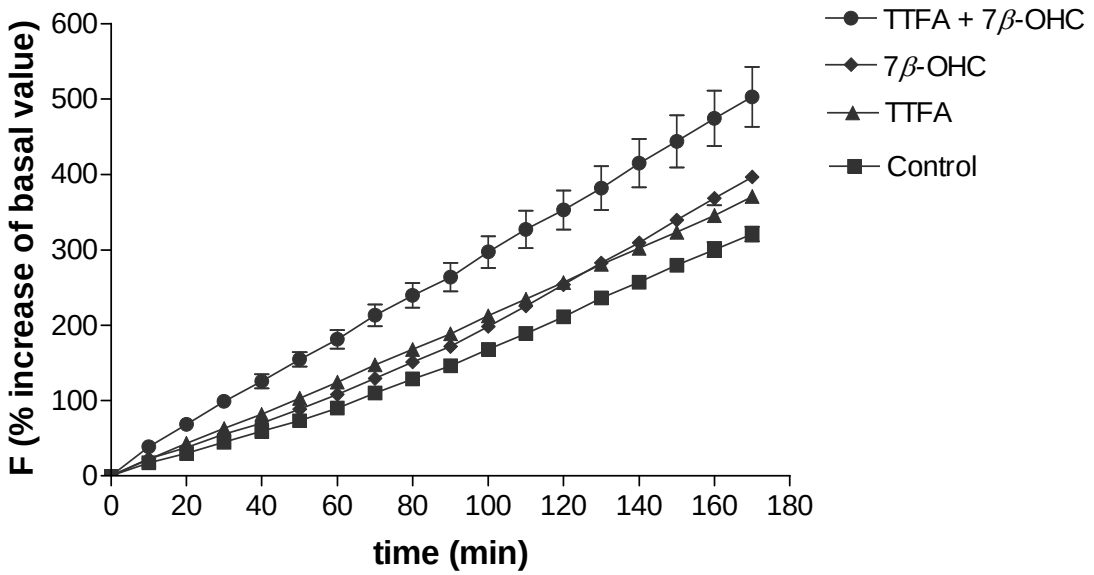

Fig. 26 Effect of (a) the complex I inhibitor rotenone or (b) complex II inhibitor tenoyltrifluoroacetate (TTFA) on 7*β*-OHC-stimulated ROS production. After loading with CM-H_2DCFDA, HUVEC were incubated with the inhibitor for 30 min, then 10 μg/mL 7*β*-OHC (or the vehicle) was added and intracellular ROS level was measured as described in methods. Data are expressed as percentage increase of basal value of fluorescence of 2 independent experiments performed in quadruplicate. Increases in ROS production were statistically significant respect to the control ($P < 0.001$). Statistical analysis were performed with non linear regression analysis and F-test.

In accordance, pretreatment of HUVEC with an uncoupler of the respiratory chain, cyanide m-chlorophenylhydrazone (CCCP), did not affect ROS production by 7β-OHC (Fig. 27). CCCP induced ROS overproduction by itself.

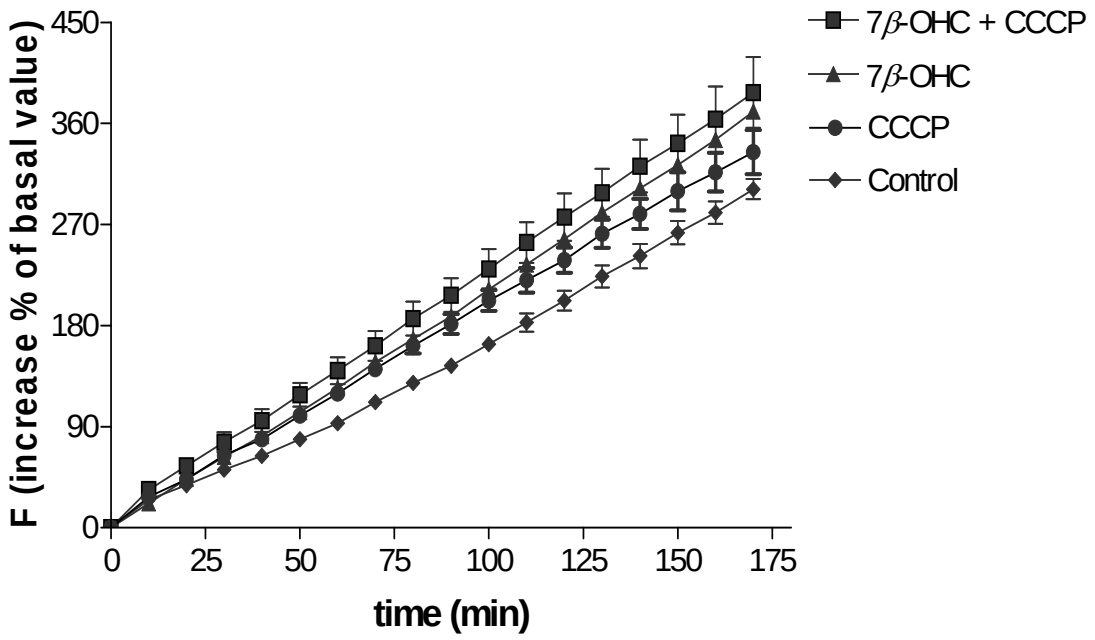

Fig. 27 Effect of the uncoupler cyanide m-chlorophenylhydrazone (CCCP) on 7β-OHC-stimulated ROS production. After loading with CM-H_2DCFDA, HUVEC were incubated with CCCP for 30 min, than 10 μg/mL 7β-OHC (or the vehicle) was added and intracellular ROS level was measured as described in methods. Data are expressed as percentage increase of basal value of fluorescence of 2 independent experiments performed in quadruplicate. Increases in ROS production were statistically significant respect to the control ($P < 0.001$). Statistical analysis were performed with non linear regression analysis and F-test.

4.4.2. Involvement of NADPH oxidase in ROS production

Many exogenous and endogenous stimuli can induce an increase in intracellular ROS production in vascular cells by stimulating the membrane-bound flavoprotein NADPH oxidase. To test the involvement of NADPH oxidase in determining the increase in intracellular ROS levels in HUVEC treated with either 7*β*-OHC, a series of experiments were performed in the presence of the NADPH oxidase inhibitor hydralazine (Münzel *et al*, 1996).

Hydralazine (25 μM) partially inhibited the increase in ROS production induced by 20 μg/mL 7*β*-OHC (Fig. 28), indicating that NADPH oxidase is a source of ROS stimulated by 7*β*-OHC.

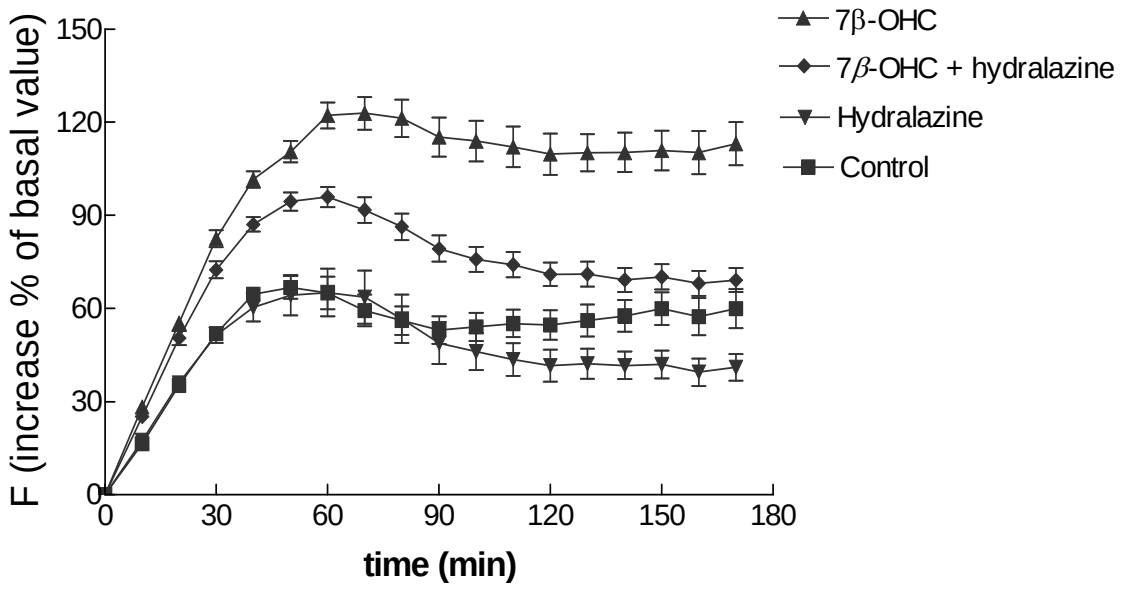

Fig. 28 Effect of hydralazine on 7*β*-OHC-stimulated ROS production. After loading with CM-H_2DCFDA, HUVEC were incubated with hydralazine for 30 min, then 20 μg/mL 7*β*-OHC (or the vehicle) was added and intracellular ROS levels were measured as described in methods. Data are expressed as percentage increase of basal value of fluorescence of 4 independent experiments performed in quadruplicate. Both increase in ROS production in presence of 7*β*-OHC alone and partially inhibition of 7*β*-OHC induced ROS production were statistically significant ($P < 0.001$). Statistical analysis were performed with non linear regression analysis and F-test.

4.5. Role of NADPH oxidase in the antiapoptotic effect of 7*β*-OHC

To investigate the role of NADPH oxidase activation in the antiapoptotic effect of *7β*-OHC, analysis of annexin-V and PI binding was performed in the presence of hydralazine (25 μM).

The antiapoptotic action of 10 μg/mL 7*β*-OHC against bFGF deprivation was not affected by hydralazine, indicating that NADPH oxidase is not involved in the protective effect of the oxysterol in HUVEC (Figg. 29, 30).

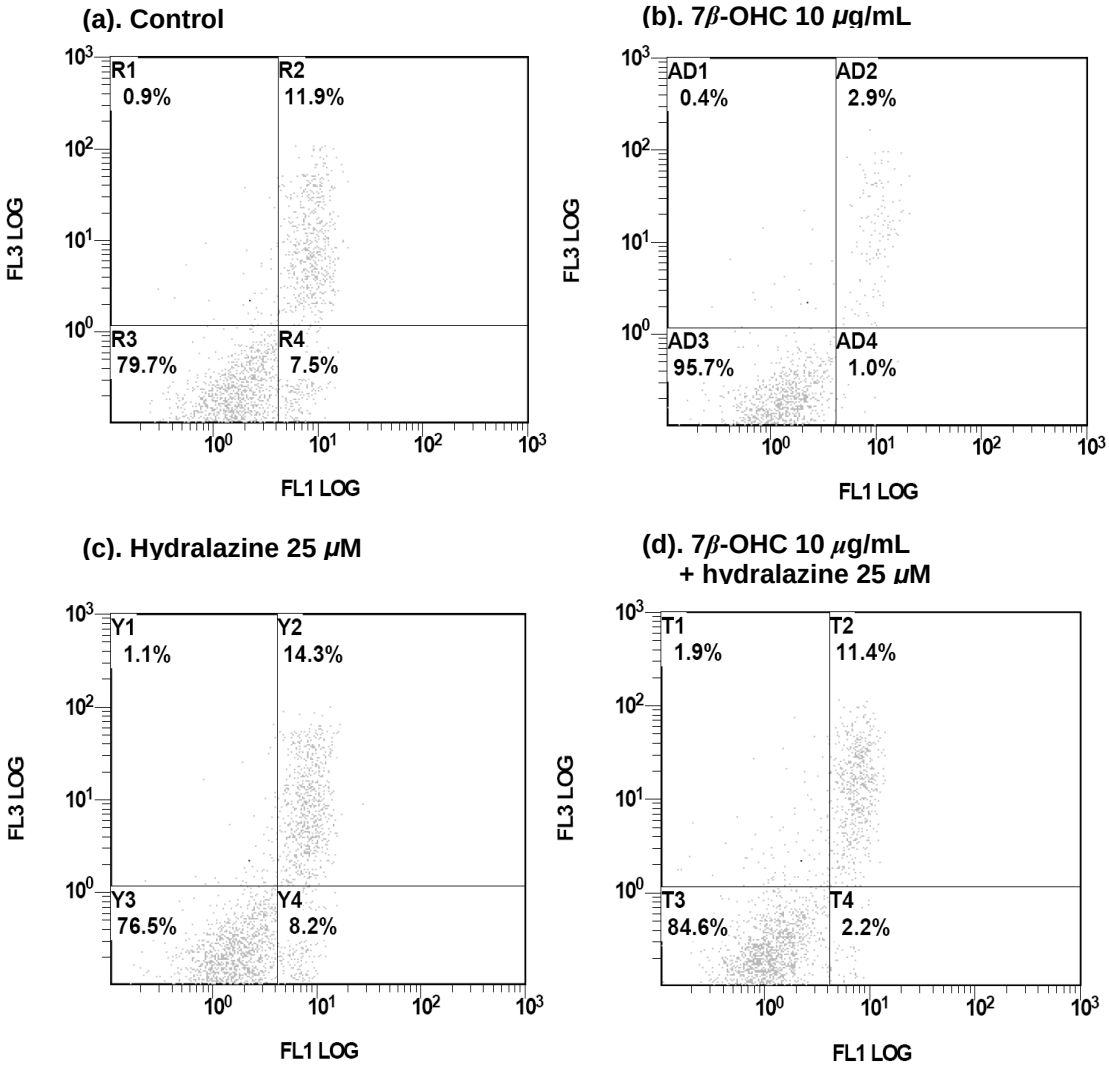

Fig. 29. Representative cytograms of annexin-V and PI binding showing the effect of hydralazine on the antiapoptotic action of 7*β*-OHC against bFGF deprivation. HUVEC were treated for 24 hours with or without 7*β*-OHC (10 *μ*g/mL) in the absence of bFGF. Where indicated, a pretreatment with hydralazine (25 *μ*M) was performed for 30min before the addition of 7*β*-OHC; the inhibitor was present during all the experiment. Unlabelled cells (viable cells) are collocated in the left quadrant on the bottom (3). Annexin-V positive cells (apoptotic cells) are collocated in the right quadrant on the bottom (4). PI positive cells (necrotic cells) are represented in the left quadrant on the top (1) of the scatter plot. Double stained cells (late apoptotic cells) are in the right quadrant on the top (2).

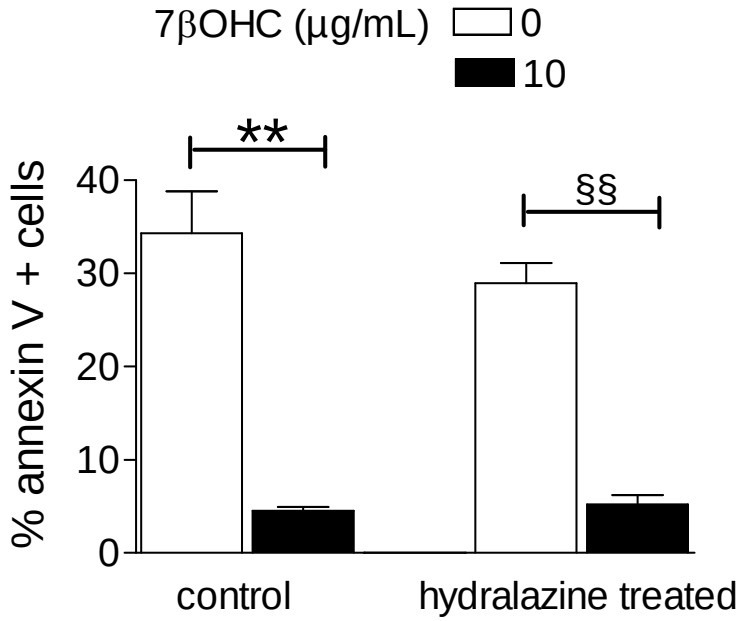

Fig. 30 Effect of NADPH oxidase inhibitor hydralazine on the antiapoptotic action of 7*β*-OHC against bFGF deprivation. HUVEC were incubated for 24 hours without bFGF in the presence or not of 7*β*-OHC (10 μg/mL). Where indicated, a pretreatment with hydralazine (25 μM) was performed for 30 min before the addition of 7*β*-OHC; the inhibitor was present during all the experiment. Results are expressed as mean $\pm$ SE of percentage of annexin-V labelled cells of 2 independent experiments performed in duplicate (***P* < 0.01, §§*P* < 0.01). Statistical analysis was performed by one-way ANOVA test and Bonferroni's multiple comparison post test.

NADPH oxidase inhibition did not block also the protective effect of 7*β*-OHC against staurosporine treatment (50 nM, 3 hours) (Fig. 31, 32).

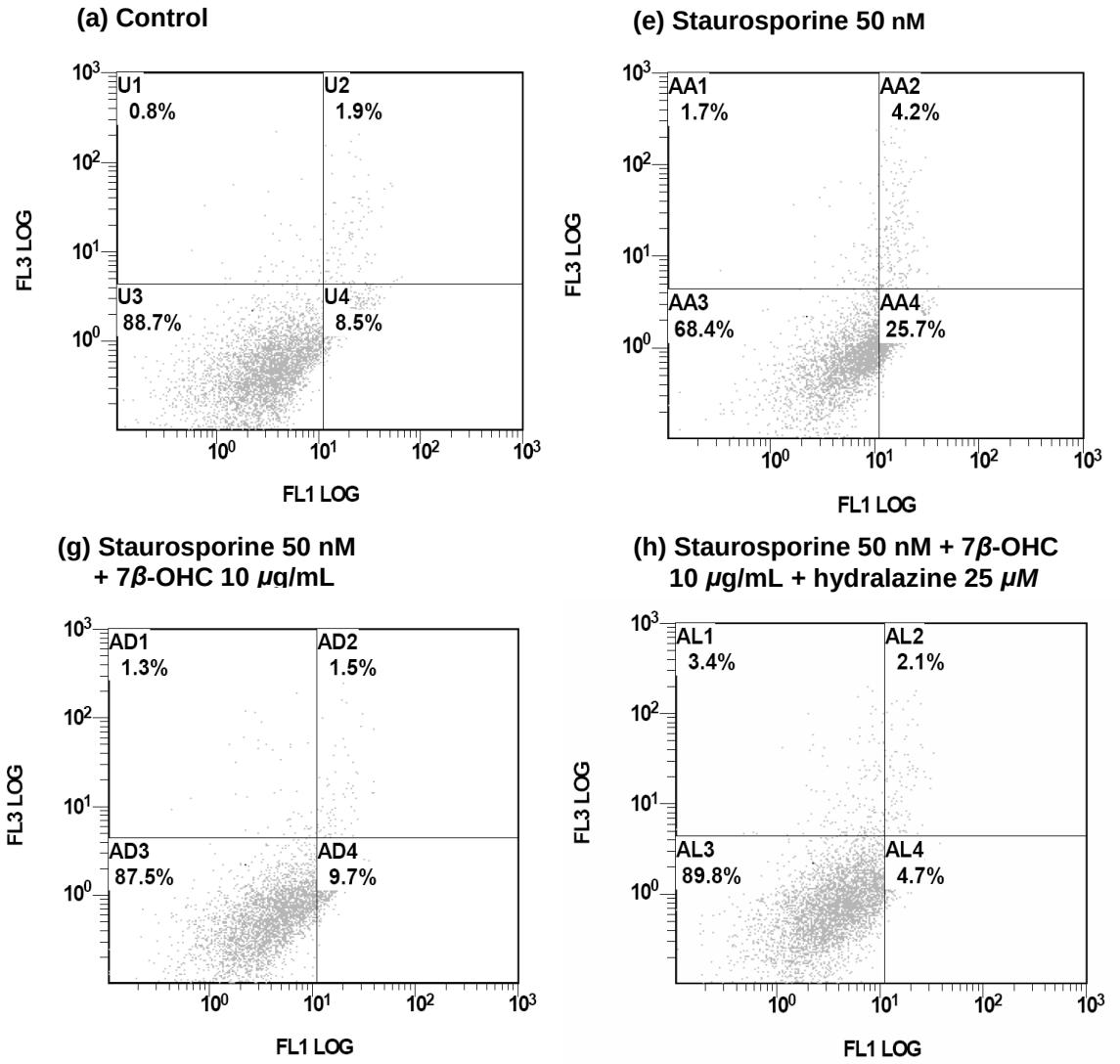

Fig. 31 Representative cytograms of annexin-V and PI binding showing the effect of hydralazine on the antiapoptotic action of 7*β*-OHC against staurosporine. HUVEC were treated for 15 hours with or without 7*β*-OHC (10 *μ*g/mL), then staurosporine (50 nM) was added for 3 hours. Where indicated, a pretreatment with hydralazine (25 *μ*M) was performed for 30min before the addition of 7*β*-OHC; the inhibitor was present during all the experiment. Unlabelled cells (viable cells) are collocated in the left quadrant on the bottom (3). Annexin-V positive cells (apoptotic cells) are collocated in the right quadrant on the bottom (4). PI positive cells (necrotic cells) are represented in the left quadrant on the top (1) of the scatter plot. Double stained cells (late apoptotic cells) are in the right quadrant on the top (2).

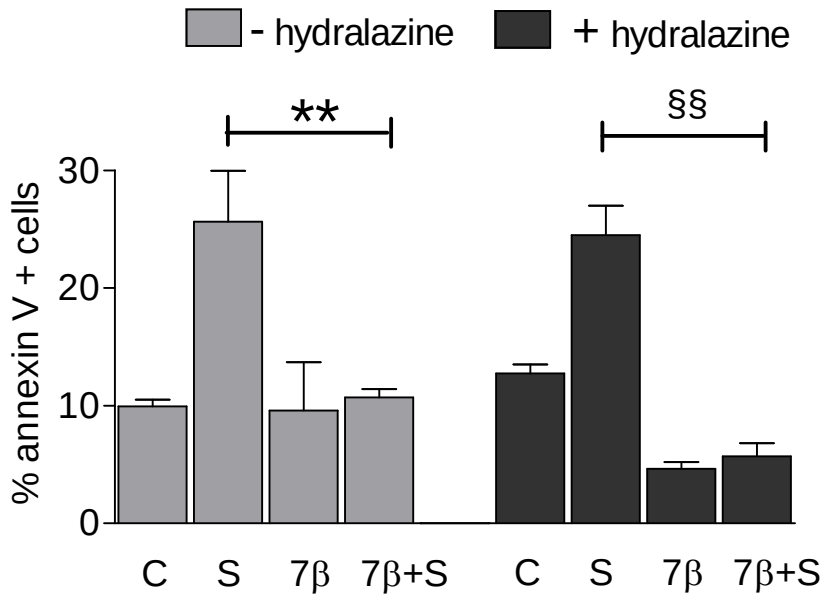

Fig. 32 Effect of the NADPH oxidase inhibitor hydralazine on the antiapoptotic action of 7*β*-OHC against staurosporine. Analysis of annexin-V binding. HUVEC were treated with or without 7*β*-OHC (10 μg/mL) for 15 hours, then staurosporine (50 nM) was added for 3 hours. Where indicated, a pretreatment with hydralazine (25 μM) was performed for 30 min before the addition of 7*β*-OHC and the inhibitor was present during all the experiment. Results are expressed as mean $\pm$ SE of percentage of annexin-V binding of 2 independent experiments performed in duplicate (**P < 0.01, §§P < 0.01). Statistical analysis was performed by one-way ANOVA test and Bonferroni's multiple comparison post test. (C = control, S = staurosporine; 7β = 7*β*-OHC).

4.6. Role of ROS in the antiapoptotic effect of 7*β*-OHC

N-acetylcystein (NAC) is a ROS scavenger acting as cystein prodrug and GSH precursor both *in vivo* and *in vitro*. This compound was used in order to verify the involvement of ROS in the antiapoptotic effect of 7*β*-OHC.

NAC (10 mM) did not antagonize the protective effect of 10 *μ*g/mL *7β*-OHC against apoptosis induced by bFGF-deprivation (Fig.33).

NAC was also ineffective to block the antiapoptotic effect of the oxysterol against apoptosis induced by staurosporine treatment (50 nM, 3 hours) (Fig. 34).

These results indicate that the antiapoptotic effect of *7β*-OHC is not dependent on the increase in ROS levels stimulated by the oxysterol.

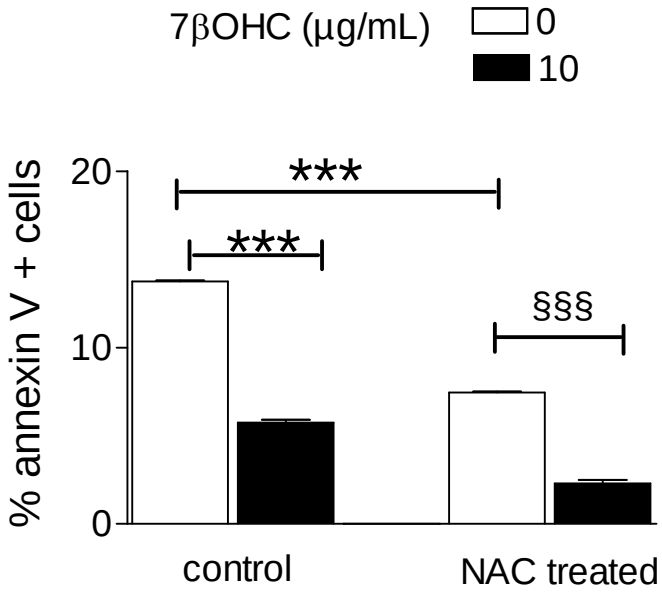

Fig. 33 Effect of the antioxidant N-acetycystein (NAC) on the antiapoptotic action of 7*β*-OHC against bFGF deprivation. HUVEC were treated with 7*β*-OHC (10 *μ*g/mL) without bFGF for 24 hours. Where indicated, a pretreatment with NAC (10 mM) was performed for 30 min before the addition of 7*β*-OHC, the inhibitor was present during all the experiment. Results are expressed as mean ± SE of percentage of annexin-V labelled cells of 2 independent experiments performed in duplicate (***P < 0.001, §§§P < 0.001). Statistical analysis was performed by one-way ANOVA test and Bonferroni's multiple comparison post test.

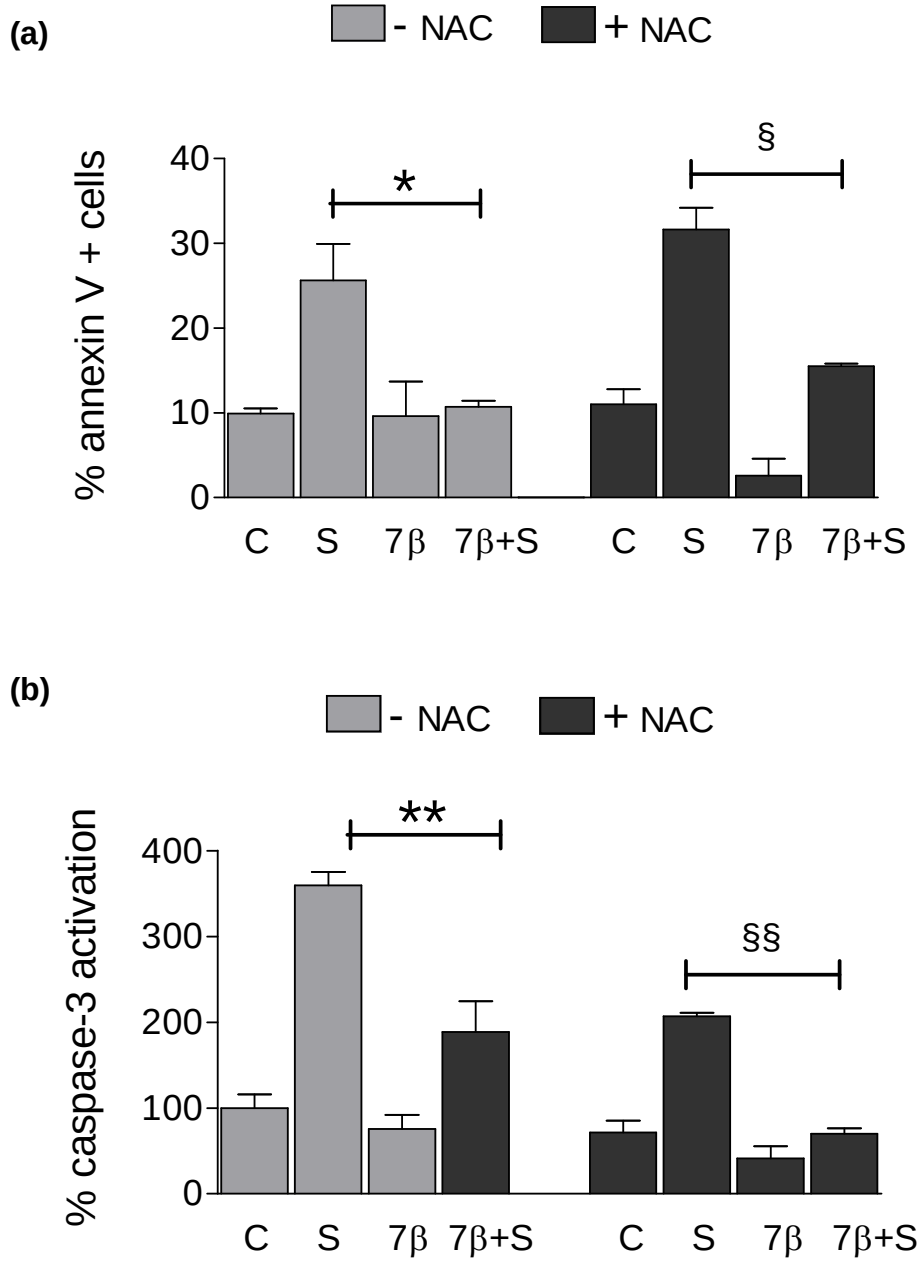

Fig. 34. Effect of the antioxidant N-acetylcystein (NAC) on the antiapoptotic action of 7*β*-OHC against staurosporine. Analysis of **(a)** annexin-V binding and **(b)** caspase-3 activation. HUVEC were treated with or without 7*β*-OHC (10 μg/mL) for 15 hours, then staurosporine (50 nM) was added for 3 hours. Where indicated, a pretreatment with NAC (10 mM) was performed for 30 min before the addition of 7*β*-OHC, the inhibitor was present during all the experiment. Results are expressed as mean $\pm$ SE of 2 independent experiments performed in duplicate of percentage of annexin-V labeled cells or caspase 3 activation (*$P < 0.05$, **$P < 0.01$, §$P < 0.05$, §§$P < 0.01$). Statistical analysis was performed by one-way ANOVA test and Bonferroni's multiple comparison post test.. (C = control, S = staurosporine; 7β = 7*β*-OHC).

4.7 Role of eNOS in the antiapoptotic effect of 7*β*-HOC

NO is an important factor produced by endothelial cells that promotes endothelial cell survival (Hürlimann *et al*, 2002). Thus, the involvement of eNOS activation in the antiapoptotic action of 7*β*-OHC was studied.

Treatment of HUVEC with the eNOS inhibitor L-NAME (1 mM) did not prevent the protective effect of 7*β*-OHC against apoptosis induced either by bFGF deprivation (Figg 35, 36) or by staurosporine (Fig. 37). Furthermore, determination of NO production by measuring total nitrite of the cell incubation media indicated that a treatment of 24 hours with 10 μg/mL *7β*-OHC did not increase NO levels (total nitrite: control = 16,5 μM $\pm$ 1,794; *7β*-OHC treated HUVEC = 18,4 μM $\pm$ 1,564).

All together these findings demonstrate that NO production by eNOS is not involved in the antiapoptotic effect of 7*β*-OHC.

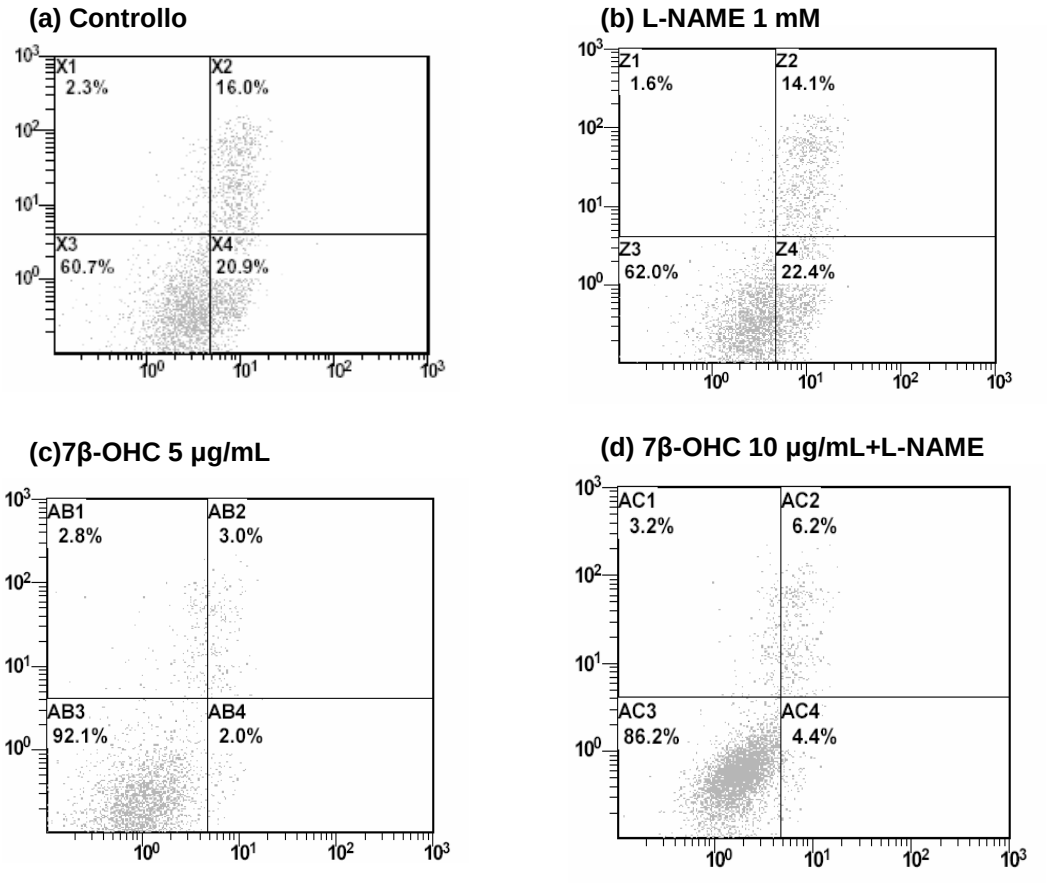

Fig. 35 Representative cytograms of annexin-V and PI binding showing the effect of 7*β*-OHC on L-NAME on the antiapoptotic action of 7*β*-OHC against bFGF deprivation. HUVEC were treated with 7*β*-OHC (10 μg/mL) for 24 hours in the absence of bFGF. Where indicated a pretreatment with L-NAME (1 mM) for 30 min was performed before the addition of 7*β*-OHC, the inhibitor was present during all the experiment. Unlabelled cells (viable cells) are collocated in the left quadrant on the bottom (3). Annexin-V positive cells (apoptotic cells) are collocated in the right quadrant on the bottom (4). PI positive cells (necrotic cells) are represented in the left quadrant on the top (1) of the scatter plot. Double stained cells (late apoptotic cells) are in the right quadrant on the top (2).

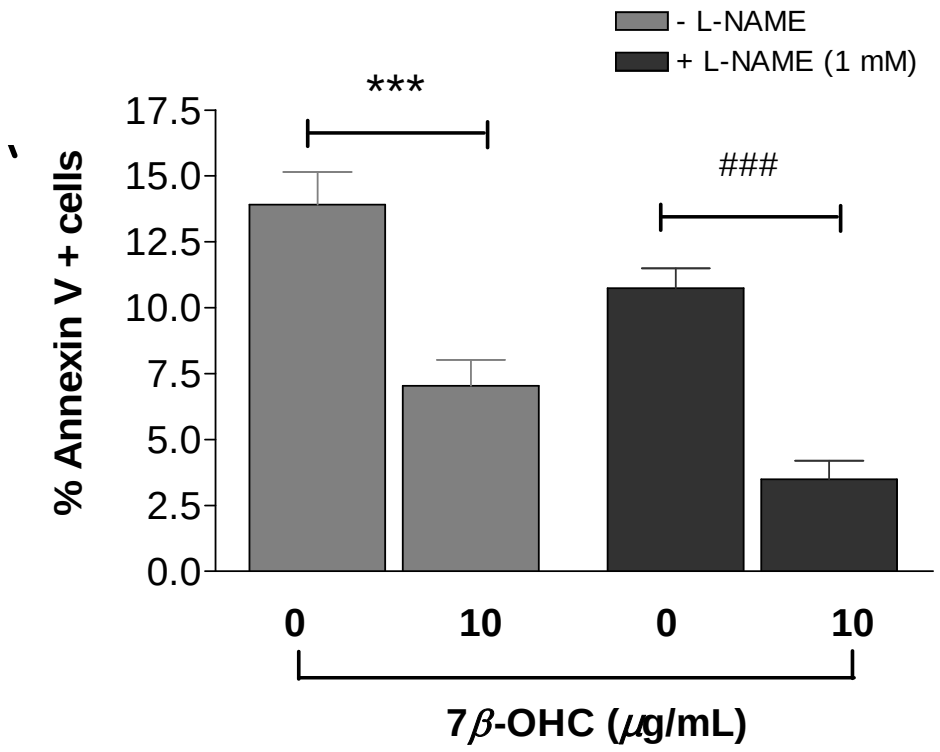

Fig. 36 Effect of L-NAME on the antiapoptotic action of 7β-OHC against bFGF deprivation. HUVEC were treated with 7β-OHC (10 μg/mL) for 24 hours in the absence of bFGF. Where indicated a pre-treatment with L-NAME (1 mM) for 30 min was performed before the addition of 7β-OHC, the inhibitor was present during all the experiment. Results are expressed as mean $\pm$ SE of percentage of annexin-V labelled cells of 2 independent experiments (***$P < 0.001$, ###$P < 0.001$). Statistical analysis was performed by one-way ANOVA test and Bonferroni's multiple comparison post test.

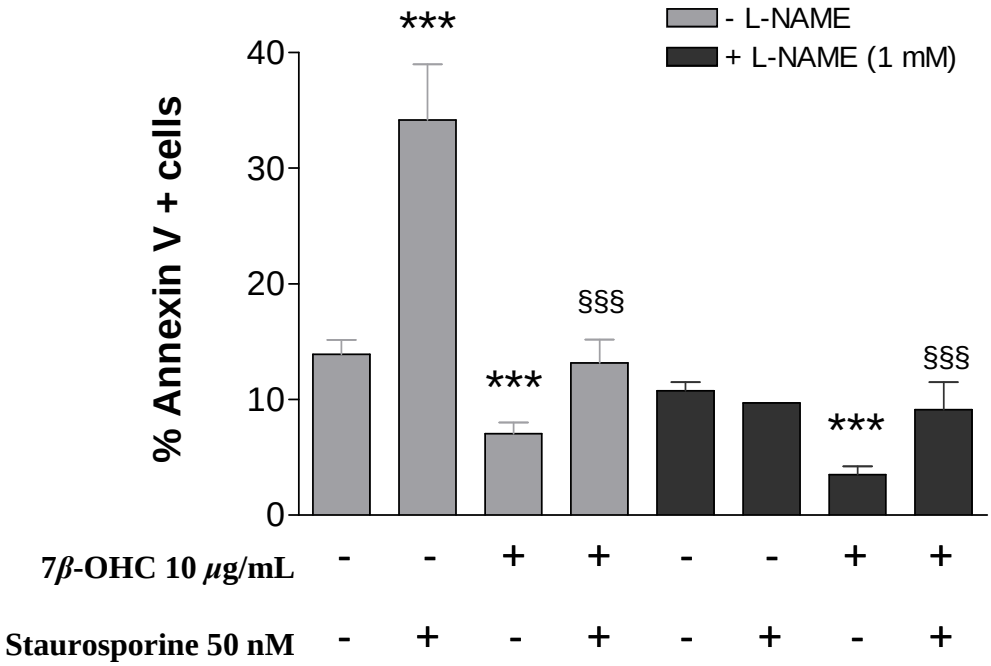

Fig. 37. **Effect of the eNOS inhibitor L-NAME on the antiapoptotic effect of 7*β*-OHC against apoptosis induced by staurosporine treatment.** HUVEC were treated with 7*β*-OHC (10 *μ*g/mL) for 15 hours, then staurosporine was added for 3 hours. Where indicated a pretreatment with L-NAME (1 mM) for 30 min was performed before the addition of 7*β*-OHC. Results are expressed as mean ± SE of percentage of annexin-V labelled cells of 2 independent experiments (***$P < 0.001$ vs. control, §§§$P < 0.001$ vs staurosporine-treated cells). Statistical analysis was performed with one-way ANOVA test and Bonferroni's multiple comparison post test.

4.8. Role of ERK in the antiapoptotic effect of 7β-OHC

To clarify the molecular mechanism of the antiapoptotic action of 7β-OHC in HUVEC, activation of MEK/ERK pathway was investigated. Generally ERK activation occurs to protect cells from death and it is triggered by activation of MEK.

ERK activation was investigated by Western blotting analysis to detect the level of phosphorylation of the enzyme (Fig. 38a). Treatment with 10 μg/mL 7β-OHC did not activate ERK. On the other hand, two different MEK inhibitors, PD98059 and UO126, were able to inhibit the antiapoptotic effect of 10 μg/mL 7β-OHC against apoptosis induced by staurosporine (50 nM, 3 hours), as demonstrated by the analysis of caspase 3 activation (Fig. 38b).

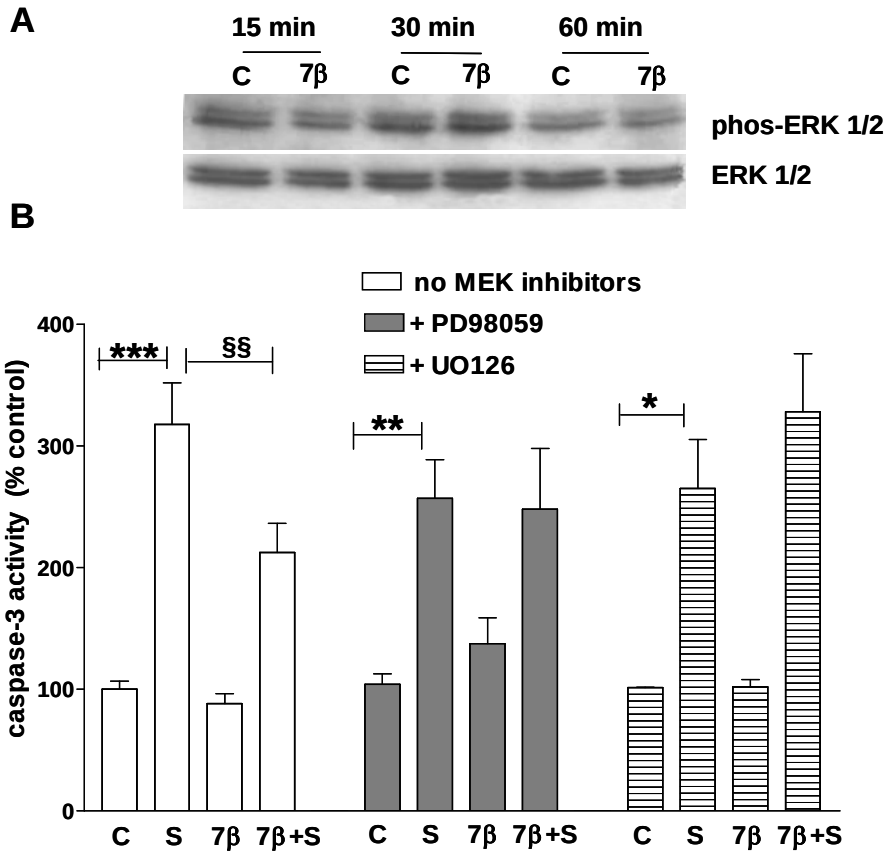

Fig. 38 Role of ERK in the antiapoptotic effect of 7*β*-OHC. (a) Western blotting analysis of ERK phosphorylation (phos-ERK 1/2) in HUVEC treated with 7*β*-OHC (10 μg/mL): 30 μg of cell lysates proteins were subjected to 10% SDS-PAGE and transferred to PVDF membrane, then phos-ERK 1/2 were detected, after stripping, the membrane was exposed to the rabbit polyclonal IgG to detect overall ERKs **(b).** Effect of MEK inhibitors PD98059 and UO126 on caspase-3 activation induced by staurosporine: HUVEC were treated with 7*β*-OHC (10 μg/mL) for 2 hours, then staurosporine (50 nM) was added for 3 hours, where indicated cells were pretreated with PD98059 (25 μM) or UO126 (25 μM) for 30 min before treatment with 7*β*-OHC, the inhibitors were present during all the experiment. Results are expressed as mean $\pm$ SE of percentage of caspase-3 activation of 3 independent experiments performed in triplicate (***$P < 0.001$, **$P < 0.01$, *$P < 0.05$, §§$P < 0.01$). Statistical analysis was performed with one-way ANOVA test and Bonferroni's multiple comparison post test.

5. DISCUSSION

Oxysterols are oxygenated derivatives of cholesterol that may be either formed endogenously or absorbed from the diet and are particularly found in highly processed foods of animal origin (Tai *et al*., 1999). They are also the major components of oxLDL which are involved in the pathogenesis of atherosclerosis and evidence suggest that oxysterols, such as 7β-OHC and 7-KC are responsible for oxLDL cytotoxicity at the vascular wall.

Otherwise, the results in this thesis show that 7β-OHC at concentrations below 40 μg/mL is able to protect HUVEC from apoptosis induced either by bFGF deprivation or by staurosporine treatment as revealed by the analysis of phosphatidylserine translocation and caspase 3 activation. The investigation of the protective effect of this oxysterol was based on the preliminary evidence, from our laboratory, about the dual effect of both 7β-OHC and 7-KC on HUVEC viability measured by the MTT assay. This dual effect is dependent on the concentrations of the oxysterols: at low concentrations (1-10 μg/mL) they induce an increase in cell viability, while at high concentration (20 μg/mL) they induce cell death, accordingly to previous experimental evidence about the proapoptotic action of 20 μg/mL 7β-OHC in HUVEC (Lizard *et al*, 1999).

Also, *in vitro* studies show that oxLDL themselves have a dual effect on endothelial cells (Galle *et al*. in 2001): at concentrations above 50 μg/mL they are cytotoxic inducing cell death through an increase in ROS levels; on the contrary, at lower concentrations they promote cell proliferation which is mediated by a lower increase in intracellular ROS produced by NADPH oxidase (Heinloth *et al*, 2000).

In accord to these findings, ROS at physiological levels are thought to be important signaling molecules involved in the regulation of many intracellular pathways concerning cell survival, proliferation and death (Tannickal *et al*, 2000). Otherwise, a dual effect of ROS on endothelial cell viability has been demonstrated, depending on their concentrations: while at high levels they are cytotoxic due to their pro-oxidant properties, at physiological levels they protect cells from apoptosis induced by serum-deprivation (Haendeler *et al*., 2004). Other experimental data support the involvement

of ROS in the proapoptotic effect of 7-KC: it has been shown that the loss of mitochondrial membrane potential induced by 7-KC is prevented by antioxidants (Lizard *et al*, 2000).

On the other hand, the protective effect of 7*β*-OHC at 20 *μ*M concentration (corresponding to 9,6 *μ*g/mL) was demonstrated (Chen *et al*, 2006). This effect is mediated by an increase in GSH levels.

All these findings indicate a role of ROS in the molecular mechanism of oxysterols at different levels, and the major source of ROS involved in these effects is NADPH oxidase. Thus, we have investigated the role of ROS in the antiapoptotic action of 7*β*-OHC in HUVEC, analyzing in particular the involvement of NADPH oxidase activity.

This study shows that both 7-KC and 7*β*-OHC are able to induce a concentration-dependent increase in ROS production in HUVEC. This ROS overproduction occurs immediately after the exposure of the cells to the oxysterols. ROS production induced by 7*β*-OHC in HUVEC is partially due to the activation of NADPH oxidase. Despite evidence summarized above, our results reveal that the activity of this enzyme is not involved in the antiapoptotic effect of the oxysterol. In fact, hydralazine, a NADPH oxidase inhibitor (Munzel *et al*., 1996), is not able to prevent the antiapoptotic action of 7*β*-OHC against apoptosis induced by either bFGF deprivation or staurosporine treatment. Actually ROS has no role in the antiapoptotic effect of oxysterols in HUVEC as demonstrated by the experiments performed in the presence of NAC, a cystein and GSH precursor acting as ROS scavenger. In fact, NAC treatment does not prevent the antiapoptotic action of 7*β*-OHC against apoptosis induced by either bFGF deprivation or staurosporine treatment.

NO is an important factor which preserves endothelial function and promotes cell survival. For this reason, the possible role of NO in the protective effect of 7*β*-OHC was studied. The involvement of NO in the antiapoptotic effect of 7*β*-OHC was excluded, since the eNOS inhibitor L-NAME does not prevent the antiapoptotic action of 7*β*-OHC against apoptosis induced by either bFGF deprivation or staurosporine treatment. Moreover incubation of HUVEC with 7*β*-OHC did not increase the levels of nitrites in the cell culture medium.

Finally we investigated the effect of the oxysterol on MEK/ERK pathway, whose activation is usually involved in the mechanisms of cell survival (Ballif and Blenis,

2001). Results reveal that 7*β*-OHC does not increase ERK activation, however the experiments performed in the presence of two different MEK inhibitors demonstrate that a basal level of MEK activity is essential for of 7*β*-OHC action, thus suggesting that the effect of the oxysterol is downstream of ERK activation. Further studies will be required to find the molecular target of 7*β*-OHC and its regulation by the MEK/ERK cascade.

In conclusion, our results offer an evidence of an unknown effect of 7*β*-OHC on human endothelial cells and suggest a role of this oxysterol as a signaling molecule that is involved in the regulation of cell survival pathways.

BIBLIOGRAPHY

Azumi H, Inoue N, Takeshita S, Rikitake Y, Kawashima S, Hayashi Y, Itoh H, and Yokoyama M, 1999. Expression of NADH/NADPH oxidase p22*phox* in human coronary arteries. *Circulation,* 100: 1494–1498,.

Babior, B. M., Lambeth, J. D. and Nauseef, W, 2002. The neutrophil NADPH oxidase. *Arch. Biochem. Biophys*, 397: 342–344.

Bader M, Muse W, Ballou DP, Gassner C, and Bardwell JC, 1999. Oxidative protein folding is driven by the electron transport system. *Cell*, 98: 217–227.

Bayraktutan U, Draper N, Lang D, and Shah AM, 1998**.** Expression of functional neutrophil-type NADPH oxidase in cultured rat coronary microvascular endothelial cells. *Cardiovasc Res,* 38: 256–262.

Bellosta S, Mahley RW, Sanan DA, Murata J, Newland DL, Taylor JM, Pitas RE, 1995. Macrophage-specific expression of human apolipoprotein E reduces atherosclerosis in hypercholesterolemic apolipoprotein E-null mice. *J Clin Invest*, 96: 2170–2179.

Biswas S, Chida AS Rahman I, 2006. Redox modifications of protein–thiols: Emerging roles in cell signaling. *Biochemical Pharmacology,* 71 551–564.

Boveris A, Oshino N, and Chance B, 1972. The cellular production of hydrogen peroxide. *Biochem J,* 128: 617–630.

Brooks-Wilson A, Marcil M, Clee SM, Zhang LH, Roomp K, van Dam M, Yu L, Brewer C, Collins JA, Molhuizen HO, Loubser O, Ouelette BF, Fichter K, Ashbourne-Excoffon KJ, Sensen CW, Scherer S, Mott S, Denis M, Martindale D, Frohlich J, Morgan K, Koop B, Pimstone S, Kastelein JJ, Genest J, Hayden MR, 1999. Mutations in ABC1 in Tangier disease and familial high-density lipoprotein deficiency. *Nat Genet*, 22: 336–345.

Brown AJ, Jessup W, 1999. Oxysterols and atherosclerosis. *Atherosclerosis*, 142: 1–28.

Brown AJ, Jessup W, 1999. Oxysterols and atherosclerosis. *Atherosclerosis,* 142: 1-28.

Cai H, Griendling KK, Harrison DG 2003. The vascular NAD(P)H oxidases as therapeutic targets in cardiovascular diseases. *Trends Pharmacol Sci 24*: 471-478.

Chen ZH, Yoshida Y, Saito Y, Sekine A, Noguchi N ¶, and Niki E, 2006. Induction of adaptive response and enhancement of PC12 cell tolerance by 7-hydroxycholesterol and 15-deoxy-_12,14-prostaglandin J2 through up-regulation of cellular glutathione via different mechanisms. *The Journal of Biological chemistry*, 281 (20): 14440–14445.

Cheng, G, Cao Z, Xu X, van Meir EG, Lambeth, JD, 2001. Homologs of gp91phox: cloning and tissue expression of Nox3, Nox4, and Nox5. *Gene*, 269: 131–140.

Choa SH, Leea CH, Ahna Y, Kima H, Kimb H, Ahnb CY, Yanga KS, LeeSR, 2004. Redox regulation of PTEN and protein tyrosine phosphatases in H_2O_2-mediated cell signaling. *FEBS Letters*, 560: 7-13.

Costet P, Luo Y, Wang N, Tall AR, 2000. Sterol-dependent transactivation of the ABC1 promoter by the liver X receptor/retinoid X receptor. *J Biol Chem* 275: 28240–28245.

Creager MA, Cooke JP, Mendelsohn ME, Gallagher SJ, Coleman SM, Loscalzo J and Dzau VJ, 1990. Impaired Vasodilation of Forearm Resistance Vessels in Hypercholesterolemic *Humans. J. Clin. Invest*, 86: 228-234.

Curtin JF, Donovan M, Cotter TG, 2002. Regulation and measurement of oxidative stress in apoptosis. *Journal of Immunological Methods* 265, 49– 72.

Curtiss LK, Boisvert WA 2000 Apolipoprotein E and atherosclerosis. *Curr Opin Lipidol*, 11: 243–251.

Dimmeler S, Fleming I, Fisslthaler B, Hermann C, Busse R, and Zeiher AM, 1999. Activation of nitric oxide synthase in endothelial cells by Akt-dependent phosphorylation. *Nature,* 399: 601–605.

Droge W, 2002. Free Radicals in the Physiological Control of Cell Function. *Physiol Rev,* 82: 47–95.

Droge W, Schulze-Osthoff K, Mihm S, Galter D, Schenk H, Eck HP, Roth S, and Gmunder H, 1994. Functions of glutathione and glutathione disulfide in immunology and immunopathology. *FASEB J,* 8: 1131–1138.

Fleming I, and Busse R, 2003. Molecular mechanisms involved in the regulation of the endothelial nitric oxide synthase. *Am J Physiol Regul Integr Comp Physiol*, 284: R1–R12.

Fleming I, Fisslthaler B, Dimmeler S, Kemp BE, and Busse R, 2001. Phosphorylation of Thr^{495} regulates Ca2_/calmodulin-dependent endothelial nitric oxide synthase activity. *Circ Res,* 88: e68–e75.

Freeman BA and Crapo JD, 1982. Biology of disease: free radicals and tissue injury. *Lab* Invest, 47: 412–426,

Freeman BA and Crapo JD, 1982. Biology of disease: free radicals and tissue injury. *Lab Invest*, 47: 412–426.

Galle J., Heinloth A., Wanner C., Heermeier K. 2001. Dual effect of oxidized LDL on cell cycle in human endothelial cells through oxidative stress. *Kidney Int. Suppl*, 78: S120-3.

Griendling KK, Minieri CA, Ollerenshaw JD, and Alexander RW, 1994. Angiotensin II stimulates NADH and NADPH oxidase activity in cultured vascular smooth muscle cells. *Circ Res* 74: 1141–1148.

Griendling KK, Sorescu D, Ushio-Fukai M 2000. NAD(P)H oxidase: role in cardiovascular biology and disease. *Circ Res 86*: 494-501.

Griendling KK, Sorescu D, Ushio-Fukai M, 2000. NAD(P)H: Oxidase Role in Cardiovascular Biology and Disease. *Circ Res*. 86: 494-501.

Guardiola F, Codony R, Addis PB, Rafecas M, Boatella J, 1996. Biological effects of oxysterols: current status. *Food Chem Toxicol,* 34: 193-11.

Gupta K, Kshirsagar S, Li W, Gui L, Ramakrishnan S, Gupta P, Law PY, Hebbel RP, 1999. VEGF prevents apoptosis of human microvascular endothelial cells via opposing effects on MAPK/ERK and SAPK/JNK signaling. *Exp Cell Res,* 247: 495–504.

Haendeler J, Hoffmann J, Tischler V, Berk BC, Zeiher AM and Stefanie Dimmeler, 2002. Redox regulatory and anti-apoptotic functions of thioredoxin depend on *S*-nitrosylation at cysteine 69. *Nature Cell Biology* 4, 743-749

Haendeler J, Tischler V, Hoffmann J, Zeiher AM, Dimmeler S, 2004, Low doses of reactive oxygen species protect endothelial cells from apoptosis by increasing thioredoxin-1 expression. *FEBS Letters* 577, 427–433

Halliwell B and Gutteridge JMC, 1989**.** *Free Radicals in Biology and Medicine.* New York: Oxford University Press, p. 22–85

Harada K, Ishibashi S, Miyashita T, et al., 1997. Bcl-2 protein inhibits oxysterol-induced apoptosis through suppressing CPP32-mediated pathway. *FEBS* Lett; 411: 63-6.

Hedges JC, Dechert MA, Yamboliev IA, Martin JL, Hickey E, Weber LA, Gerthoffer WT, 1999. A role for p38(MAPK)/HSP27 pathway in smooth muscle cell migration. *J Biol Chem,*. 274: 24211–24219.

Heinloth A, Heermeier K, Raff U, Wanner C, Galle J, 2000. Stimulation of NADPH Oxidase by Oxidized Low-Density Lipoprotein Induces Proliferation of Human Vascular Endothelial Cells. *J Am Soc Nephrol*, 11: 1819–1825.

Hodis HN, Crawford DW, Sevanian A, 1991. Cholesterol feeding increases plasma and aortic tissue cholesterol oxide levels in parallel: further evidence for the role of cholesterol oxidation in atherosclerosis. *Atherosclerosis*, 89: 117-26.

Hoffmann J, Haendeler J, Zeiher AM and Dimmeler S, 2001, TNFα and ox-LDL reduce protein S-nitrosylation in endothelial cells. *The journal of biolological chemistry* 276 (44), 41383-41387)

Horton JD, Joseph L. Goldstein and. Brown Michael S, 2002 SREBPs: activators of the complete program of cholesterol and fatty acid synthesis in the liver. *J Clin Invest*. 109(9): 1125–1131.

Huie RE and Padmaja S, 1993The reaction of NOz with superoxide. *Free Radic Res Commun* 18: 195–199.

Hürlimann D, Ruschitzka F, and Lüscher TF, 2002. The relationship between the endothelium and the vessel wall. *European Heart Journal Supplements* **4** *(Supplement A),* A1–A7

Hwang J, Ing MH, Salazar A, Lassegue B, Griendling K, Navab M, Sevanian A, Hsiai TK 2003. Pulsatile versus oscillatory shear stress regulates NADPH oxidase subunit expression: implication for native LDL oxidation. *Circ Res 93*: 1225-1232.

Irani K, 2000. Oxidant Signaling in Vascular Cell Growth, Death, and Survival A Review of the Roles of Reactive Oxygen Species in Smooth Muscle and Endothelial Cell Mitogenic and Apoptotic Signaling. *Circ Res* 87: 179-183.

Jones SA, O'Donnell VB, Wood JD, Broughton JP, Hughes EJ, Jones OT, 1996. Expression of phagocyte NADPH oxidase components in human endothelial cells. *Am J Physiol*, 271: H1626–H1634.

Kabir J, Lobo M, Zachary I. 2002 Staurosporine induces endothelial cell apoptosis via focal adhesion kinase dephosphorylation and focal adhesion disassembly independent of focal adhesion kinase proteolysis. *J. Biochem.* 367: 145-155.

Kumar S., 1999. Mechanisms mediating caspase activation in cell death. *Cell Death Differ*; 6: 1060-6.

Lee T-S, Chau L-Y, 2001. Fas/Fas ligand-mediated pathway is involved in oxLDL-induced apoptosis in vascular smooth muscle cells. *Am J Physiol Cell Physiol*, 280: 709-18.

Leonarduzzi G, Sottero B, Poli G, 2002. Oxidised products of cholesterol: dietary and metabolic origin, and proatherosclerotic effects (review). *J Nutr Biochem*, 13: 700-10.

Lizard G, Gueldry S, Sordet O, 1998. Glutathione is implied in 7-ketocholesterol-induced apoptosis, which is associated with radical oxygen species production. *FASEB J*, 12: 1651-63.

Lizard G, Lemaire S, Monier S, Gueldry S, Neel D, Gambert P., 1997. Induction of apoptosis and of interleukin-1b secretion by 7b-hydroxycholesterol and 7-ketocholesterol: partial inhibition by Bcl-2 overexpression. *FEBS Lett*; 419: 276-80.

Lizard G, Miguet C, Bessede G, *et al.* 2000. Impairment with various antioxidants of the loss of mitochondrial transmembrane potential and of the cytosolic release of cytochrome *c* occurring during 7-ketocholesterol-induced apoptosis. Free Radic Biol Med; 28: 743-56.

Lizard G., Monier S., Cordelet C., Gesquière L., Deckert V., Gueldry S., Lagrost L., Gambert P. (1999) Characterization and comparison of the mode of cell death, apoptosis versus necrosis, induced by 7β-hydroxycholetserol and 7-ketocholesterol in the cells of the vascular wall. *Arterioscler*. *Thromb*. *Vasc*. *Biol*. 19, 1190-1200.

Maejima Y, Adachi S, Morikawa K, Ito H, Isobe M, 2005. Nitric oxide inhibits myocardial apoptosis by preventing caspase-3 activity via S-nytrosilation. *Journal of Molecular and Cellular Cardiology*, 38, 163-174.

Mak PA, Laffitte BA, Desrumaux C, Joseph SB, Curtiss LK, Mangelsdorf DJ, Tontonoz P, Edwards PA 2002 Regulated expression of the apolipoprotein E/C-I/C-

IV/C-II gene cluster in murine and human macrophages. A critical role for nuclear liver X receptors and . J Biol Chem 277:31900–21908.

McKelvey TG, Hollwarth ME, Granger DN, Engerson TD, Landler U, and Jones HP, 1988 Mechanisms of conversion of xanthine dehydrogenase to xanthine oxidase in ischemic rat liver and kidney *Am J Physiol Gastrointest Liver Physiol* 254: G753-G760.

Miguet-Alfonsi C, Prunet C, Monier S, et al. 2002. Analysis of oxidative processes and of myelin figures formation before and after the loss of mitochondrial transmembrane potential during 7b-hydroxycholesterol and 7-ketocholesterol-induced apoptosis: comparison with various pro-apoptotic chemicals. *Biochem Pharmacol*; 64: 527-41.

Miguet-Alfonsi C, Prunet C, Monier S, *et al.,* 2002. Analysis of oxidative processes and of myelin figures formation before and after the loss of mitochondrial transmembrane potential during 7*β*-hydroxycholesterol and 7-ketocholesterol-induced apoptosis: comparison with various pro-apoptotic chemicals. *Biochem Pharmacol*, 64: 527-41.

Münzel T, Kurz S, Rajagopalan S, Thoenes M, Berrington WR, Thompson JA, Freeman BA, Harrison DG. Hydralazine Prevents, 1996. Nitroglycerin Tolerance by Inhibiting Activation of a Membrane-bound NADH Oxidase A New Action for an Old Drug. *J. Clin. Invest.*. 98: 1465–1470.

Nordberg J and. Arnér ESJ, 2001 Reactive oxygen species, antioxidants, and the mammalian thioredoxin system. *Free Radical Biology & Medicine*, Vol. 31, No. 11, 1287–1312.

Peng SK, Taylor BC, Hill JC, Morin RJ, 1985. Cholosterol oxydation derivatives and arterial endothelial damage. *Atherosclerosis*, 54: 121-133.

Porasuphatanaa S, Tsaib P, Rosen GM, 2003. The generation of free radicals by nitric oxide synthase. *Comparative Biochemistry and Physiology* Part C 134 281–289.

Puddu GM, Cravero E, Arnone G, Muscari A and Puddu P, 2005. Molecular aspects of atherogenesis: new insights and unsolved questions. *Journal of Biomedical Science* 12, 839–853.

Radomski MW, Palmer RMJ, and Moncada S. The anti-aggregating properties of vascular endothelium: interactions between prostacyclin and nitric oxide. *Br J Pharmacol* 92: 639–646, 1987.

Ray R and Shah AM, 2005. NADPH oxidase and endothelial cell function. *Clinical Science* 109, 217–226

Robertson JD, Orrenius S. Role of mitochondria in toxic cell death. *Toxicology* 2002; 181-182: 491-6.

Rosenblat M, Aviram M, 2002. Oxysterol-induced activation of macrophage NADPH-oxidase enhances cell-mediated oxidation of LDL in the atherosclerotic apolipoprotein E deficient mouse: inhibitory role for vitamin E. *Atherosclerosis*, 160: 69-80.

Rossi, F, Bellavite, P, Berton, G, Grzeskowiak, M, Papini E, 1985. Mechanism of production of toxic oxygen radicals by granulocytes and macrophages and their function in the inflammatory process. *Pathol. Res. Pract.* 180**,** 136–142.

Rueckschloss U, Galle J, Holtz J, Zerkowski HR, Morawietz H 2001. Induction of NAD(P)H oxidase by oxidized low-density lipoprotein in human endothelial cells: antioxidative potential of hydroxymethylglutaryl coenzyme A reductase inhibitor therapy. Circulation 104, 1767–1772

Sa´nchez FA, Savalia NB, Dura´n RG, Lal BK., Boric MP and Dura´n WN, 2006. Functional significance of differential eNOS translocation. *Am J Physiol Heart Circ Physiol* 291, H1058–H1064

Saitoh M, Nishitoh H, Fujii M, Takeda K, Tobiume K, Sawada Y, Kawabata M, Miyazono K and Ichijo H, 1998. Mammalian thioredoxin is a direct inhibitor of

apoptosis signal-regulating kinase (ASK) 1 *The EMBO Journal* Vol.17 No.9 pp.2596–2606.

Schroepfer GJ, 2000. Oxysterols: modulator of cholesterol metabolism and other processes. *Physiological Reviews,* Vol 80 n. 1.

Schroepfer GJ. Oxysterols, 2000. Modulators of cholesterol metabolism and other processes. *Physiol Rev*, 80: 361-554.

Seshiah PN, Weber DS, Rocic P, Valppu L, Taniyama Y, Griendling KK 2002. Angiotensin II stimulation of NAD(P)H oxidase activity: upstream mediators. *Circ Res 91*: 406-413.

Slee EA, Adrain C, Martin SJ., 1999. Serial killers: ordering caspase activation events in apoptosis. *Cell Death Differ*, 6: 1067-74.

Sulciner DJ, Irani K, Yu ZX, Ferrans VJ, Goldschmidt-Clermont P, Finkel T, 1996. Rac1 Regulates a cytokine-stimulated, redox-dependent pathway necessary for NF-kB activation. *Mol Cell Biol*, 16: 7115–7121.

Tai C-Y, Chen YC, Chen BH, 1999. Analysis, formation and inhibition of cholesterol oxidation products in foods: an overview (part I). *J Food Drug Anal*, 7: 243-57.

Tamura DY, Moore EE, Johnson JL, Zallen G, Aiboshi J, Silliman CC, 1998. p38 Mitogen-activated protein kinase inhibition attenuates intercellular adhesion molecule-1 up-regulation on human pulmonary microvascular endothelial cells. *Surgery*, 124: 403–407.

Tanaka T, Nakamura H, Yodoi J, Bloom ET, 2005, Redox regulation of the signaling pathways leading to eNOS phosphorylation. *Free Radical Biology & Medicine* 38, 1231– 1242.

Thannickal VJ, and Fanburg BL, 2000. Reactive oxygen species in cell signaling. *Am J Physiol Lung Cell Mol Physiol* 279, L1005–L1028.

Thum T, Borlak J 2004. Mechanistic role of cytochrome P450 monooxygenases in oxidized low-density lipoprotein-induced vascular injury: therapy through LOX-1 receptor antagonism *Circ Res 94*: e1-13.

Tontonoz P and Mangelsdorf DJ, 2003 Liver X Receptor Signaling Pathways in Cardiovascular Disease Molecular Endocrinology 17(6):985–993.

Touyz RM, Yao G, Schiffrin EL 2003. c-Src induces phosphorylation and translocation of p47phox: role in superoxide generation by angiotensin II in human vascular smooth muscle cells. *Arterioscler Thromb Vasc Biol 23*: 981-987.

Ushio-Fukai M and Alexander RW, 2004. Reactive oxygen species as mediators of angiogenesis signaling Role of NAD(P)H oxidase. *Molecular and Cellular Biochemistry*, 264: 85–97.

Ushio-Fukai M, Alexander RW, Akers M, Griendling KK, 1998. p38 Mitogen-activated protein kinase is a critical component of the redox-sensitive signaling pathways activated by angiotensin II. Role in vascular smooth muscle cell hypertrophy. *J Biol Chem*, 273:15022–15029.

Ushio-Fukai M, Tang Y, Fukai T, Dikalov SI, Ma Y, Fujimoto M, Quinn MT, Pagano PJ, Johnson C, Alexander RW 2002. Novel role of gp91(phox)-containing NAD(P)H oxidase in vascular endothelial growth factor-induced signaling and angiogenesis. *Circ Res 91*: 1160-1167.

Wang N, Verna L, Hardy S, Zhu Y, Ma KS, Birrer MJ, Stemerman MB, 1999. c-Jun triggers apoptosis in human vascular endothelial cells. *Circ Res*, 85: 387–393.

Zhou Q, Wasowicz E, Handler B, Fleischer L, Kummerow F A, 2000. An excess concentration of oxysterols in the plasma is cytotoxic to cultured endothelial cells. *Atherosclerosis*, 149: 191-197.

Zhua Y, Liaoa HL, Niub X, Yuana Y, Lina T, Vernaa L,. Stemerman MB, 2003. Low density lipoprotein induces eNOS translocation to membrane caveolae: the role of

RhoA activation and stress fiber formation. *Biochimica et Biophysica Acta* 1635, 117–126.